



The  
University  
Of  
Sheffield.

# Determining The Role Of CD68 Positive Macrophages In Muscle Damage And Disease

Hannah Roberts

*Thesis submitted for degree of Doctor of Philosophy September 2019.  
Department of Oncology and Metabolism  
Faculty of Medicine, Dentistry and Health  
The University of Sheffield*

# Summary

---

Macrophages play an essential role in the immune response, responding to pathogens, inflammation and tissue damage. Proinflammatory macrophages are prevalent in the X-linked life limiting muscle wasting disease, Duchenne Muscular Dystrophy (DMD), where they are thought to exacerbate muscle damage. We hypothesise that reducing numbers of a specific subset of macrophages may reduce the muscle damage seen in DMD without effecting regeneration of the muscle. The MacLow mouse model allows the doxycycline inducible depletion of CD68 positive (CD68+) macrophages. We crossed the mdx mouse model of DMD with the MacLow model to generate the mdx-MacLow model (MacLowMD). This study aimed to determine the effects of macrophage depletion on muscle damage and regeneration in muscular dystrophy using the MacLowMD model.

Doxycycline treated MacLowMD mice had a 33% reduction in total macrophage population in the liver ( $P < 0.05$ ). No difference was found in the number of CD68+ cells in Tibialis Anterior (TA) and quadricep muscle of doxycycline treated MacLowMD mice compared to mdx mice, but a 30% reduction ( $P < 0.05$ ) was observed in diaphragm and heart muscle. A significant increase in numbers of M2, CD206 positive (CD206+) and CD163 positive (CD163+) macrophages was observed throughout all muscles studied ( $P < 0.05$ ). A significant ( $P < 0.05$ ) reduction in muscle fibre damage was observed between doxycycline treated MacLowMD muscle compared to mdx muscle, and doxycycline treatment and CD68+ macrophage depletion had no negative effects on the regenerative capacity in any of the muscles studied.

These results demonstrate that the MacLowMD model is a good model for studying the role of proinflammatory CD68+ macrophages in disease progression, muscle damage and muscle regeneration.

# Acknowledgements

---

First and foremost, I would like to express my deepest gratitude to my brilliant supervisors, Dr Gaynor Miller and Professor Alison Gartland. Their continued encouragement, support and guidance have helped me at every stage of my PhD; from guiding me during my practical laboratory work, to providing me with wonderful support during the writing of my project. They were always willing to assist me and provide me with advice, and for this I am extremely grateful.

I would also like to thank Dr Neil Chapman and his group for their suggestions and advice during Western Blotting, the Biological Service Unit for their kind help and support while I was undertaking the animal work as well as thanking Dr Karan Shah for his guidance during qPCRs.

Finally, and most importantly, I thank my parents and sister for their patience, understanding and endless support throughout my PhD.

## Authors Declaration

---

I declare that the work presented within this thesis is my own work and has not been previously submitted for any other degree.

# Table of Contents

---

Summary.....	I
Acknowledgments.....	III
Authors Declaration.....	IV
Table of Contents .....	V
List of Figures.....	XI
List of Tables.....	XIV
Abbreviations.....	XV
1. Introduction.....	1
1.1 Duchenne Muscular Dystrophy in Human.....	1
1.1.1 Duchenne Muscular Dystrophy Background.....	1
1.1.2 Mutations in the DMD Gene.....	2
1.1.3 Dystrophin.....	3
1.1.4 Clinical Presentation of DMD.....	7
1.1.5 Inflammation and the Immune Response in Human DMD.....	8
1.1.5.1 Inflammation and the Immune Response in Healthy Muscle....	8
1.1.5.2 Inflammation and the Immune Response in DMD.....	9
1.2 The mdx Mouse Model.....	10
1.2.1 Background to the mdx Mouse Model.....	10
1.2.2 Inflammation and the Immune Response in the mdx Model.....	10
1.2.3 Advantages and Limitations of the mdx Model.....	12
1.3 Previous Studies on Macrophages in DMD and the mdx Mouse Model.....	15
1.4 Current Therapeutic Strategies for DMD.....	22
1.4.1 Glucocorticoid Steroids.....	22
1.4.2 Genetic Therapies.....	24
1.4.2.1 Exon Skipping.....	24

14.2.2 Stop Codon Read Through Agents.....	25
1.4.2.3 Dystrophin Gene Editing.....	26
1.5 Targeting Macrophages.....	27
1.5.1 Historical Background of Macrophage Targeting.....	27
1.5.2 The Macrophage Low (MacLow) Model.....	30
1.6 Previous Findings From Our Laboratory.....	33
1.7 Hypothesis.....	35
1.8 Aims and Objectives.....	35
2. Materials and Methods.....	38
2.1 Animal Work.....	38
2.1.1 Animal Husbandry.....	38
2.1.2 Macrophage Depletion.....	39
2.1.3 Tissue Harvest.....	39
2.2 Genotyping.....	40
2.2.1 Cell Lysate Preparation.....	40
2.2.2 Genomic Analysis of mdx.....	41
2.2.2 Genomic Analysis of CD68 and tetDTA.....	43
2.3 Tissue Sectioning .....	45
2.4 Immunohistochemistry.....	45
2.4.1 Quantification of F4/80 Macrophages in Liver.....	45
2.5 Immunofluorescence.....	48
2.5.1 General Immunofluorescence Protocol.....	48
2.5.2 CD68 Staining and Analysis.....	50
2.5.3 CD206 Staining and Analysis.....	50
2.5.4 CD163 Staining and Analysis.....	51
2.5.5 IgG Staining and Analysis.....	52
2.5.6 Laminin Staining and Analysis.....	52

2.5.6.1 Quantification of the Regenerative Capacity of Muscle Fibres, Total Number of Fibres and Percentage of Regenerating Fibres.....	53
2.5.7 Collagen Staining and Analysis.....	54
2.6 Western Blot.....	55
2.6.1 Myomesin Western Blot and Analysis.....	55
2.7 Molecular Biology.....	58
2.7.1 RNA Extraction .....	58
2.7.2 DNase Treatment .....	58
2.7.3 Reverse Transcription .....	59
2.7.4. TaqMan® Real Time Quantitative PCR (qPCR).....	59
2.8 Statistical Analysis.....	60
3. The Impact of CD68+ Macrophage Depletion on Macrophage Phenotype in Muscle .....	62
3.1 Introduction.....	62
3.2 Results.....	67
3.2.1 Effect of Six Week Doxycycline Treatment on Macrophages in Liver..	67
3.2.2 Effect of Six Week Doxycycline Treatment on CD68 Positive Macrophages in Muscle.....	70
3.2.2.1 Tibialis Anterior.....	70
3.2.2.2 Quadriceps.....	72
3.2.2.3 Diaphragm.....	74
3.2.2.4 Heart.....	76
3.2.3 Effect of Six Week Doxycycline Treatment on CD206 Positive Macrophages in Muscle.....	78
3.2.2.1 Tibialis Anterior.....	78
3.2.2.2 Quadriceps.....	80
3.2.2.3 Diaphragm.....	82

3.2.2.4 Heart.....	84
3.2.4 Effect of Six Week Doxycycline Treatment on CD163 Positive Macrophages in Muscle.....	86
3.2.2.1 Tibalis Anterior.....	86
3.2.2.2 Quadriceps.....	88
3.2.2.3 Diaphragm.....	90
3.2.2.4 Heart.....	92
3.3 Discussion.....	94
4. The Impact of CD68+ Macrophage Depletion on the Level of Muscle Damage.....	98
4.1 Introduction.....	98
4.2 Results.....	101
4.2.1 Effect of Two Week Doxycycline Treatment on Muscle Fibre Damage.....	101
4.2.1.1 Tibalis Anterior.....	101
4.2.2 Effect of Six Week Doxycycline Treatment on Muscle Fibre Damage.....	104
4.2.2.1 Tibalis Anterior.....	104
4.2.2.2 Quadriceps.....	107
4.2.2.3 Diaphragm.....	109
4.2.2.4 Heart.....	111
4.2.3 Effect of Six Week Doxycycline Treatment on Myomesin Blood Serum Levels .....	114
4.3 Discussion.....	116
5. The Impact of CD68+ Macrophage Depletion on The Regenerative Capacity of Muscle.....	120
5.1 Introduction.....	120
5.2 Results.....	126

5.2.1 Effect of Two Week Doxycycline Treatment on the Regenerative Capacity of Muscle Fibres and Total Fibre Number .....	126
5.2.2 Effect of Six Week Doxycycline Treatment on the Percentage of Regenerating Muscle Fibres.....	129
5.2.2.1 Tibalis Anterior.....	129
5.2.2.2 Quadriceps.....	131
5.2.2.3 Diaphragm.....	133
5.2.3 Effect of Six Week Doxycycline Treatment on the Regenerative Capacity of Muscle Fibres and Total Fibre Number.....	135
5.2.3.1 Tibalis Anterior.....	135
5.2.3.2 Quadriceps.....	139
5.2.3.3 Diaphragm.....	142
5.2.4 Effect of Six Week Doxycycline Treatment on the Level of Fibrosis.....	145
5.2.4.1 Tibalis Anterior.....	145
5.2.4.2 Quadriceps.....	147
5.2.4.3 Diaphragm.....	149
5.2.4.4 Heart.....	151
5.2.5 Effect of Six Week Doxycycline Treatment on the Expression of Proinflammatory and Anti-inflammatory Cytokines .....	153
5.3 Discussion.....	156
6. General Discussion and Future Work.....	162
6.1 Discussion.....	162
6.2 Future Work.....	170
6.2.1. The Impact of the MacLowMD Model and CD68+ Macrophage Depletion on Cytokine Expression.....	171

6.2.2 The Impact of the MacLowMD Model and CD68+ Macrophage Depletion on Muscle Strength and Mobility.....	173
6.2.3 The Identification of Potential Druggable Targets.....	177
7. Bibliography.....	179
8. Appendices.....	199
8.1 Appendix I Complete IgG Stained Six Week Doxycycline Treated MacLowMD TA.....	199
8.2 Appendix II Complete Laminin Stained Six Week Doxycycline Treated MacLowMD TA.....	200
8.3 Appendix III Animal Work Reagents.....	201
8.4 Appendix IIII Immunohistochemistry and Immunofluorescent Antibodies and Reagents.....	202
8.5 Appendix V Western Blot Antibodies and Reagents.....	204

# List of Figures

---

Figure 1.1.1: Localisation of dystrophin and the DAPC in a healthy individual.....	2
Figure 1.1.2: Location of costameres within muscle fibres .....	3
Figure 1.1.3: Gowers manoeuvre method of standing.....	4
Figure 1.2.2: The TH1 Inflammatory Response in DMD .....	11
Figure 1.3.1: Main Cytokines Involved in the Induction of M1 and M2 macrophages. .....	17
Figure 1.3.2: Macrophage expression and properties following muscle damage in mdx mice.....	19
Figure 1.5.2: The molecular mechanism of the MacLow model.....	32
Figure 1.6.1: Doxycycline treatment results in a 50% reduction in the number of CD68+ macrophages in the MacLowMD mouse model .....	34
Figure 1.6.2: Doxycycline treatment results in a 33% reduction in the number of regenerating muscle fibres in the MacLowMD mouse model.....	35
Figure 2.2.1.1 HincII recognition site for point mutation in DMD gene.....	43
Figure 3.1.1 Changes in the balance of muscle macrophages within mdx mice.....	63
Figure 3.2.1 Effect of six week doxycycline treatment on total macrophage number in liver .....	69
Figure 3.2.2.1. Effect of six week doxycycline treatment on number of CD68+ macrophages in TA .....	71
Figure 3.2.2.2. Effect of six week doxycycline treatment on number of CD68+ macrophages in quadricep .....	73
Figure 3.2.2.3. Effect of six week doxycycline treatment on number of CD68+ macrophages in diaphragm .....	75

Figure 3.2.2.4. Effect of six week doxycycline treatment on number of CD68+ macrophages in heart.....	77
Figure 3.2.3.1. Effect of six week doxycycline treatment on number of CD206 macrophages in TA .....	79
Figure 3.2.3.2. Effect of six week doxycycline treatment on number of CD206 macrophages in quadricep .....	81
Figure 3.2.3.3. Effect of six week doxycycline treatment on number of CD206 macrophages in diaphragm .....	83
Figure 3.2.3.3. Effect of six week doxycycline treatment on number of CD206 macrophages in heart .....	85
Figure 3.2.4.1. Effect of six week doxycycline treatment on number of CD163 macrophages in TA .....	87
Figure 3.2.4.2. Effect of six week doxycycline treatment on number of CD163 macrophages in quadriceps .....	89
Figure 3.2.4.3. Effect of six week doxycycline treatment on number of CD163 macrophages in diaphragm .....	91
Figure 3.2.4.4. Effect of six week doxycycline treatment on number of CD163 macrophages in heart .....	93
Figure 4.2.1. Effect of two week doxycycline treatment on IgG staining in MacLowMD TA muscle.....	103
Figure 4.2.2.1. Effect of six week doxycycline treatment on IgG staining in MacLowMD and mdx TA muscle.....	106
Figure 4.2.2.2. Effect of six week doxycycline treatment on IgG staining in MacLowMD and mdx quadricep muscle.....	108
Figure 4.2.2.3. Effect of six week doxycycline treatment on IgG staining in MacLowMD and mdx diaphragm.....	110
Figure 4.2.2.4. Effect of six week doxycycline treatment on IgG staining in MacLowMD and mdx heart .....	112

Figure 4.2.3. Effect of six week doxycycline treatment on myomesin blood levels in MacLowMD and mdx mice .....	115
Figure 5.2.1. Effect of two week doxycycline treatment on fibre regenerative capacity and number of fibres in MacLowMD TA muscle .....	128
Figure 5.2.2.1. Effect of six week doxycycline treatment on the percentage of regenerating TA muscle fibres .....	130
Figure 5.2.2.2. Effect of six week doxycycline treatment on the percentage of regenerating quadricep muscle fibres .....	132
Figure 5.2.2.3. Effect of six week doxycycline treatment on the percentage of regenerating diaphragm muscle fibres .....	134
Figure 5.2.3.1. Effect of six week doxycycline treatment on fibre regenerative capacity and total fibre number in mdx and MacLowMD TA muscle .....	138
Figure 5.2.3.2. Effect of six week doxycycline treatment on fibre regenerative capacity and total fibre number in mdx and MacLowMD quadricep muscle .....	141
Figure 5.2.3.3. Effect of six week doxycycline treatment on fibre regenerative capacity and total fibre number in mdx and MacLowMD diaphragm muscle .....	144
Figure 5.2.4.1. Effect of six week doxycycline treatment on the percentage of fibrotic TA tissue.....	146
Figure 5.2.4.2. Effect of six week doxycycline treatment on the percentage of fibrotic quadricep tissue.....	148
Figure 5.2.4.3. Effect of six week doxycycline treatment on the percentage of fibrotic diaphragm tissue.....	150
Figure 5.2.4.4. Effect of six week doxycycline treatment on the percentage of fibrotic heart tissue.....	152
Figure 5.2.5 Effect of Six Week Doxycycline Treatment on the Expression of Proinflammatory and Anti-inflammatory Cytokines in TA and Diaphragm muscle.....	155
Figure 5.3.1. Comparison of histopathology of twelve weeks-old muscles.....	159

# List of Tables

---

Table 2.1.1: Summary of genotypes used throughout six week doxycycline treatment.....	39
Table 2.2.1.1. Details of mdx primers, amplicon size, annealing temperatures and annealing cycle numbers .....	41
Table 2.2.1.2. Details of PCR conditions for mdx genotyping .....	42
Table 2.2.2. Details of CD68 and tetDTA primers, amplicon size, annealing temperatures and annealing cycle numbers.....	44
Table 2.5.1.1. General immunofluorescence protocol used throughout study.....	49
Table 4.2.2.1 Summary of percentage of IgG stained tissue for two and six week doxycycline treatment.....	113
Table 6.1.1. Comparison of previous macrophage depletion models.....	167

# Abbreviations

---

%	Percent
6MWT	6 Minute Walk Test
AON	Antisense Oligonucleotide
BMD	Becker Muscular Dystrophy
BSA	Bovine Serum Albumin
CCL4	Chemokine Ligand 4
CCR2	Chemokine Receptor Type 2
cDNA	Complementary DNA
CK	Creative Kinase
DAB	3 3'-Diaminobenzidine
DAG1	Dystroglycan Gene
DAPC	Dystrophin-Associated Protein Complex
DAPI	4',6-diamidino-2-phenylindole
DMD	Duchenne Muscular Dystrophy
Dox	Doxycycline
DTA	Diphtheria Toxin A
DTT	Dithiothreitol
ECL	Enhanced Chemiluminescent
ECM	Extra Cellular Membrane
EGFP	Enhanced Green Fluorescent Protein
F4/80+	F4/80 Positive
GAPDH	Glyceraldehyde 3-phosphate dehydrogenase
HRP	Horseradish Peroxidase
IFN $\gamma$	Interferon Gamma
IgG	Immunoglobulin G

IL1R	Interleukin 1 receptor
IL4	Interleukin 4
IL6	Interleukin 6
IL10	Interleukin 10
IL13	Interleukin 13
iNOS	Inducible Nitric Oxide Synthase
iRES	Internal Ribosome Entry Site
JAK/ STAT	Janus Kinase/ Signal Transducers
L <sub>o</sub>	Optimal muscle length
MRC1	Mannose Receptor C Type 1
mRNA	Messenger RNA
MYOM3	Myomesin-3
NO	Nitric Oxide
nNOS	Neuronal Nitric Oxide Synthase
OCT	Optimal Cutting Temperature
rtTA	Reverse Tetracycline Transactivator
PBS	Phosphate Buffered Saline
PBST	Phosphate Buffered Saline with Tween
pCD68	Macrophage Specific Human CD68 Promoter
PCR	Polymerase Chain Reaction
SEM	Standard Error of the Mean
TA	Tibialis Anterior
TBST	Tris Buffered Saline with Tween
TG1	Transgene 1
TG2	Transgene 2
TLR4	Toll- Like Receptor 4
TNF $\alpha$	Tumour Necrosis Factor Alpha
TRE	Tetracycline Response Element

$\mu\text{m}$

Micrometre

# Chapter 1: Introduction

---

## **1.1 Duchenne Muscular Dystrophy In Human**

### **1.1.1 Duchenne Muscular Dystrophy Background**

Despite being beneficial in a healthy individual, the inflammatory immune response can be detrimental in a number of conditions, including the x-linked muscular wasting disease, Duchenne Muscular Dystrophy (DMD). Of the 60 muscular dystrophies, DMD is the most common and has recently been shown to affect up to 1 in 3600 male births worldwide, making it both the most prevalent neuromuscular disorder and the most common inherited muscle disease of childhood worldwide (Mah *et al.*, 2014).

In general, the muscular dystrophies are a group of inherited diseases that cause progressive muscle wasting and weakness (Mercuri and Muntoni, 2013). The majority of muscular dystrophies are caused by mutations in genes of the dystrophin- associated protein complex (DAPC, see Figure 1). The DAPC consists of sarcoplasmic proteins (i.e. nitric oxide synthase), transmembrane proteins (i.e.  $\beta$  dystroglycan), extracellular proteins (i.e. laminin), and the dystrophin protein. The DAPC produces a strong mechanical connection between the extracellular matrix (ECM) and the cytoskeleton (Davies and Nowak, 2006). The components of the DAPC are shown in Figure 1.1.1.

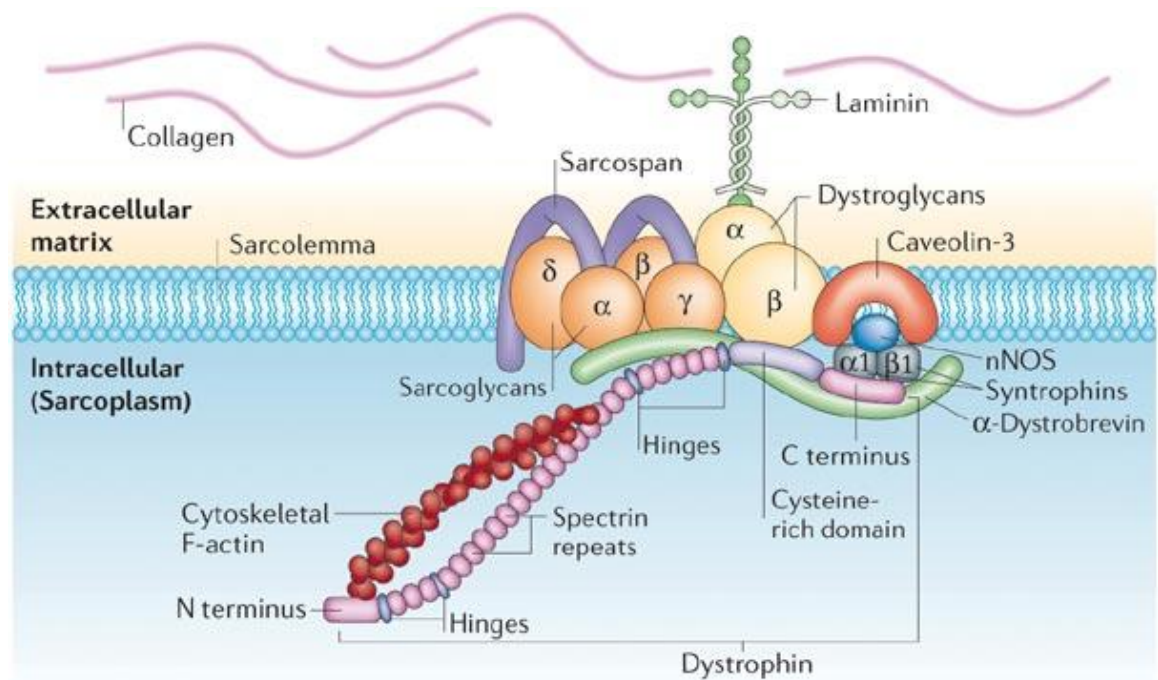


**Figure 1.1.1: Localisation of dystrophin and the DAPC in a healthy individual.** Davies and Nowak, 2006, reproduced with permission from Nature Publishing Group.

### **1.1.2 Mutations in the DMD Gene**

DMD is an X- linked recessive allelic disorder caused by nonsense and out of frame mutations in the *DMD* gene, which codes for the dystrophin protein, a key protein involved in the stabilisation of muscle. The *DMD* gene is found on the X chromosome, meaning that usually only boys are affected (Kunkel *et al.*, 1985). The *DMD* gene is the longest human gene, comprising 2.4 megabases of DNA and forming approximately 1% of chromosome X DNA (Kunkel *et al.*, 1985).

If a mutation in the DMD gene is out of frame the dystrophin protein will be lost or truncated, resulting in the severe DMD phenotype. Dystrophin immunoblotting of DMD muscles has shown a complete absence of dystrophin

in the vast majority of muscle, cardiac and diaphragm fibres (Neri *et al.*, 2007). Becker Muscular Dystrophy (BMD) is less severe than DMD. BMD occurs when a mutation in the DMD gene is in frame and results in a partially functional form of dystrophin being present in muscles.

### **1.1.3 Dystrophin**

In healthy muscle, dystrophin acts as a major scaffolding protein, linking microtubules, cytoskeleton actin and intermediate filaments to the ECM (Le Rumeur, 2015). In DMD, the lack of dystrophin results in the transmission of forces from the cytosol to the ECM being impaired at the costameres (Ayalon *et al.*, 2008), causing the plasma membrane to rupture frequently during muscle contractions (Le Rumeur, 2015). Location of costameres within muscle fibres is highlighted in Figure 1.1.2.

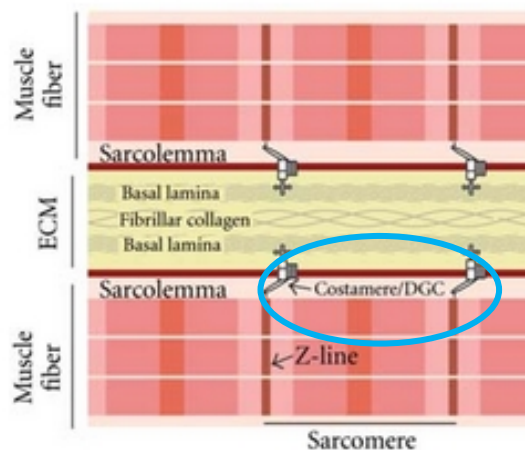


**Figure 1.1.2: Location of costameres within muscle fibres.** Gumerson and Michele, 2011, reproduced with permission from Journal of Biomedicine and Biotechnology (Gumerson and Michele, 2011).

Rupturing of the plasma membrane results in cellular components, such as creatine kinase and myomesin, leaking from the interior of muscle cells into

the bloodstream. As such, serum levels of creatine kinase are often used as a diagnostic marker for DMD, with higher than average levels usually observed in children suffering from the disease (Mariol and Ségalat, 2001). Furthermore, plasma membrane rupture allows immune cells such as macrophages, neutrophils and T cells to enter the muscle in order to clear away and repair the muscle damage. Recruitment of immune cells has been found to be initiated by expression of CXCL1 and CXCL5 chemokines (Nedachi *et al.*, 2009).

Dystrophin has also been found to have a significant role in calcium signalling. A notable pathophysiological change in DMD patients is the disruption of intracellular calcium homeostasis. Maintenance of calcium homeostasis is necessary for cell growth and function, particularly in muscle where calcium fluctuation is essential for generation of contraction and relaxation cycles (Batchelor and Winder, 2006). Skeletal muscle biopsies from DMD patients show an increased level of intracellular calcium (Bertorini *et al.*, 1982). Increased levels of intracellular calcium can contribute to muscle degeneration through abnormal activation of calcium dependant proteases, leading to muscle fibres being more susceptible to necrosis (Batchelor and Winder, 2006). DMD dystrophin deficiency results in destabilisation of the linkage between the actin cytoskeleton and the extracellular matrix component, laminin, which results in the muscle being more susceptible to micro-rupturing (Ruegg *et al.*, 2002). This, in turn, triggers a calcium dependent membrane resealing process. The influx of extracellular calcium ions initiates an event that adds plasma membrane patches to seal the disrupted muscle. Calcium

leak channels present in the newly introduced patches cause an increased influx of calcium into the cytoplasm of dystrophic fibres (Ruegg *et al.*, 2002).

Calcium is highly implicated in excitation–contraction coupling, an essential element of the signal from nerve to muscle. Included in this signal is depolarization-induced activation of the T-tubule dihydropyridine receptors (DHPRs). These receptors, through direct interaction, open the ryanodine receptors (RYRs), which enables the movement of calcium from the sarcoplasmic reticulum into the sarcoplasm (Batchelor and Winder, 2006). Muscle fibres have a negative feedback mechanism caused by uncoupling of the DHPR and RYR by increased intracellular calcium levels. Using mechanically skinned muscle fibres from control and mdx mice Plant and Lynch, 2003, demonstrated that, compared to control fibres, mdx fibres showed a quicker decrease in calcium release levels. This was suggested to be due to increased uncoupling of the DHPR and RYR that occurred in the absence of dystrophin. Although dystrophin is not present in the T-tubules where DHPR is located, the increased intracellular calcium levels and reduced sarcoplasmic reticulum calcium-buffering activity that are a result of dystrophin loss likely contribute to the increased uncoupling (Plant and Lynch, 2003). Johnson, Scheuer and Catterall, 2005, also found that loss of dystrophin in mdx mice diminished the voltage-dependence of activation of the DHPR and calcium channel activity ((Johnson, Scheuer and Catterall, 2005). These findings suggest that the absence of dystrophin could stabilise the closed state of the DHPR and could provide a mechanism for DHPR and RYR uncoupling

and the impaired excitation-contraction coupling observed in the mdx mouse and DMD.

Dunmont *et al.*, 2015, also indicated that an absence of dystrophin has a significant impact on muscle stem cells (satellite cells) polarity (Dumont *et al.*, 2015). Dystrophin is highly expressed in satellite cells, where it associates with the serine-threonine kinase Mark2, a key regulator of cell polarity. When dystrophin is lacking (such as in DMD), there is downregulated expression of Mark2 protein, leading to the inability to localise the cell polarity regulator Pard3 to the opposite side of the cell. This results in the number of asymmetric divisions being greatly reduced in dystrophin-deficient satellite cells, which also display a loss of polarity, prolonged cell divisions, impaired mitotic spindle orientation and abnormal division patterns (Dumont *et al.*, 2015). Together, these defects significantly reduce the generation of resultant muscle cells that are needed for proper muscle regeneration. Dunmont *et al.*'s findings show that dystrophin plays a vital role in the regulating satellite cell polarity and indicate that muscle wasting in DMD is exacerbated by impaired regeneration due to satellite cell dysfunction (Dumont *et al.*, 2015).

Dystrophin has also been shown to undertake a vital role as a tumour suppressor in numerous human mesenchymal cancers. Genome- single-nucleotide polymorphism (SNP) assays revealed the intragenic deletion of the dystrophin-encoding DMD gene in 96% of metastatic gastrointestinal stromal tumours (26 out of 27 patient biopsies), 100% of metastatic embryonal rhabdomyosarcoma tumours (9 out of 9 patient biopsies) and 62% of

metastatic leiomyosarcoma tumours (8 out of 13 biopsies) (Wang *et al.*, 2014b). By contrast, intragenic DMD deletions were not found in 20 benign tumour counterparts for gastrointestinal stromal tumour, rhabdomyosarcoma and leiomyosarcoma, indicating that dystrophin absence is a mechanism by which myogenic tumours progress to lethal, high-grade sarcomas (Wang *et al.*, 2014b).

#### **1.1.4 Clinical Presentation of DMD**

DMD is characterised by progressive muscle weakness and wasting, which occur due to the lack of dystrophin (Falzarano *et al.*, 2015). The clinical signs of DMD are not present at birth and remain uncharacterised until around the age of 3 years old, when patients first exhibit the early symptoms of muscle weakness (Wu *et al.*, 2014), namely the use of the Gowers manoeuvre method of standing (Kang, 2013). The Gowers manoeuvre is used by individuals with a weakness in leg muscles, such as DMD patients, and involves patients using their hands to 'walk' their body from a squatting position (Chang and Mubarak, 2012) (Figure 1.1.3).

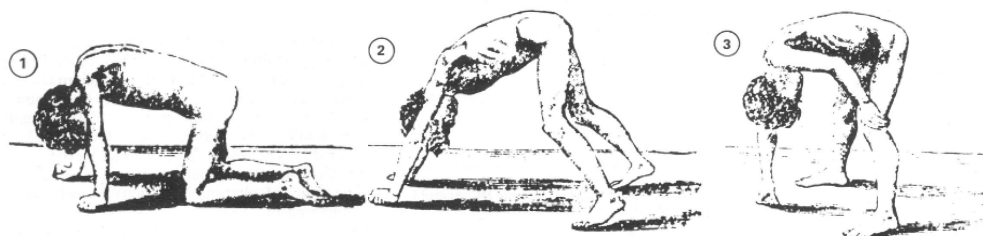


**Figure 1.1.3: Gowers manoeuvre method of standing** (Wallace and Newton, 1989). Reproduced with permission from BMJ Publishing Group Ltd.

Falling over, struggling to run, weakness and a delay in the achievement of motor milestones are also exhibited in the early stages of DMD (Chung *et al.*,

2015). The disease then progresses rapidly, with loss of ambulation occurring in the early teens, and the use of a wheelchair becoming a necessity (Wu *et al.*, 2014). Continuous cycles of muscle degeneration and repair occur throughout life and leads to muscle tissue being replaced by fat and collagen. During the later stages of DMD, fibrosis occurs. Fibrosis is characterised by progressive collagen deposition in the muscle.

Sufferers of DMD develop severe cardiomyopathy and respiratory problems due to degeneration of heart and diaphragm muscles respectively (Falzarano *et al.*, 2015). The average age of death of DMD patients is in the mid- 20s and occurs due to cardiac and respiratory failure (Wu *et al.*, 2014).

The lifespan of DMD patients has steadily increased over recent years due to the use of artificial respirators (Passamano *et al.*, 2012). Furthermore, since the 1990s, ambulation has been prolonged due to the use of glucocorticoid steroids, which target the inflammatory response and promote muscle growth (Wu *et al.*, 2014). Despite this, there is currently still no cure for DMD.

### **1.1.5 Inflammation and the Immune Response in Human DMD**

#### **1.1.5.1 Inflammation and the Immune Response in Healthy Muscle**

In healthy muscle, inflammation is the cellular response to damage and injury, and is necessary for functional regeneration (Chazaud, 2015).

Upon muscle damage, an inflammatory response occurs; this response involves a series of distinct phases, beginning with the infiltration of immune

cells into the site of injury and the release of pro-inflammatory factors, followed by the resolution of inflammation and muscle repair and regeneration.

Immune cells known to infiltrate damaged muscle include neutrophils, mast cells, regulatory T cells and B and T lymphocytes. However, macrophages are the predominant immune cell present throughout the inflammatory response to muscle damage. Following damage or injury, macrophages infiltrate damaged muscle and phagocytose debris. They then change to an anti-inflammatory phenotype and are involved in the repair of muscle.

#### 1.1.5.2 Inflammation and the Immune Response in DMD

The inflammatory immune response in healthy individuals is essential for repair and regeneration of muscle. However, in DMD, due to the loss of the dystrophin protein, muscles of patients are extremely weak and prone to contraction-induced damage. This results in continuous cycles of muscle damage, inflammation, and repair, which leads to muscle regenerative capacity being exhausted, and acts as a moderator of muscle pathology, degeneration and necrosis (Nedachi *et al.*, 2009). Nedachi *et al.*, 2009, compared blood from 24 DMD patients with healthy age matched controls. Levels of Fas receptor, FasL ligand and Bax/Bcl-2 were measured as markers of apoptosis. The growth factor vascular endothelial growth factor (VEGF) was measured as markers of regeneration. RT-PCR indicated that DMD patients showed significantly increased expression of Fas, FasL and Bax compared to healthy controls. Expression of Bcl-2 and VEGF was found to be significantly decreased (Nedachi *et al.*, 2009).

Continuous damage of DMD muscle results in an over-accumulation of immune cells, predominately macrophages, and causes additional inflammation (Rosenberg *et al.*, 2015). This results in further damage of the already damaged muscle.

In order to study DMD, as well as the role of the immune response in DMD, in greater detail, a number of models are widely used.

## **1.2 The mdx Mouse Model**

### **1.2.1 Background to the mdx Mouse Model**

The mdx mouse model is the most researched model of DMD. The model arose due to a spontaneous mutation causing a premature stop codon in exon 23 of the dystrophin gene (Bulfield *et al.*, 1984). This means that mdx mice produce a small, non-functional form of the dystrophin protein. Since its discovery in 1984 the mdx mouse model has been used extensively to study the pathophysiology of DMD.

### **1.2.2 Inflammation and the Immune Response in the mdx Model**

The initial inflammatory response in the mdx mouse had been characterised as the TH1 inflammatory response, which is detailed in Figure 1.2.2. This TH1 inflammatory response is mirrored in DMD patients.

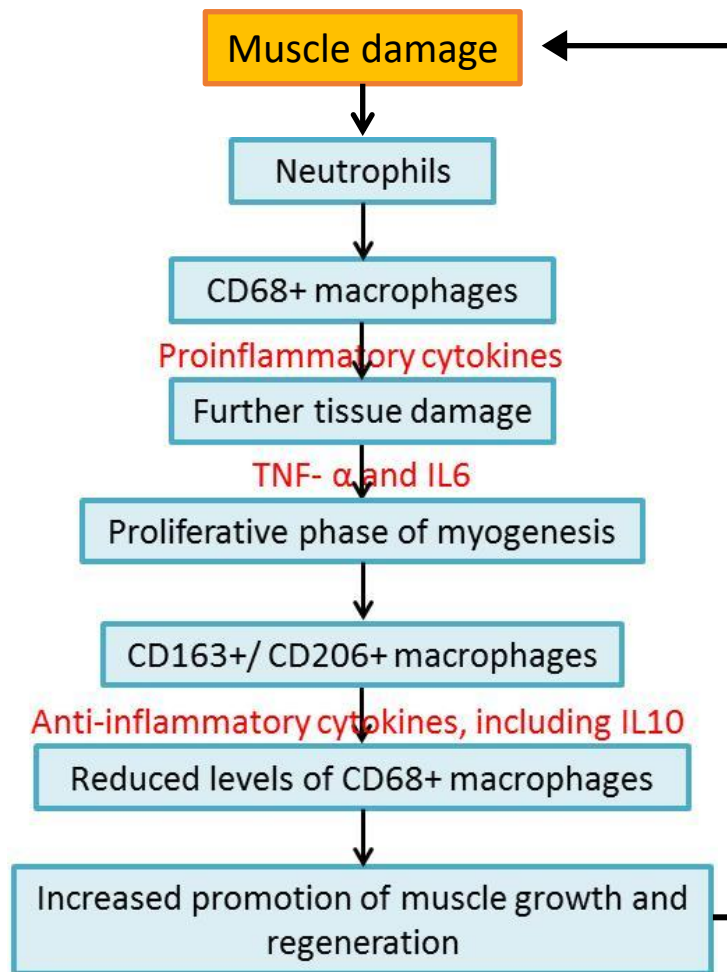


**Figure 1.2.2: The TH1 Inflammatory Response in DMD.** (Tidball and Villalta, 2010).

Following contraction induced muscle damage in mdx mice, the TH1 inflammatory response is dominated by neutrophils, followed by CD68+ 'M1' macrophages. CD68+ macrophages propagate the inflammatory response by the release of proinflammatory cytokines (Tidball and Villalta, 2010). Further tissue damage occurs, and mechanisms mediated by TNF $\alpha$  and IL6 stimulate the proliferative phase of myogenesis in myeloid cells. CD163+/CD206+ 'M2' macrophages subsequently invade the muscle, and release anti-inflammatory cytokines such as IL10, which cause the levels of CD68+ macrophages to be

reduced (Tidball and Villalta, 2010). This leads to a promotion of muscle growth and regeneration (Tidball and Villalta, 2010).

Genetic and pharmacological inhibition of inflammatory markers (i.e. Interferon Gamma (IFN $\gamma$ )) has been shown to reduce the severity of muscle pathology in the mdx mouse model of DMD (Villalta *et al.*, 2011a). The accumulation of inflammatory cytokines in the muscles of mdx mice and DMD patients is evidence that the immune system plays a key role in the pathogenesis of DMD.

### **1.2.3 Advantages and Limitations of the mdx Model**

Whilst there are many advantages of using the mdx as a mouse model of DMD, there are a number of limitations that are important to consider.

Importantly for this study, as previously detailed in Chapter 1.3.2, the inflammatory response in the mdx mouse mirrors that of human. Changes in pro-inflammatory cytokines (including TNF $\alpha$  and IL6 (Abdel-Salam, Abdel-Meguid and Korraa, 2009)) are detected early in mdx mice, and the inflammatory response becomes more severe as the disease progresses (Messina *et al.*, 2011). Chronic inflammation is also seen in the muscles of mdx mice (Grounds *et al.*, 2008).

Whilst the mdx mouse is genetically comparable to the human form of DMD, the phenotypical changes in some muscles differ to greater extents between mdx and human.

As previously mentioned, skeletal muscles of DMD patients are very weak and prone to contraction-induced damage, resulting in continuous cycles of muscle damage, inflammation, and repair and eventual necrosis. mdx skeletal muscle also exhibits cycles of damage, regeneration and repair starting from the age of two weeks old, although the extent of skeletal muscle degeneration is somewhat less (Grounds *et al.*, 2008). However, unlike in the human form of DMD, dystrophic mouse skeletal muscles do not display a comparable degree of fibrosis (Coulton *et al.*, 1988). Furthermore, the loss of function in limb muscles is markedly less in mdx mice than the human form of DMD (Coulton *et al.*, 1988).

The pathology of mdx diaphragm more closely resembles that of the human form of DMD. Extensive areas of fibrotic tissue are seen in the diaphragm of mdx mice from the age of twelve weeks (Gosselin and Williams, 2006). Although not as severe as human DMD, fibrosis continues to develop in mdx diaphragm until death (Huang *et al.*, 2009).

Previous studies have also shown widespread presence of revertant fibres in muscles of mdx mice. Revertant fibres is a term for muscle fibres that are positive for dystrophin expression. A study by Pigozzo *et al.* in 2013 demonstrated that in TA muscle from 8 week old mice, an average of 1.96% of fibres were revertant fibres. This increased to 3.39% in 26 week old mice. A similar percentage, of revertant fibres, as well as an increase in percentage with age, was found throughout all other mdx muscles (Pigozzo *et al.*, 2013).

Furthermore, degeneration appears to resolve itself in the mdx mouse (Partridge, 2013). This is highly contrasting with human DMD.

The effects of lack of dystrophin on cardiac muscle in mdx mice is highly comparable to that in the human form of DMD. Both forms display cardiac fibrosis as well as arrhythmias and conduction irregularities due to lack of dystrophin protein. Similarly, both mdx and human irregularities progress throughout the course of the disease (Romfh and McNally, 2010).

One of the main differences between the mdx mouse and human form of DMD is the presence of utrophin. Utrophin is an autosomal analog of dystrophin, with an 80% similarity between the two proteins (Kleopa *et al.*, 2006). In healthy individuals, where dystrophin is expressed, utrophin is downregulated. However, when dystrophin is absent, utrophin is able to compensate for dystrophin's stabilising function and preserve the function of muscles. In mdx mice, utrophin upregulation restores the integrity of plasma membranes and spares some level of muscle degeneration (Gilbert *et al.*, 1999). However, although utrophin is upregulated in human DMD, levels are insufficient to prevent the progression of disease (Love *et al.*, 1989). As a result, not only is the level of muscle degeneration less in mdx mice than humans with DMD, but whilst mdx mice die somewhat younger than healthy mice, this is to a substantially lesser extent than human patients with DMD and more closely resembles a normal lifespan.

### **1.3 Previous Studies on Macrophages in DMD and the mdx Mouse Model**

Macrophages are a plastic population and have the potential to exist in two separate subsets: 1) Classically activated or M1 macrophages, which are pro-inflammatory and polarized by TH1 cytokines; and 2) alternatively activated or M2 macrophages, which are anti-inflammatory and immunoregulatory and polarized by TH2 cytokines (Shapouri-Moghaddam *et al.*, 2018). In health, M2 macrophages maintain homeostasis by aiding the repair and replacement of lost or damaged cells. Macrophages also form part of the host defence against pathogens due to their unique plasticity from their M2 (repair) phenotype to an M1 (proinflammatory) phenotype (Mills, Lenz and Ley, 2015). In disease, over expression of M2 macrophages contributes to chronic infections, fibrosis, allergy, and cancer (Mills, Lenz and Ley, 2015). Tumour-associated macrophages (TAMs) are the major infiltrating cells of tumour micro-environment and a major link between inflammation and cancer (Belgiovine *et al.*, 2016). TAMs generally display an M2-like phenotype. They produce growth factors for cancer cells and have an immuno-suppressive activity (Belgiovine *et al.*, 2016). Conversely, M1 macrophage- dominant activity is greatly implicated in atherosclerosis, chronic inflammatory conditions and autoimmunity (Mills, Lenz and Ley, 2015). Macrophages are major player in the pathogenesis of many chronic inflammatory and autoimmune diseases including Rheumatoid Arthritis (RA), Multiple Sclerosis (MS), Crohn's disease, and Inflammatory Bowel Disease (IBD) (Wynn, Chawla and Pollard, 2013). In these diseases, M1 macrophages are an important source of many of the inflammatory cytokines including TNF- $\alpha$ , IL-1 $\beta$  and IL-

23 that have been identified as mediators and drivers of these conditions (Udalova, Mantovani and Feldmann, 2016), (Cuda, Pope and Perlman, 2016).

As previously stated in Section 1.1.5.2, macrophages are the predominant cell type involved in the inflammatory response to muscle damage. A 2001 study by Wehling *et al.* showed that the ablation of muscle macrophages from mdx mice through repeated intraperitoneal injections of anti-F4/80 antibodies, resulted in a 75% reduction in muscle cell necrosis being observed with immunofluorescent staining, indicating a primary role for macrophages in DMD pathogenesis (Wehling, Spencer and Tidball, 2001).

In muscle, macrophages are a phenotypically variable population, capable of promoting both tissue injury and repair. Classically activated M1 macrophages participate in the TH1 immune response and are induced by proinflammatory cytokines (Figure 1.3.1). On the other hand, M2 macrophages participate in the TH2 immune response and have the potential to encourage tissue repair. M2 macrophages comprise three different subpopulations a - c, each of which are activated by different cytokines (Figure 1.3.1).

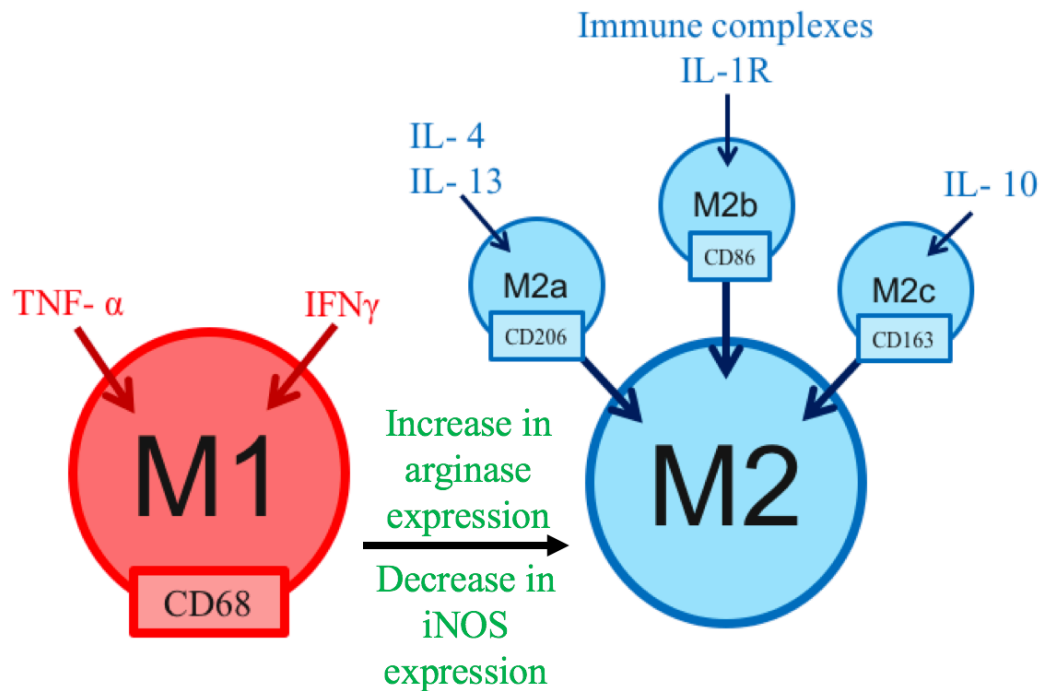


**Figure 1.3.1: Main Cytokines Involved in the Induction of M1 and M2 macrophages.** M1 macrophages are induced by TNF $\alpha$  and IFN $\gamma$ , M2a by IL4 and IL13, M2b by immune complexes, toll like receptor ligands (Röszer, 2015) and IL1R ((Martinez and Gordon, 2014) and M2c by IL10 (Villalta *et al.*, 2009).

In DMD, monocytes are the first cell to invade damaged muscle. They then progress to M1 macrophages, expressing the cell surface marker CD68. Later invading macrophages express the CD206 and CD163 marker. CD206 is a marker of the M2a phenotype and CD163 is a marker of the M2c phenotype. These later invading M2 macrophages are responsible for promoting muscle regeneration.

Macrophages shift from an M1 to an M2 phenotype through an increase in the expression of arginase by macrophages, accompanied by a decrease in the expression of inducible nitric oxide synthase (iNOS).

A 2009 study by Villalta *et al.* has shown that macrophages shift from an M1 to an M2 phenotype with age in dystrophin deficient muscle of mdx mice. At four weeks of age (the age of initial macrophage involvement in muscle necrosis, as well as stage of highest muscle necrosis) immunofluorescent staining of mdx muscle showed high levels of proinflammatory M1 macrophages, expressing CD68. After the age of four weeks, ongoing cycles of muscle damage and repair occur until the age of twelve weeks. Macrophages begin to shift to the M2 phenotype, as seen by an increase in the expression of the CD163 marker. By the age of twelve weeks, real time PCR results show a major increase in the number of CD163 expressing M2c macrophages, accompanying the shift towards peak muscle regeneration. This shift from an M1 to M2 macrophage phenotype in mdx mice is also observed in DMD patients during muscle regeneration.

The expression of macrophage phenotype, cytokines and macrophage markers and their impact on DMD pathology following muscle damage is detailed in Figure 1.3.2.

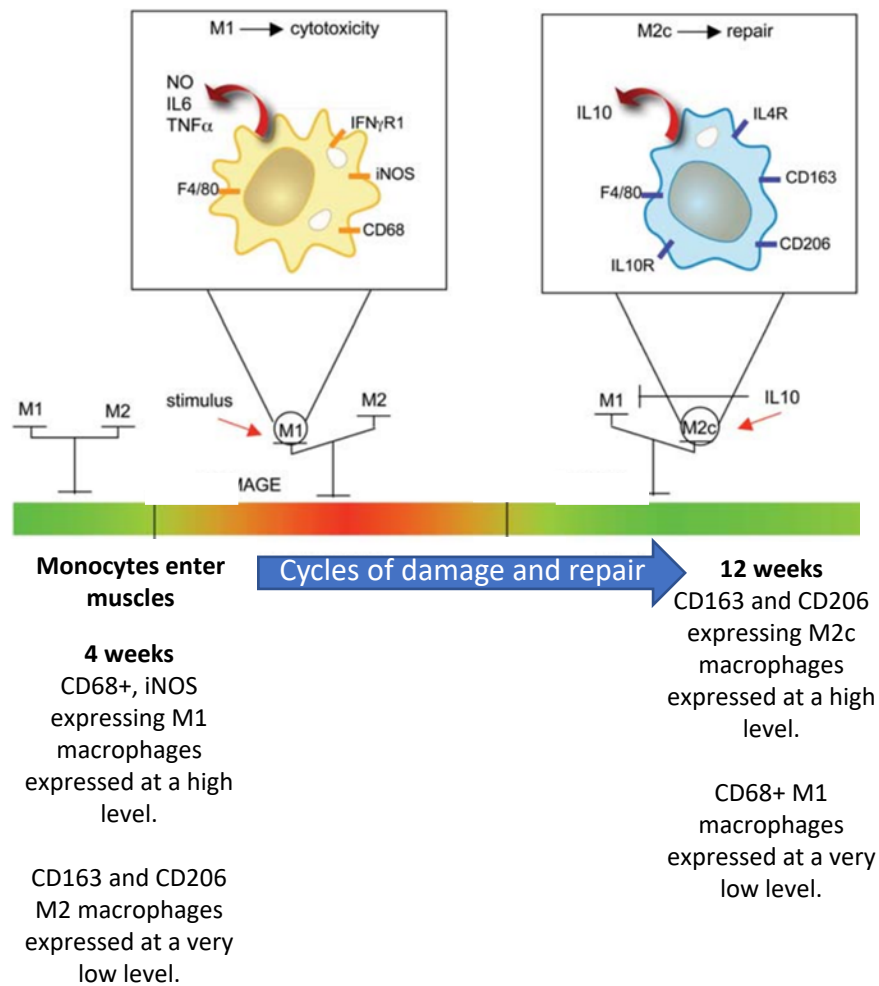


**Figure 1.3.2: Macrophage expression and properties following muscle damage in mdx mice.** Following muscle damage, macrophages become involved in muscle, and the acute phase of muscle necrosis occurs, with CD68+, iNOS expressing M1 macrophages being expressed at a substantially greater level than M2 macrophages. M1 macrophages are activated by TNF $\alpha$  and IFN $\gamma$ . Cycles of muscle damage and repair then begin, and muscle shifts to the peak regenerative phase at the age of twelve weeks, with an accompanying increase in the expression of CD163 and CD206, markers of M2c macrophages. M2c macrophages are activated by IL10. A reduction in the number of M1 macrophages and levels of iNOS are also observed. Villalta *et al.*, 2011b, reproduced with permission from Oxford University Press.

As previously mentioned, a number of cytokines drive the immune response of DMD, including proinflammatory cytokines such as TNF $\alpha$  and IFN $\gamma$ , as well as IL4, IL6 and IL1Ra, which are involved in the anti-inflammatory response.

These cytokines include IL-10, which is imperative for M2c macrophage activation.

A study by Villalta *et al.*, in 2011, provided a greater understanding of the role of IL-10 and immunity in DMD. The group used IL-10 deficient mice and observed influx of Procion orange dye as an indicator of membrane damage, and showed that muscle membrane damage was increased, indicating that IL-10 reduces the disease pathology in dystrophin deficient mice (Villalta *et al.*, 2011b). Furthermore, the group isolated macrophages from mdx mice and stimulated them with IL10. The expression of CD163 and CD206 was increased, indicating that IL-10 was able to modulate the activation of M2c macrophages. Results also showed that IL-10 was capable of deactivating the M1 phenotype and allowing progression to the M2 macrophage phenotype in mdx muscle macrophages. IL10 was found to be specifically inhibiting the expression of iNOS by M1 macrophages, seen through the isolation and treatment of mdx muscle macrophages with IL-10. This implies a specialised strategy for IL-10 to reduce mdx muscle pathology during the early acute stage of DMD (Villalta *et al.*, 2011b).

IL-10 was also found to play a role in the induction of CD163 expression and the activation of M2c macrophages in mdx muscles, suggesting IL-10 also influences the balance between the M1 and M2c macrophage phenotypes (Villalta *et al.*, 2011b). Villalta *et al.* showed that ablation of IL-10 signalling in mdx mice resulted in the shift in macrophage phenotype from M1 to M2c being prevented (Villalta *et al.*, 2011b). Due to the repair and regeneration

characteristics associated with the M2 macrophages, it is suggested that the IL-10 mediated shift in macrophage phenotype may contribute to the process of regeneration that occurs in mdx muscle following the acute phase of disease pathology (Villalta *et al.*, 2011b).

Investigations have found that dystrophin deficiency results in epigenetic silencing of the gene that encodes Klotho. Klotho is a transmembrane protein that is expressed at highest levels in kidney, skin and brain, as well as also being expressed at low levels in skeletal muscle (Kuro-O, *et al.*, 1997). Reduced expression of Klotho in healthy, non dystrophic muscles has been found to reduce muscle strength and mass (Wehling-Henricks, *et al.*, 2016).

Silencing of Klotho in dystrophic muscles has been shown to contribute to several, major components of the dystrophic pathology. Expression of a Klotho transgene in 6 month old *mdx* mice resulted in reduced muscle loss, reduced muscle fibrosis and increased the numbers of muscle-resident stem cells required for muscle regeneration (Wehling-Henricks, *et al.*, 2016). Wehling-Henricks, *et al.*, 2016, show that expression of Klotho in mdx mice significantly reduces at the stage of peak muscle degeneration and extensive inflammation when mice are approximately 4 weeks old (Wehling-Henricks, *et al.*, 2016). This suggests that inflammatory mediators may play a role in Klotho down-regulation in dystrophic muscle.

A 2018 study by Wehling-Henricks, *et al.*, found that the onset of muscle inflammation, and stage of lowest Klotho expression, in the *mdx* mouse model

coincided with large increases in expression of pro-inflammatory cytokines including TNF $\alpha$  and IFN $\gamma$ , accompanied by dramatic reductions Klotho in both muscle cells and pro-regenerative, CD206+ macrophages (Wehling-Henricks, *et al.*, 2018). Wehling- Henricks, *et al.*, also found that Klotho also acted directly on macrophages, stimulating their secretion of TNF $\alpha$  (Wehling-Henricks, *et al.*, 2018).

To summarise, macrophages play a substantial role in the progression of DMD. Monocytes first invade damaged muscle before advancing to Pro-inflammatory M1, CD68+ macrophages. The expression of certain cytokines, including IL10, then drive macrophages towards an anti- inflammatory M2 repair phenotype, and an accompanying regeneration of muscle is seen. Currently, there is a lack of understanding of why regeneration peaks at the age of 12 weeks, and why extent of subsequent degeneration is limited. It is possible that, as a major step in muscle regeneration is the remodelling and reorganizing of muscle ECM and DAPC, the presence of utrophin is sufficient to stabilise this complex, and as such reduce levels of intracellular calcium levels leading to a halt in muscle degeneration.

## **1.4 Current Therapeutic Strategies for DMD**

### **1.4.1 Glucocorticoid Steroids**

Currently, there is no cure for DMD, however, the role of inflammation in disease progression has been therapeutically targeted, with anti- inflammatory glucocorticoid steroids being the main treatment used. These drugs are used for their immunosuppressant properties and have been shown to prolong

ambulation, increase muscle mass and improve muscle strength in DMD through stimulation of insulin like growth factors.

The success of immunosuppressants has been attributed to their ability to decrease the expression of molecules that assist in extravasation and trafficking of inflammatory cells into tissues (Burzyn *et al.*, 2013).

One of the most common glucocorticoid steroids, prednisone, has been shown to decrease the levels of macrophages in dystrophic muscle and produce a reduction in the lysis of muscle membranes in patients (Wehling-Henricks, Lee and Tidball, 2004). This further supports the theory that the beneficial effects of glucocorticoids lie in their anti-inflammatory properties.

Despite the benefits of the use of glucocorticoids, long-term use results in a number of detrimental side effects. These include substantial weight gain, cushingoid (puffiness) appearance, increased susceptibility to infection and inhibition of bone formation (Angelini and Peterle, 2012).

Glucocorticoids target the early signs of DMD, with little focus on the later stages. Therefore, whilst skeletal muscle function is improved, fibrosis remains, as does degeneration of diaphragm and cardiac muscle seen in later stages of disease. However, it is now widely accepted that the treatment of DMD may require more than one approach, with a number of therapies currently in development, including genetic therapies and therapies targeting muscle repair and growth, to be used alongside glucocorticoids. An ideal

therapy would target both the underlying molecular causes and the damaging immune response in not only skeletal muscle but also in heart and diaphragm muscle as well.

## **1.4.2 Genetic Therapies**

### **1.4.2.1 Exon Skipping**

Exon skipping involves the use of synthetic antisense oligonucleotide (AON) sequences to skip specific exons in *DMD* gene mutations. The aim of this strategy is to change DMD to a milder BMD phenotype (Yin *et al.*, 2010). DMD and BMD occur as a result of different mutations in the *DMD* gene, with mutations in BMD being in-frame and DMD being out of frame. In-frame mutations result in smaller truncated dystrophin proteins being present. Depending on the location of the exon, this can result in varying degrees of muscle improvement. Symptoms of BMD are much less severe than DMD and patients have a significantly longer life (Wein, Alfano and Flanigan, 2015).

Diverse chemical backbones, including peptide nucleic acids, are used to transfer synthesised AONs into the cell. Specific exons are skipped during pre-messenger RNA splicing of the *DMD* gene. This causes the reading frame to be restored, and an internally truncated protein to be produced (Malerba, Boldrin and Dickson, 2011). 83% of patients with DMD have the potential for treatment using exon skipping (Malerba, Boldrin and Dickson, 2011).

Drisapersen is an exon skipping drug designed to skip exon 51 (Malerba, Boldrin and Dickson, 2011).<sup>12</sup> DMD patients receiving weekly doses of

Drisapersen as part of a phase II clinical trial showed an improvement in a 6 minute walk test (6MWT) as well as an increase in dystrophin in all muscles (Goemans *et al.*, 2011). A subsequent phase III clinical trial involving 186 DMD patients found no significant improvement in the 6MWT. However, a subset of 80 boys with baseline 6MWT of 300- 400 metres and the ability to stand up off the floor before treatment made a significant improvement in their 6MWT (Goemans *et al.*, 2018) following 48 weeks of Drisapersen treatment. This suggests that Drisapersen may be effective when used in severely affected patients.

The limitations of exon skipping include low cellular uptake, requirement of frequent admissions due to fast clearance from the circulatory system to ensure therapeutic targets are reached and poor efficiency in diaphragm and cardiac muscles (Yu *et al.*, 2015).

#### 1.4.2.2 Stop Codon Read- Through Agents

Premature stop codons account for 10- 15% of *DMD* mutations (Cirak *et al.*, 2012). They are nucleic triplets within mRNA that result in the dissociation of ribosomal subunits and the terminations of protein translation. Nonsense suppression therapy induces read- through of premature stop codons by binding to the ribosomes and preventing recognition of stop signals. This allows a full- length dystrophin protein to be generated (Malik *et al.*, 2010a).

Genamicin, a nonsense suppression agent, has been shown to induce higher expression of dystrophin and increase resistance to contraction induced

damage in mdx mice (Malik *et al.*, 2010a). However, in human trials, whilst a significant reduction in serum creatine kinase levels and increase in dystrophin expression were seen, there was no improvement in timed function tests. (Malik *et al.*, 2010b). Ataluren, a small molecule read-through agent, has been shown to result in clinically significant improvement in the 6MWT distance of 174 DMD patients in a double-blind placebo-controlled phase IIB study. However, a number of side effects including vomiting and dizziness were reported in 10% of patients (Namgoong and Bertoni, 2016).

#### 1.4.2.3 Dystrophin Gene Editing

Recently, CRISPR/Cas9 systems have been used for efficient *DMD* gene editing. CRISPR/Cas9, delivered using adeno-associated viral vectors, has allowed functional recovery in mdx mice, as well as reversal of dystrophic changes, including muscle damage, in skeletal and cardiac muscle fibres (El Refaey *et al.*, 2017).

The deltaE50-MD dog model of DMD possesses a mutation in a region of the canine gene that corresponds to a mutational “hot spot” in the human DMD gene. A recent study by Amoasii *et al.*, 2018, used adeno-associated viruses to systemically deliver CRISPR gene editing components to four dogs. On average, six weeks post-delivery, dystrophin was restored to levels, 90% of normal, depending on muscle type. In cardiac muscle, dystrophin levels reached 92% of normal and diaphragm 58% of normal (Amoasii *et al.*, 2018).

As yet, there have been no human clinical trials using CRISPR/Cas9 systems.

## 1.5 Targeting Macrophages

### 1.5.1 Historical Background of Macrophage Targeting

There have been numerous attempts to study the impact of macrophage depletion using a variety of methods. These include liposome assisted delivery of clodronate (Van Rooijen and Sanders, 1994), use of transgenic models to express the diphtheria toxin receptor (Duffield *et al.*, 2005) and the use of transgenic models to induce apoptosis via Fas based suicide genes (Burnett *et al.*, 2004).

Van Rooijen and Sanders (1994), used liposome assisted delivery of clodronate as a method of inducing macrophage suicide to specifically target phagocytic cells of the mononuclear phagocyte system. The phagocytic cells of the mononuclear phagocyte system were specifically targeted as phagocytosis is the natural fate of lymphocytes. The macrophages ingest the clodronate- carrying liposomes, and the phospholipid bilayers of the liposomes are disrupted, resulting in clodronate being released intracellularly, thus killing the macrophages (Van Rooijen and Sanders, 1994). A 2016 study by Kawanishi *et al.* also used clodronate to deplete macrophages (Kawanishi *et al.*, 2016). They found that macrophage depletion by clodronate liposome injection led to a significant reduction in the number of muscle fibres stained positive following anti IgG antibody staining after exhaustive exercise in male C57BL/6J mice. Presence of IgG in the muscle fibre cytosol indicates the presence of muscle membrane lesions, signifying muscle fibre damage. Clodronate is delivered and released into phagocytic macrophages using liposome vehicles (Summan *et al.*, 2006). Clodronate accumulates

intracellularly and irreversibly damages the cell causing the macrophage to die by apoptosis. This mechanism allows clodronate liposome mediated depletion of macrophages, as identified by histological analysis using pan-macrophage marker, F4/80. A 2017 study by Lui *et al.* also found that macrophage depletion via clodronate injection resulted in muscle regeneration being impaired. Macrophage depletion was induced in C57BL/6 male mice through intraperitoneal injections of clodronate-containing liposomes. Muscle injury was stimulated by skeletal muscle contusion. Lui *et al.* found that the size of regenerating muscle fibres in mice treated with clodronate-containing liposomes was significantly smaller 14 days after muscle injury than control mice lacking macrophage depletion, indicating impaired muscle regeneration (Liu *et al.*, 2017).

Duffield *et al.*, 2005, developed transgenic models to express the diphtheria toxin receptor and induce macrophage depletion by injection of diphtheria toxin. However, as this model required injection of diphtheria toxin to induce macrophage depletion, it had limited longevity without repeat administration of diphtheria toxin.

Burnett *et al.*, 2004 created transgenic mice expressing an inducible suicide gene which allowed the systemic and reversible elimination of macrophages. A drug-inducible suicide gene was expressed in transgenic mice that lead to Fas-mediated apoptosis of 70- 95% of macrophages in the vast majority of tissues. However, transgenic mice displayed numerous abnormalities and animals were unable to survive for more than 7 days post treatment.

A number of previous studies have indicated that macrophage depletion results in an improved DMD disease pathology.

A 2001 study by Wehling *et al.* showed that the ablation of muscle macrophages from mdx mice through repeated intraperitoneal injections of anti-F4/80 antibodies resulted in a 75% reduction of muscle cell necrosis observed through immunofluorescent staining (Wehling, Spencer and Tidball, 2001).

Mojumdar *et al.*, 2014, genetically and pharmacologically (using CCR2-inhibiting 'fusokine' molecule) ablated CC cytokine receptor 2 (CCR2). CCR2 is critically involved in macrophage recruitment. CCR2 depletion resulted in a reduction in macrophage accumulation in dystrophic diaphragms. CCR2 depletion by Mojumdar *et al.* improved DMD disease pathology (reduced central nucleation, increased regenerating fibre size) as well as increasing the force-generating capacity of the diaphragm (Mojumdar *et al.*, 2014).

A subsequent study by Giordano *et al.* (2015) genetically ablated toll like receptor 4 (TLR4). TLR4 is a pattern recognition receptor that is able to recognise and respond to molecules associated tissue inflammation. Genetic ablation of TLR4 resulted in an alleviation of DMD progression, with a significant reduction in the expression of pro-inflammatory genes, as well as a reduction in macrophage infiltration being exhibited. Muscle macrophages

were also found to shift to a more anti-inflammatory phenotype (Giordano *et al.*, 2015).

In 2014 Wang *et al.* used transgenic mice expressing the CD11b-diphtheria toxin receptor to transiently deplete macrophages before and after cardiotoxin induced muscle injury. Macrophage depletion resulted in smaller regenerating fibres compared to control mice, signifying impaired/ delayed regeneration. Fat accumulation was also increased, which is an indicator of irregular muscle regeneration (Wang *et al.*, 2014a).

Unfortunately, the previous methodologies used to induce macrophage ablation described were hindered by issues with specificity, durability and poor health, including lymphadenopathy and thymic atrophy (Burnett *et al.*, 2004).

To overcome the problems with durability and specificity seen in previous studies the MacLow model was developed by our group to directly and inducibly deplete CD68+ macrophages (Gheryani *et al.*, 2013).

### **1.5.2 The Macrophage Low (MacLow) Model**

The MacLow model is a novel transgenic mouse model generated in our laboratory that allows the inducible depletion of macrophages by treatment with doxycycline.

The MacLow model consists of two transgenes. The first transgene comprises of the reverse tetracycline transactivator (rtTA), under the control of the

macrophage specific human CD68 promoter (PCD68) (Gheryani *et al.*, 2013). It also contains an internal ribosome entry site (IRES), which drives expression of enhanced green fluorescent protein (EGFP), which acts as a marker for expression of the transgene. The second transgene contains the diphtheria toxin A gene (DTA) downstream of a tetracycline response element (TRE) (Gheryani *et al.*, 2013a).

A schematic of the molecular mechanism of the MacLow model is shown in Figure 1.5.2.

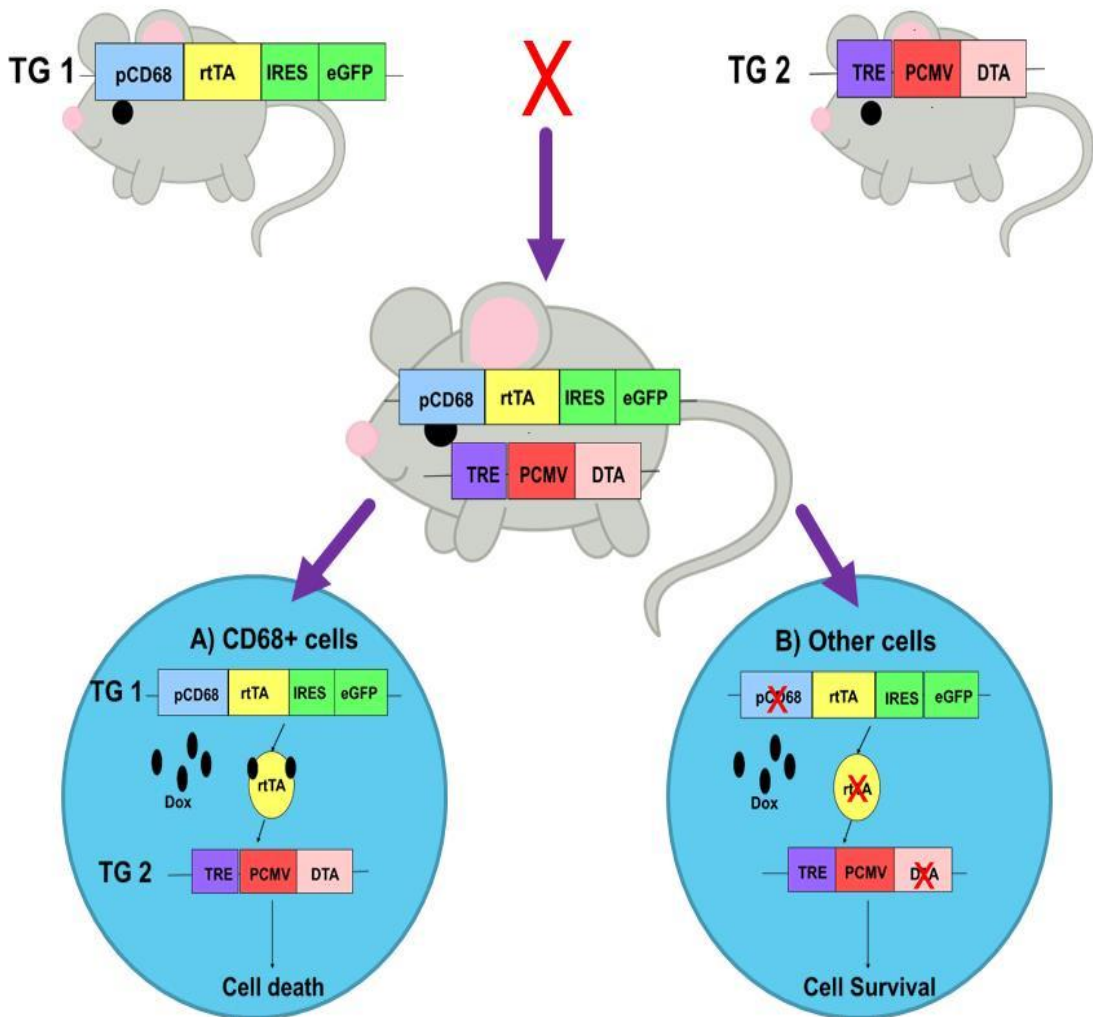


**Figure 1.5.2: The molecular mechanism of the MacLow model.** Double transgenic mice were generated by crossing the two transgenic lines TG1 and TG2. Transgene 1 (TG1) contains the CD68 promoter upstream of reverse tetracycline transactivator (rtTA), internal ribosome entry site (IRES) and enhanced green fluorescent protein (eGFP). A) In CD68+ cells, doxycycline binds to rtTA the two then bind to the tetracycline response element (TRE) on the second transgene (TG2). This leads to the expression of diphtheria toxin A gene (DTA) which results in cell death. B) In all other cells, the CD68 promoter is not active and transgene 1 is not expressed, as such, cells survive even in the presence of both transgenes and doxycycline (Gheryani *et al.*, 2013).

Gheryani *et al.* found that 2-6 weeks of doxycycline treatment in adult animals resulted in a significant 50% reduction in CD68+ cells in liver, spleen and bone. Additionally, remaining macrophages were found to be smaller and functionally impaired (Gheryani *et al.*, 2013). It is important to note that, unlike previous models, no other detrimental health effects were reported despite the large decrease in macrophage number (Gheryani *et al.*, 2013).

## 1.6 Previous Findings from Our Laboratory

To determine the effect of depleting CD68 positive macrophages on the progression of muscular dystrophy the MacLow mouse was crossed with the mdx mouse model of DMD to generate the MacLowMD model. This provides a model of CD68+ macrophage depletion in DMD. Macrophage depletion was induced for two weeks when the MacLowMD animals were four weeks of age. Four weeks of age was chosen as it is the stage of peak muscle necrosis and is when the inflammatory response is first seen, and as such is the stage where the highest number of CD68 positive M1 macrophages are present in the muscle (Villalta *et al.*, 2009).

Previous findings from our laboratory showed that CD68+ macrophage numbers were decreased by 50% in doxycycline treated MacLowMD mice (Doherty *et al.*, unpublished data) (Figure 1.6.1). The observed 50% reduction in CD68+ M1 macrophages is expected to have a beneficial impact on the pathology of DMD due to a decrease in their damaging proinflammatory property.

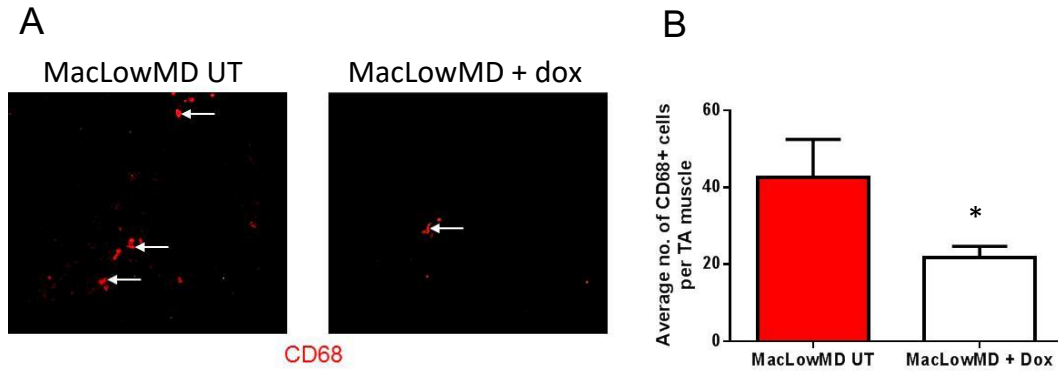


**Figure 1.6.1: Doxycycline treatment results in a 50% reduction in the number of CD68+ macrophages in the MacLowMD mouse model.** Frozen 8 $\mu$ m transverse sections of tibialis anterior muscle from the MacLowMD mice treated with doxycycline (T) or untreated animals as a negative control (UT) were stained for antibodies for CD68 (red). Treated MacLowMD TA muscle showed a 50% reduction in the number of CD68+ stained cells. n=3. p= <0.05.

In addition, a 50% decrease in CD68+ cells led to a 33% decrease in the number of regenerating muscle fibres in MacLowMD muscle (Doherty *et al.*, unpublished data) (Figure 1.6.2)

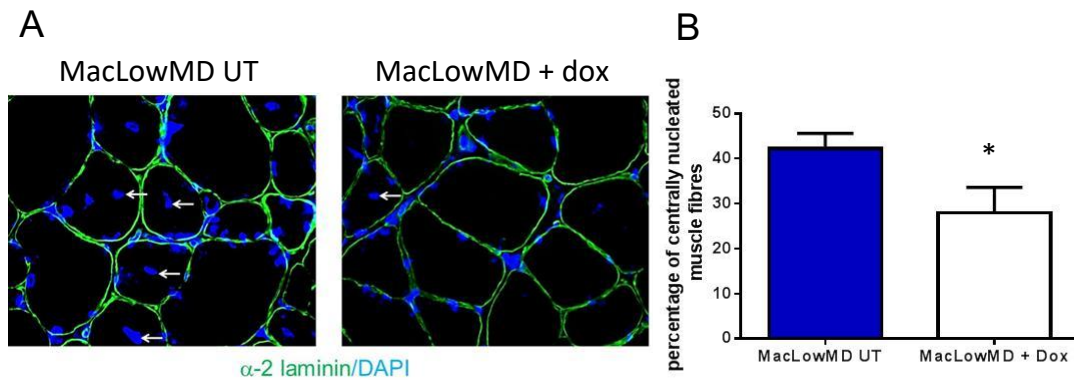


**Figure 1.6.2: Doxycycline treatment results in a 33% reduction in the number of regenerating muscle fibres in the MacLowMD mouse model.** Frozen  $8\mu\text{m}$  transverse sections of tibialis anterior muscle from the MacLowMD mice treated with doxycycline (T) or untreated animals as a negative control (UT) were stained for antibodies for nuclei (blue) and laminin (green). Image A shows fluorescent staining muscle fibres, with central nucleation being indicated by arrows. Central nucleation was used as a method of measuring muscle fibre regeneration. Treated MacLowMD TA muscle showed a 33% reduction in the number of centrally nucleated regenerating fibres.  $p = <0.05$ .

## 1.7 Hypothesis

Based on the previous data from our laboratory and the need for new treatment options for DMD, we hypothesise that reducing numbers of proinflammatory CD68+ macrophages will reduce fibre damage in MacLowMD mice without affecting the regenerative capacity of the muscle.

## 1.8 Aims and Objectives

Following on from the research previously performed in our laboratory, the present study continued to analyse the 2 week doxycycline treated MacLowMD tissues to understand if the previously observed reduction in

muscle fibre regeneration in the MacLowMD model occurred due to: a reduction in muscle fibre damage; an impairment of the regenerative capacity of muscle fibres or a delay in muscle fibre regeneration.

In addition, the impact of a longer, six week treatment with doxycycline will also be determined. The impact of CD68+ macrophage depletion following six week doxycycline treatment will be assessed for three main criteria-

**1. The Impact of CD68+ Macrophage Depletion on Macrophage Phenotype in Muscle- Chapter 3.**

This will be achieved by determining the impact of six week doxycycline treatment on the numbers of F4/80+, CD68+, CD163+ and CD206+ macrophages, determined through immunohistochemical staining.

**2. The Impact of CD68+ Macrophage Depletion on the Level of Muscle Damage- Chapter 4.**

This will be achieved by determining the impact of six week doxycycline treatment on muscle fibre damage, determined through immunohistochemical staining, and myomesin blood serum levels, determined through Western Blots.

This will test the hypothesis that reduced fibre damage will be seen in the MacLowMD mice, following CD68+ macrophage depletion.

**3. The Impact of CD68+ Macrophage Depletion on the Regenerative Capacity of Muscle- Chapter 5.**

This will be achieved by determining the impact of six week doxycycline treatment on muscle fibre size, the percentage of regenerating fibres,

the total number of muscle fibres and the percentage of fibrotic tissue, determined through immunohistochemical staining.

This will test the hypothesis that the regenerative capacity of the muscle in the MacLowMD mice will not be affected by reducing numbers of CD68+ macrophages.

## Chapter 2: Materials and Methods

---

### **2.1 Animal Work**

#### **2.1.1 Animal Husbandry**

All animals were maintained in a high health status facility at The University of Sheffield according to the UK Home Office guidelines. All animal studies were approved by the ethical committee at The University of Sheffield and the Home Office. (PPL no. 70/8118). All two week doxycycline treatment work was undertaken by Louise Nugent, The University of Sheffield.

Mdx mice were crossed with MacLow mice to generate the four genotypes required for analysis (mdx, MacLow, MacLowMD and wildtype). The inducible macrophage depletion line, MacLow, is on an FVB/n background. Only age matched male mice were used. In the two week study only MacLowMD animals were used, whilst all genotypes were used throughout the six week study. The phenotypes of all the genotypes of mice used throughout this study are represented in the table overleaf (Table 2.1.1).

<b>Genotype</b>	<b>Disease phenotype</b>	<b>CD68+ Macrophage Depletion?</b>
<b>Mdx</b>	Diseased	No
<b>MacLowMD</b>	To be determined by CD68+ macrophage depletion	Yes
<b>MacLow</b>	Healthy	Yes
<b>Wild Type</b>	Healthy	No

**Table 2.1.1: Summary of genotypes used throughout six week doxycycline treatment.** mdx and MacLowMD mice have diseased, dystrophic muscle, with MacLowMD mice possessing CD68+ macrophage depletion when treated with doxycycline. MacLow and wild type mice are healthy controls, with MacLow mice possessing CD68+ macrophage depletion when treated with doxycycline.

Animals were regularly monitored for any side effects; weight loss (mice were weighed weekly) or physical abnormalities (unkempt coat, squinted eyes). Prior to dissection, blood was obtained via tail vein incision.

### **2.1.2 Macrophage Depletion**

Animals were fed a diet containing doxycycline (5g per mouse per day) (Teklad custom rodent diet TD.01306, 625mg/kg doxycycline, Envigo, Madison, WI, USA) (in order to induce CD68+ macrophage depletion) or normal food (untreated controls) between the ages of four and six weeks old for two weeks study, or between the ages of four and ten weeks old for six weeks study.

### **2.1.3 Tissue Harvest**

Prior to euthanasia tail bleeds were performed to obtain a maximum of 100 $\mu$ l of blood. Mice were placed on heat mats in order to increase the accessibility

of tail veins. Blood was collected via small incisions were made on minor tail veins. Mice were euthanised by cervical dislocation. Quadriceps, Tibialis Anterior (TA), soleus, gastrocnemius and hamstring, diaphragm and heart muscle were dissected from all mice and frozen, as well as spleen and liver (half frozen, half stored in formalin (see Appendix III for recipe)), and leg bones (stored in formalin). For freezing, tissues were covered in OCT cryoprotective embedding medium (Thermo Scientific, Cheshire, UK), frozen rapidly in liquid nitrogen-cooled 2-methylbutane and stored at -80°C. Blood from tail bleeds was incubated at 4°C overnight (to allow clots to form) before being centrifuged at 3000rpm at 4°C for 10 minutes. Clear serum was removed and spun for another 10 minutes at 3g at 4°C. Serum was removed, aliquoted and stored at -80°C.

## **2.2 Genotyping**

Due to heterozygous breeding of the two different strains (mdx and MacLow) genotyping of the offspring is needed to ensure mice carry the required genes.

### **2.2.1 Cell Lysate Preparation**

Ear biopsies were taken from three week old mice and incubated overnight at 55°C in 150µl lysis buffer (1M Tris- HCl, 0.5M Ethylenediaminetetraacetic acid, 10% Tween 20) supplemented with 300µg/ml Proteinase K (see Appendix III for recipe). Samples were then incubated at 100°C to inactive the Proteinase K and 600µl dH<sub>2</sub>O added to each sample.

### **2.2.2 Genotypic Analysis of mdx**

Cell lysate (2µl) from each ear biopsy was added to 13µl of PCR master mix in a sterile PCR tube. The master mix volume per reaction consisted of: 3µl 5x green GoTaq Flexi Buffer (Promega, Wisconsin, USA), 1.5µl 2.5mM dNTP, 0.9µl of 25mM MgCl<sub>2</sub>, 2µl of 10pmol/µl forward primer 2µl of 10pmol/µl reverse primer, 0.12µl GoTaq G2 Flexi polymerase (5U/µl) (Promega, Wisconsin, USA) and 3.38µl DEPC treated water. Details of mdx primers can be found in Table 2.2.1.1.

Gene	Forward primer	Reverse primer	Base pairs	Annealing °C	Annealing cycle number
HincIImdx	5'GCAAA GTTCTTT GAAAGG TAA3'	5'CACCAACTG AGGAAAGTT3'	157bp	58°C	35

**Table 2.2.1.1. Details of mdx primers, amplicon size, annealing temperatures and annealing cycle numbers.**

The PCR was performed using the cycling conditions in Table 2.2.1.2 in a BioRad My Cycler Thermal Cycle PCR machine:

Number of Cycles	Temperature	Time
1	94°C	2 minutes
35- denaturation	94°C	30 seconds
35- annealing	58°C	30 seconds
35- extension	72°C	30 seconds
1	72°C	2 minutes

**Table 2.2.1.2. Details of PCR conditions for mdx genotyping.**

Restriction enzyme digestion was performed as mdx genotyping relies on mismatch PCR. Mismatch PCR is a method of detecting point mutations. The mdx mouse has a point mutation in the dystrophin gene. The point mutation giving rise to dystrophin deficiency in mice carrying the mdx allele of the *DMD* gene is shown in bold and underlined in the schematic below. Following PCR, 10µl of PCR product was added to 10µl digestion mix and incubated at 37°C for 3.5 hours. The digestion reaction consisted of: 2µl 10x buffer 3, 0.2µl 100x BSA (Sigma- Aldrich)/, 0.5U *HincII* enzyme (New England Biolabs, Massachusetts) and 7.3µl DEPC treated water.

The sequence of the forward primer is shown in italics and stops just before the point mutation giving rise to the mdx phenotype. *HincII* recognition sequence GTYRAC in the amplified product from wild-type mice alone is underlined, and digestion with *HincII* would result in a 20 base pair smaller fragment. Therefore, PCR products for mdx animals are 157 base pairs, whilst PCR products for wild type animals are 137 base pairs.

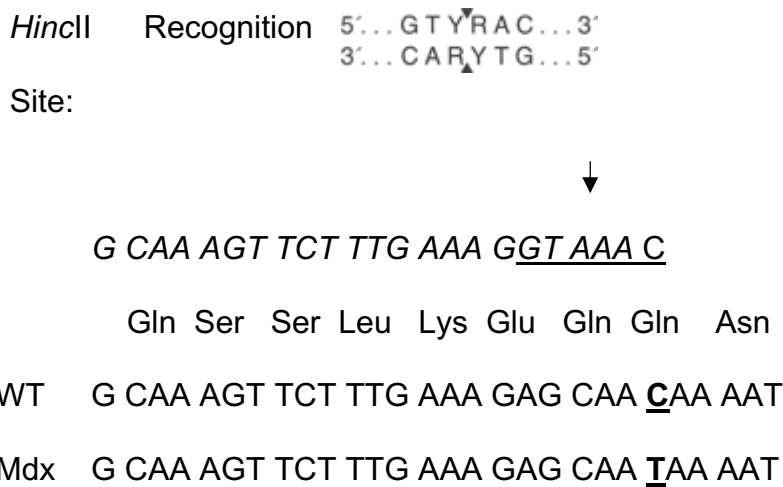


**Figure 2.2.1.1** *HincII* recognition site for point mutation in DMD gene.

15µl of *HincII* digested PCR product was loaded on 4% agarose (Fischer Scientific, Leicester, UK) gel containing 5% ethidium bromide (Sigma- Aldrich, Missouri, USA) and run for approximately 60 minutes at 160 volts. 4% agarose gel was used to allow clear separation of digested and non-digested bands. 0.5µg of low molecular weight ladder (#N3233, New England Biolabs) was also run on the gel using 1x TBE running buffer (see Appendix III for recipe).

### **2.2.3 Genotypic Analysis of CD68 and tetDTA**

Along with mdx PCRs, CD68 and tetDTA PCRs are necessary as the expression of these transgenes varies within the different genotypes used in this study. The mdx genotype is only present in mice with the dystrophic phenotype (mdx and MacLowMD). MacLowMD and MacLow mice have the potential for expression of the CD68 promoter in their transgene (TG1, CD) (MacLowMD and MacLow). These are the mice in which CD68+ macrophage

depletion is possible. tetDTA is expressed in all genotypes, although it is only activated in mice with the CD68 promoter and treated with doxycycline (TG2, TD) (see Figure 1.62 in Introduction chapter). 2µl of cDNA sample was added to 13µl of master mix in a new PCR tube. The master mix volume per reaction is the same as in Section 2.2.1. Details of CD68 and tetDTA primers can be found in **Table 2.2.2**.

Gene	Forward primer	Reverse primer	Base pairs	Annealing °C	Annealing cycle number
CD68	5'GACGTAAA CGGCCACAA GTT3'	5'TGCTCAGGT AGTGGTTGTC G3'	526	57°C	30
tetDTA	5'TCGTACCA CGGGACTAA ACC3'	5'ACTTGCTCC ATCAACGGTT C3'	300	57°C	30

**Table 2.2.2. Details of CD68 and tetDTA primers, amplicon size, annealing temperatures and annealing cycle numbers.**

The PCR was performed using the cycling conditions described in Table 2.2.1.2 (with an altered annealing temperature of 57°C) in a BioRad My Cycler Thermal Cycle PCR machine.

15µl of PCR products were loaded on 2% agarose (Fischer Scientific) gel containing 5% ethidium bromide (Sigma- Aldrich) and run for approximately

60 minutes at 80 volts. 0.5µg of low molecular weight ladder (New England Biolabs) was also run on the gel using 1x TBE running buffer.

## **2.3 Tissue Sectioning**

Following harvesting, muscle tissue was covered in OCT cryoprotective embedding medium (Thermo Scientific, Cheshire, UK), frozen rapidly in liquid nitrogen cooled 2-methylbutane and stored at -80°C. 8µm transverse sections of TA, quadricep, diaphragm and heart muscle were cut using a Leica CM3050S cryostat and placed on slides (Thermo Scientific).

Liver and spleen sections were stored in formalin at 4°C before being paraffin embedded and cross sectioned at 3µm using a HistoCore BIOCUT microtome.

For each experiment, all muscle sections analysed were of a comparable size between each genotype and treatment group.

## **2.4 Immunohistochemistry**

### **2.4.1 Quantification of F4/80 Macrophages in Liver**

F4/80 positive (F4/80+) macrophages in the liver were quantified in order to investigate the impact of treatment with doxycycline on the total macrophage population. F4/80 is a mouse cell surface glycoprotein expressed in high levels on a variety of macrophages of both the M1 and M2 phenotype (Kinoshita *et al.*, 2010). Liver was chosen for analysis as it is a hub for tissue resident F4/80+ Kupffer cells (macrophages of the liver) and acts as a comparison with our previous study and published findings (Gheryani *et al.*, 2013); (Rumney *et*

*al.*, 2017). Quantification of the number of F4/80+ macrophages was used to verify that the MacLow model was allowing successful macrophage depletion, as expected, in MacLow mice, as well as when crossed with mdx mice.

F4/80 staining was performed on paraffin embedded liver for wild type, MacLow, mdx and MacLowMD muscle, for both doxycycline treated and control fed mice.

Slides were dewaxed by two successive 10 minute immersions in xylene before being transferred through an ethanol gradient (100%- 70%) and then briefly being washed in distilled water followed by phosphate buffered saline (PBS). In order to allow antigen retrieval, slides were placed in cassettes of a pressure cooker and covered in Dako Target Retrieval Buffer (Agilent, California, USA) diluted 1:10 in distilled water. Slides were incubated in the pressure cooker for 30 minutes according to manufacturer's instructions. Slides were removed from the pressure cooker and rinsed twice in PBS.

Liver sections were encircled by a Hydrophobic Barrier from MAKE PAP pen and a number of steps were then performed in order to block any non-specific antibody binding. Sections were covered in 3% hydrogen peroxide diluted in PBS for 20 minutes before being washed with PBS. Tissues that contain red blood cells, such as liver, possess endogenous peroxidases, which result in non-specific staining. Hydrogen peroxide blocks these endogenous peroxides and reduces background staining. Sections were then incubated with Avidin D solution (Vector Laboratories, California, USA) for 15 minutes, washed in PBS

and covered in biotin solution (Vector Laboratories, California, USA) for 15 minutes before another PBS wash. This stage ensures that endogenous biotin, biotin receptors, and avidin binding sites present in tissues are blocked. As a final blocking step, sections were incubated in 10% rabbit serum block (Vector Laboratories) diluted in 0.1% triton/1% BSA/ PBS for 60 minutes (see Appendix III) Serum is a blocking agent that contains antibodies that bind to non-specific sites in tissue. Serum that matches the species of the secondary antibody, in this case rabbit, is used. Rabbit serum block was removed and 50µl rat anti-F4/80 antibody (Abcam) diluted 1:100 in 1% BSA /PBS added to sections and incubated overnight at 4°C.

Following overnight incubation slides were washed three times in PBS with tween 20% (PBST). Sections were incubated for 60 minutes at room temperature with 50µl biotinylated rabbit anti-rat IgG antibody (Vector Laboratories). Avidin and biotin complex (ABC complex kit) (Vector Laboratories, see Appendix III for recipe) was made 30 minutes prior to adding to sections. This allowed the biotinylated Horseradish Peroxidase (HRP) enzyme in the ABC kit to form avidin–biotin–enzyme complexes. Slides were washed three times in PBST and incubated for 30 minutes with the previously prepared avidin and biotin complex. Any remaining biotin binding sites on the avidin in the ABC kit bind to the biotinylated rabbit anti-rat IgG antibody. Slides were washed three times in PBST and incubated with DAB Peroxidase (chromogen) for approximately 3 minutes, or until brown stain appears. DAB reaction was stopped using excess tap water and slides counterstained for 60 seconds in haematoxylin (Sigma- Aldrich), washed twice

in PBS and rinsed in tap water. Slides were dehydrated by being transferred through ethanol (70%- 100%) to xylene before being mounted using DPX mountant (Sigma- Aldrich).

An isotype control was created by adding a rat IgG control antibody (Vector Laboratories) to tissue sections in place of rat anti-F4/80 antibody.

Slides were stored in slide boxes at room temperature until visualised using a Leica DMI4000 Fluorescent microscope.

F4/80+ DAB stained macrophages were manually quantified using FIJI version 2 software. Five random fields were analysed for each tissue section.

## **2.5 Immunofluorescence**

### **2.5.1 General Immunofluorescence Protocol**

Immunofluorescence staining is used multiple times throughout this study in order to detect inflammatory cells, areas of muscle damage and muscle fibres. However, despite being used to detect different markers, the general immunofluorescence protocol is similar throughout each experiment.

The general immunofluorescence protocol is detailed in Table 2.5.1.1. Any alterations to this protocol will be detailed in subsequent immunofluorescence subchapters. A complete list of all primary and secondary antibodies used in immunohistochemistry and immunofluorescence can be found in Appendix IV.

Step		Time
1	Slides were brought to room temperature in a humidified chamber.	5 minutes
2	Sections drawn around with a PAP pen.	
3	Block to prevent non- specific antibody binding	60 minutes
4	Primary antibody.	60 minutes
5	3 x wash	5 minutes per wash
6	Secondary antibody	60 minutes
7	3 x wash	5 minutes per wash
8	Coverslips mounted using 5 $\mu$ l Vectorshield mounting media with DAPI (Vector Laboratories).	
9	Slides covered in foil and stored at 4°C until visualized using Leica DMI4000 Fluorescent microscope.	

**Table 2.5.1.1. General immunofluorescence protocol used throughout study.**

Immunofluorescence was performed on frozen TA from MacLowMD for both doxycycline and control fed mice in the two week study.

Throughout the six week study all immunofluorescence was performed on frozen TA, diaphragm, quadricep and heart muscle for MacLowMD, mdx, MacLow and wild type muscle, for both doxycycline treated and control fed mice.

For each stain a negative control of secondary antibody only was prepared to ensure that the secondary antibody did not bind to the tissue non-specifically.

### **2.5.2 CD68 Staining and Analysis**

CD68 staining followed the general immunofluorescence protocol detailed in Table 2.5.1.1 with blocking being performed using 1% BSA. 1:10 CD68 alexafluor647 conjugated antibody (BioRad, California, USA) diluted in 1% BSA (Sigma- Aldrich), PBST was added at the primary antibody stage. The antibody used in CD68 staining is a conjugate antibody so no secondary antibody is needed.

An isotype control was created by adding a rat IgG1 antibody (BioRad) to tissue sections. Slides were visualised using Leica AF6000 Time Lapse microscope. Far- red fluorescence stained CD68+ macrophages were manually quantified using FIJI version 2 software. Whole tissue sections were analysed for each genotype and muscle type, with genotype being blinded to avoid bias.

### **2.5.3 CD206 Staining and Analysis**

CD206 staining followed the general immunofluorescence protocol detailed in Table 2.5.1.1 with the following alterations:

After step 1 slides were flooded with ice- cold acetone in order to fix tissue samples for 10 minutes. Without acetone fixation, antibody detection of CD206 was unsuccessful. Following fixation, slides were air dried at room temperature for 20 minutes. Tissue was encircled using a PAP pen and rehydrated with PBST for 10 minutes before proceeding to step 4. Anti- MRC1 (an alternative name for CD206) antibody (BioLegend, California, USA) diluted

1:200 in PBST was added to tissue. In these studies, the control was prepared by only adding secondary antibody (Anti- MRC1) to tissue sections, but continuing the rest of the stain as normal.

Green fluorescence stained CD206+ macrophages were manually quantified using FIJI version 2 software. Whole tissue sections were analysed for each genotype and muscle type, with genotype being blinded to avoid bias.

#### **2.5.4 CD163 Staining and Analysis**

CD163 staining followed the general immunofluorescence protocol detailed in Table 2.5.1.1 with blocking being performed with 5% BSA (Sigma- Aldrich)/ 2% normal goat serum (Vector Laboratories)/ 0.05% triton x100/ PBS. Primary antibody used was CD163 antibody (Abcam) diluted 1:200 in 2% normal goat serum (Vector Laboratories). Secondary antibody was goat anti rabbit IgG antibody diluted 1:1000 in 2% normal goat serum (Vector Laboratories). A no primary control was created by only adding secondary antibody (goat anti rabbit IgG antibody) and DAPI stain as normal.

Green fluorescence stained CD163+ macrophages were manually quantified using FIJI version 2 software. Whole tissue sections were analysed for each genotype and muscle type, with genotype being blinded to avoid bias.

### **2.5.5 IgG Staining and Analysis**

IgG staining followed the general immunofluorescence protocol detailed in Table 2.5.1.1. Blocking was performed using in 50µl 5% BSA (Sigma- Aldrich)/PBS. Primary antibody used in IgG staining was 1:500 diluted biotin labelled mouse IgG (Vector Laboratories) in 2% normal goat serum in PBS. 1:250 50µl FITC conjugated streptavidin (Vector Laboratories) diluted in 2% normal goat serum in PBS was used as the secondary antibody. Negative controls were prepared by only adding secondary antibody (FITC conjugated streptavidin) and DAPI stain as normal.

FIJI version 2 software was used to measure the cross-sectional area of damaged muscle fibres. Whole tissue sections were analysed for each genotype and muscle type, with genotype being blinded to avoid bias. The scale bar was measured and converted to microns and IgG stained fibres were manually drawn around. The area of IgG stained tissue was calculated as a percentage of the total area of each tissue section.

### **2.5.6 Laminin Staining and Analysis**

Laminin staining followed the general immunofluorescence staining protocol in Table 2.5.1.1 with sections being blocked in 50µl 1% BSA (Sigma- Aldrich) /PBS. 1:500 laminin antibody  $\alpha$ 1 (Enzo Laboratories) diluted in 1% BSA (Sigma- Aldrich), 0.05% PBST was used as the primary antibody. The secondary antibody was 1:200 anti-rat secondary fluorescein antibody (Vector Laboratories). An isotype control was created by adding rat IgG1 antibody (BioRad) to tissue sections.

### **2.5.6.1 Quantification of the Regenerative Capacity of Muscle Fibres, Total Number of Fibres and Percentage of Regenerating Fibres**

Feret's minimum diameter was used to measure the diameter of laminin stained muscle fibres and takes in to consideration whether a section has been cut at a plane. This means that Feret's minimum diameter allows a more accurate representation of muscle fibre size than traditional cross-sectional area measurements.

FIJI version 2 software was used to measure Feret's minimum diameter. The scale bar was measured and converted to microns and all muscle fibres within a section were manually drawn around. FIJI produces a Feret's minimum diameter measurement for each individual fibre. All fibres within each muscle were measured. Whole tissue sections analysed for each genotype and muscle type, with genotype being blinded to avoid bias.

Feret's minimum diameter measurements were obtained for all fibres within a section and arranged in order of size. Number of fibres were 'binned' into a range of Feret's minimum measurements, i.e. 6- 10, 11- 15, 16- 20, and were quantified and calculated as a percentage of total number of fibres. This allowed histograms to be generated detailing diameter of muscle fibres, as indicated by Feret's minimum diameter measurements, throughout whole tissue sections. Feret's minimum diameter measurements were analysed in histograms for both regenerating fibres and the total fibres (both regenerating

and non- regenerating) within each tissue. Regenerating fibres were indicated by central nuclei and non- regenerating by peripheral nuclei.

As Feret's minimum diameter measurements had been obtained for all fibres within a section this also was used as a quantification of total number of muscle fibres in a tissue. Furthermore, as Feret's minimum diameter measurements were obtained for both regenerating fibres specifically, it was possible to quantify these and establish the percentage of regenerating fibres out of the total fibre number for each tissue.

### **2.5.7 Collagen Staining and Analysis**

Collagen staining was performed following the general immunofluorescence protocol detailed in Table 2.5.1.1 with the following alterations:

Sections were blocked in 5% BSA (Sigma- Aldrich)/ 1% normal goat serum (Vector Laboratories)/ 0.5% Triton x 100/ PBS. Following this primary collagen 1 antibody (Merck Millipore), diluted 1:500 in 1% normal goat serum (Vector Laboratories)/ 0.05% Triton x 100/ PBS was added to section and incubated overnight at 4°C. Following overnight incubation, slides were washed three times in 1% normal goat serum (Vector Laboratories)/ 0.05% Triton x 100/ PBS solution. Secondary antibody goat anti-rabbit alexa fluor 488 was diluted 1:50 in 1% normal goat serum (Vector Laboratories)/ 0.05% Triton x 100/ PBS. In these studies, a negative control was prepared by only adding secondary antibody (Goat anti-rabbit Alexa Fluor 488) and DAPI stain as normal.

FIJI version 2 software was used to measure the level of tissue fibrosis. Whole tissue sections were analysed for each genotype and muscle type, with genotype being blinded to avoid bias. The scale bar was measured and converted to microns. Colour threshold was adjusted to RGB and areas of green collagen stained tissue selected. FIJI measured the area of collagen stained tissue, thus allowing the calculation of collagen stained tissue a percentage of the total area of each tissue section.

## **2.6 Western Blot**

### **2.6.1 Myomesin Western Blot and Analysis**

Myofibrillar structural protein myomesin-3 (MYOM3) is a biomarker of muscle damage in DMD. Myomesin is a protein normally located in muscle that leaks into blood following rupturing of muscle plasma membrane. Western blot analysis of blood serum from six week doxycycline treated mice using the myomesin MYOM3 biomarker allowed levels of myomesin in blood to be assessed. Levels of myomesin in the blood is used as a measure of the effect of six week doxycycline treatment and CD68+ macrophage depletion on muscle damage.

1µl of blood serum was diluted 1 in 4 in water and added to 4µl laemelli buffer + DTT before being incubated at 65°C for 15 minutes. Laemelli buffer contained 4% 10% ultrapure SDS (ThermoFisher), 20% glycerol, 120mM 1m Tris- Cl, 0.02% bromophenol blue (BioRad) and was made to a final volume

of 10ml with distilled water. 50 $\mu$ l DTT (Fischer Scientific) was added to 950 $\mu$ l laemelli buffer. After incubation electrophoresis was performed.

Electrophoresis apparatus consisted of a 4–15% Mini-PROTEAN® TGX™ Precast Protein gel (BioRad) fixed into a BIORAD gel tank containing 1x Running buffer (consisting of 25mM Tris, 190mM glycine and 0.1% SDS) filled to the appropriate level. 5 $\mu$ l of BLUeye prestained 10- 245kDa protein ladder (Geneflow, Lichfield, UK) and 8 $\mu$ l of the samples were loaded into the wells. Electrophoresis was run at 150 volts for approximately 60 minutes.

A semi- dry transfer stack was prepared, covered in Towbin Buffer (comprised of 25mM tris base, 193mM glycine, distilled water and methanol) and kept at 4°C during electrophoresis.

Following electrophoresis, the Towbin Buffer soaked transfer stack was placed in the transblot (BioRad). The gel cast was prised open to obtain the gel. The gel was placed on the nitrocellulose membrane with three pieces of blotting paper on top and the transblot ran at 20 volts for 8 minutes. Protein was transferred to the membrane from the gel.

After protein transfer, the nitrocellulose membrane was cut to the desired size and transferred to 3% Blocking Buffer (non-fat dairy milk powder in 1x Tris-Buffered Saline Tween (TBST)) for 60 minutes on an orbital shaker. This blocked any non-specific antibody binding. The membrane was washed in TBST for 15 minutes on an orbital shaker. TBST was removed and membrane

incubated in fresh TBST for 5 further minutes on an orbital shaker. Two primary antibodies were used during western blotting- MYOM3, rabbit polyclonal (Proteintech, Manchester, UK) and GAPDH, rabbit monoclonal (Abcam, Cambridge, UK), as a housekeeping protein to normalise MYOM3 expression to. The MYOM3 primary antibody was diluted 1:500 in TBST, and the GAPDH primary antibody 1:10,000 in TBST. Membranes were covered in diluted antibodies and incubated overnight at 4°C on orbital shaker.

Following overnight incubation, membranes were washed quickly in TBST, placed in TBST for 15 minutes on orbital shaker. TBST was removed and membranes incubated in fresh TBST for 5 minutes on orbital shaker. Polyclonal goat anti- rabbit immunoglobulins antibody (Agilent Technologies, California, USA) was used as a secondary antibody for both MYOM3 and GAPDH and was diluted at 1:20.000 in TBST. Membranes were covered with diluted secondary antibody and incubated at room temperature for 60 minutes before being washed three times in TBST.

Excess TBST was drained off and nitrocellulose membrane placed on a debris free clear plastic film. 1ml of constituted Enhanced Chemiluminescent (ECL) reagent (Geneflow) was added drop wise to the membrane and incubated for 1 minute. Excess ECL was removed and nitrocellulose transferred to a fresh plastic film and covered. The wrapped membrane was immediately visualised using a G:Box Chemiluminescent Image Visualiser (Syngene, Cambridge, UK).

Genetools software (version 4.3.8) was used to manually quantify protein bands. Results from MYOM3 western blots were normalised to those from GAPDH.

## **2.7 Molecular Biology**

### **2.7.1 RNA Extraction**

RNA was extracted from three 6 week doxycycline treated and three 6 week untreated TA and diaphragm muscles to determine the effect of macrophage depletion on the expression of TNF $\alpha$ , IL4 and IL10 at gene level. Small pieces of TA ranging from 78.9-112.1 mg and diaphragm ranging from 89.5- 119.3 mg was ground to a fine powder in a mortar and pestle under liquid nitrogen before being homogenised in lysis buffer (QIAGEN RNeasy fibrous tissue midi kit) using a dounce homogeniser, followed by repeated uptake and expulsion through a 19- gage syringe. RNA extraction was performed through the use of a QIAGEN RNeasy fibrous tissue midi kit (QIAGEN), following manufacturer's guidelines.

Following RNA extraction, mRNA concentration of samples was determined through the use of a Nanodrop Spectrophotometer (Thermo Scientific).

### **2.7.2. DNase Treatment**

Due to high levels of genomic DNA, an additional DNase treatment was undertaken. Prior to reverse transcription, RNA samples were DNase treated through the use of Promega RQ1 RNase- Free DNase kit (1U/ $\mu$ l) (Promega), following manufacturer's guidelines. This ensured that no DNA would be

present in RT PCR reactions. This is confirmed by using the no RT RNA control in the subsequent PCR reaction. During DNase treatment all samples were standardised to a concentration of 600ng/ $\mu$ l.

### **2.7.3. Reverse Transcription**

5 $\mu$ l of DNase treated RNA was reverse transcribed by the addition 1 $\mu$ l 10mM dNTP mix, 0.5 $\mu$ g/ $\mu$ l oligo dt and 3 $\mu$ l RNA free water and heated at 65°C for 5 minutes. 9 $\mu$ l of the 2x reaction mix was added to each RNA/ primer mix and incubated at 42°C for 2 minutes. 2x reaction mix volume per reaction consisted of 2 $\mu$ l 10x RT buffer, 4 $\mu$ l 25mM MgCl<sub>2</sub>, 2 $\mu$ l 0.1M DTT and 1 $\mu$ l RNase out. 1 $\mu$ l SuperScript II RT was added to each reaction, with water in place for RT negative controls. Samples were re-incubated at 42°C for 50 minutes before being transferred to 70°C for 15 minutes to terminate the reaction. Samples were chilled on ice and 1 $\mu$ l RNase H was added to each reaction before being incubated at 37°C for 15 minutes.

cDNA was stored at -20°C short term, -80°C long term. All reagents used in reverse transcription reaction were taken from SuperScript First-Strand Synthesis System kit (InvitrogeA Life Technologies, California, USA).

### **2.7.4. TaqMan® Real Time Quantitative PCR (qPCR)**

Equipment was treated using a UV light hood for 45 minutes prior to undertaking the reaction, which was carried out in a 384 well plate. Each 20 $\mu$ l reaction consisted of 10 $\mu$ l 2x Universal Master Mix (ThermoFisher, Massachusetts, USA), 1 $\mu$ l of the TaqMan® gene expression assay, 8 $\mu$ l

nuclease free water and 1 $\mu$ l cDNA template. Plates were sealed and centrifuged at 300g for 1 minute. The qPCR was carried out on an Applied Biosystems 7900HT Real- Time PCR Machine (Biosystems, California, USA). The following TaqMan® probes were used: Mouse GAPDH gene expression assay ID: Mm05724508\_g1, Catalogue: 4351372, Mouse TNF $\alpha$  gene expression assay ID: Mm00443258\_m1, Catalogue: 4331182, IL4 gene expression assay Catalogue: Mm00445259\_m1, Catalogue: 4331182 and IL10 gene expression assay ID: Mm01288386\_m1, Catalogue: 4331182 (ThermoFisher).

## **2.8 Statistical analysis**

All quantitative data were evaluated using GraphPad Prism 7 software (La Jolla, USA). All data are expressed as means  $\pm$  SEM. All results were tested for normality using the D'Agostino-Pearson normality test. In order to test the impact of six week doxycycline treatment on numbers of F4/80+ macrophages one- way ANOVA was used. The impact of six week doxycycline treatment on number of CD68+ macrophages was analysed using one- tailed unpaired student's T-test. One- tailed analysis was used as there was an assumption of outcome- doxycycline treatment will result in CD68+ macrophage number being reduced. To address whether doxycycline treatment and CD68+ macrophage depletion affected the expression of M2 macrophages, level of muscle fibre damage, myomesin blood serum levels, number of muscle fibres, percentage of regenerating fibres and level of fibrosis, two-tailed unpaired student's t-test was used. Two tailed tests were performed as there was no prior indication of outcome. One-way ANOVA was used for F4/80 analysis

because a variable in three or more groups- number of F4/80+ macrophages in all four genotypes. All other experiments were tested using unpaired student's T-tests. This is because two sets of measurements were compared- MacLowMD + Dox and mdx + Dox. Differences were considered statistically significant in all tests when p value less than 0.05 (Confidence intervals > 95%).

## Chapter 3: The Impact of CD68+ Macrophage Depletion on Macrophage Phenotype in Muscle

---

### 3.1 Introduction

As previously described in Chapter 1.4, CD68+ macrophages are a subset of M1, proinflammatory macrophages that propagate the inflammatory response in DMD and the mdx mice. The changes in the balance of muscle macrophages during the development of mdx disease are represented in Figure 3.1.1. Following muscle damage, the acute phase of disease peaks at the begins at the age of four weeks and lasts until the age of twelve weeks. CD68+, iNOS- expressing M1 macrophages are seen at much higher levels than M2 macrophages. These proinflammatory M1 macrophages are capable of lysing muscle fibres by NO- mediated cytotoxicity. Arginase-expressing CD206+ M2a macrophages compete with iNOS for arginine, and thereby reduce the cytotoxicity of M1 macrophages (Rőszer, 2015). CD206+ macrophages assist in the removal of damaged muscle tissue (Rőszer, 2015). Cycles of damage and regeneration occur throughout the age of four to twelve weeks, with regeneration peaking at the age of twelve weeks. An increase in the levels of IL10 results in deactivation of M1 macrophages, a reduction in iNOS expression and an accompanying increase in the expression of CD163+ M2c macrophages (Rőszer, 2015). At this stage, low levels of muscle cytotoxicity is seen, the expression of anti- inflammatory cytokines, such as IL10, are increased, and muscle growth is promoted.

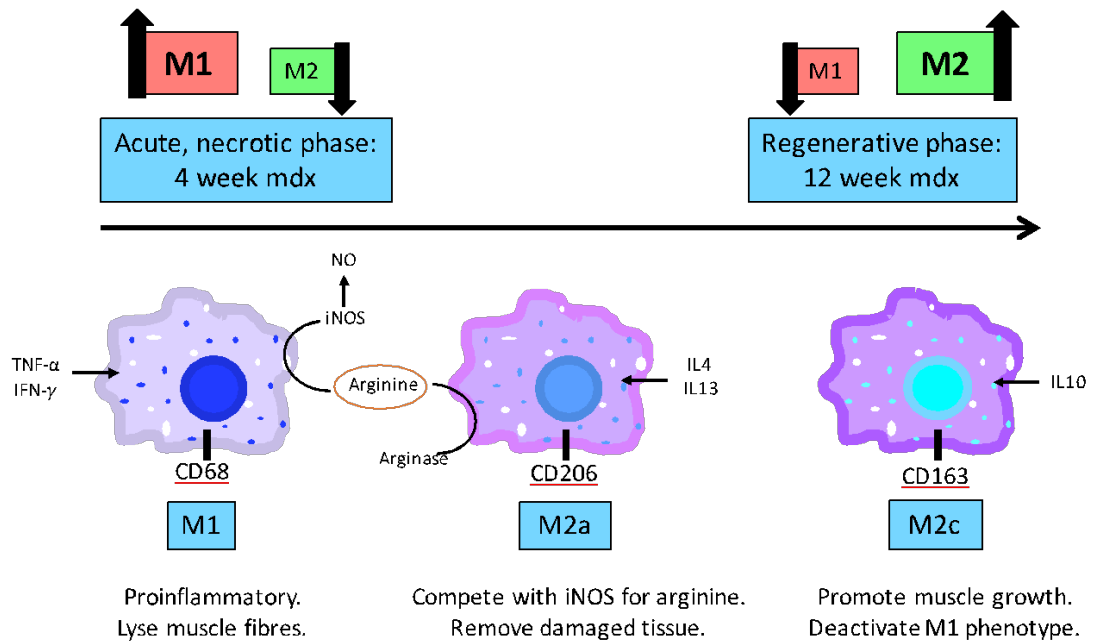


**Figure 3.1.1. Changes in the balance of muscle macrophages within mdx mice.**

Previous findings from our laboratory indicated that when the mdx mouse model of DMD was crossed with the MacLow model of inducible macrophage depletion, two weeks of doxycycline treatment resulted in a 50% reduction in the number of both F4/80 positive (F4/80+) macrophages in the liver and CD68 positive (CD68+) macrophages in TA muscle (Miller *et al.*, unpublished). However, the effect of six week doxycycline treatment on the number of CD68+ macrophages as well the balance of the inflammatory muscle macrophages as outlined above in the MacLowMD model has not been investigated.

In this current study the number of F4/80+ macrophages in the liver was used to assess the impact of treatment with doxycycline on total macrophage population. Liver was chosen for analysis as it is a hub for tissue resident F4/80+ Kupffer cells (macrophages of the liver) and acts as a comparison with

our previous study and published findings (Gheryani *et al.*, 2013), (Rumney *et al.*, 2017). Furthermore, studying the number of F4/80+ macrophages allowed us to ensure that the MacLow model was allowing successful reduction in numbers of macrophages, as expected, when crossed with mdx mice. The F4/80 antigen is a mouse cell surface glycoprotein expressed in high levels on a variety of macrophages, including Kupffer cells, of both the M1 and M2 phenotype.

CD68 is a highly expressed protein marker on M1, proinflammatory macrophages, and is specifically targeted for inducible depletion by doxycycline in the MacLow model. Studying levels of CD68+ macrophages in muscle allowed us to see if six week doxycycline treatment is effective in depleting CD68+ macrophages in MacLowMD mice. The effects of CD68+ macrophage depletion on the levels of M2 anti-inflammatory macrophages, CD206 and CD163 were also studied.

The membrane protein CD206 is a marker for M2a macrophages. CD206 positive (CD206+) macrophages are induced by IL4 and IL13 and play a major role in removal of damage tissue (Martinez and Gordon, 2014). Evaluating the levels of CD206+ macrophages in muscle allowed us to understand the impact of CD68+ macrophage depletion on the number of M2a macrophages.

CD163, a cell surface glycoprotein, is a protein marker for M2c macrophages. CD163 positive (CD163+) macrophages are induced by IL10 and have vital roles in tissue remodelling and anti-inflammatory immune regulation (Martinez

and Gordon, 2014). Studying the number of CD163+ macrophages allowed us to see the effects of CD68+ macrophage depletion on the levels of M2c macrophages.

The balance of macrophage phenotype was studied in four muscle types- TA, diaphragm, quadriceps and heart. TA and quadriceps are two of the most commonly used limb muscles in murine studies of muscular dystrophy. Diaphragm and heart are the two tissues affected in later stages of DMD and are the most severely affected muscles in both DMD patients and the mouse model of DMD (Ameen and Robson, 2010). These four muscles were used throughout this project.

Findings in this and further results chapters focus on comparisons between mdx and MacLowMD doxycycline treated muscle. This ensures that any observed effects in diseased tissue are due to a reduction in the numbers of CD68+ macrophages, and not just the effects of doxycycline.

The objectives of this results chapter were:

1. To determine the effect of six week doxycycline treatment on total macrophage number by quantifying F4/80 stained cells in liver sections.
2. To determine the effect of six week doxycycline treatment on the number of CD68+ macrophages in muscle by quantifying CD68+ macrophages in a variety of muscles.

3. To determine the effect of CD68+ macrophage depletion on the number of CD206+ macrophages in muscle by quantifying CD206+ macrophages in a variety of muscles.
4. To determine the effect of CD68+ macrophage depletion on the number of CD163+ macrophages in muscle by quantifying CD163+ macrophages in a variety of muscles.

## 3.2 Results

Macrophages were quantified for all genotypes (wild type, MacLow, mdx and MacLowMD).

### **3.2.1 Effect of Six Week Doxycycline Treatment on Macrophages in Liver**

In order to assess the impact of six week doxycycline treatment on total macrophage number immunohistochemistry was performed on formalin fixed liver sections using the pan macrophage marker F4/80. Macrophages that were positive for F4/80 were stained brown and had the ring-like appearance that is characteristic of macrophages (**Figure 3.2.1. A, arrows**).

Five sections with an 5µm depth were chosen at random from six age matched doxycycline treated and untreated MacLowMD, mdx, MacLow and wild type liver samples.

Six week doxycycline treatment had no impact on the number of F4/80+ macrophages in wild type or mdx liver. This was expected as wild type and mdx mice lack the MacLow transgenes required for inducible macrophage depletion. Six week doxycycline treatment resulted in a significant 27% reduction in numbers of F4/80+ macrophages in doxycycline treated MacLow mice compared to untreated MacLow mice ( $100.76 \pm 2.57$  compared to  $139.40 \pm 2.82$ ,  $p < 0.0001$ ) (**Figure 3.2.1. B**). Furthermore, a 33% reduction in the numbers of F4/80+ macrophages in MacLowMD liver compared to untreated

MacLowMD liver was also observed ( $97.81 \pm 2.74$  compared to  $145.13 \pm 2.78$ ,  $p < 0.0001$ ) (**Figure 3.2.1. B**).

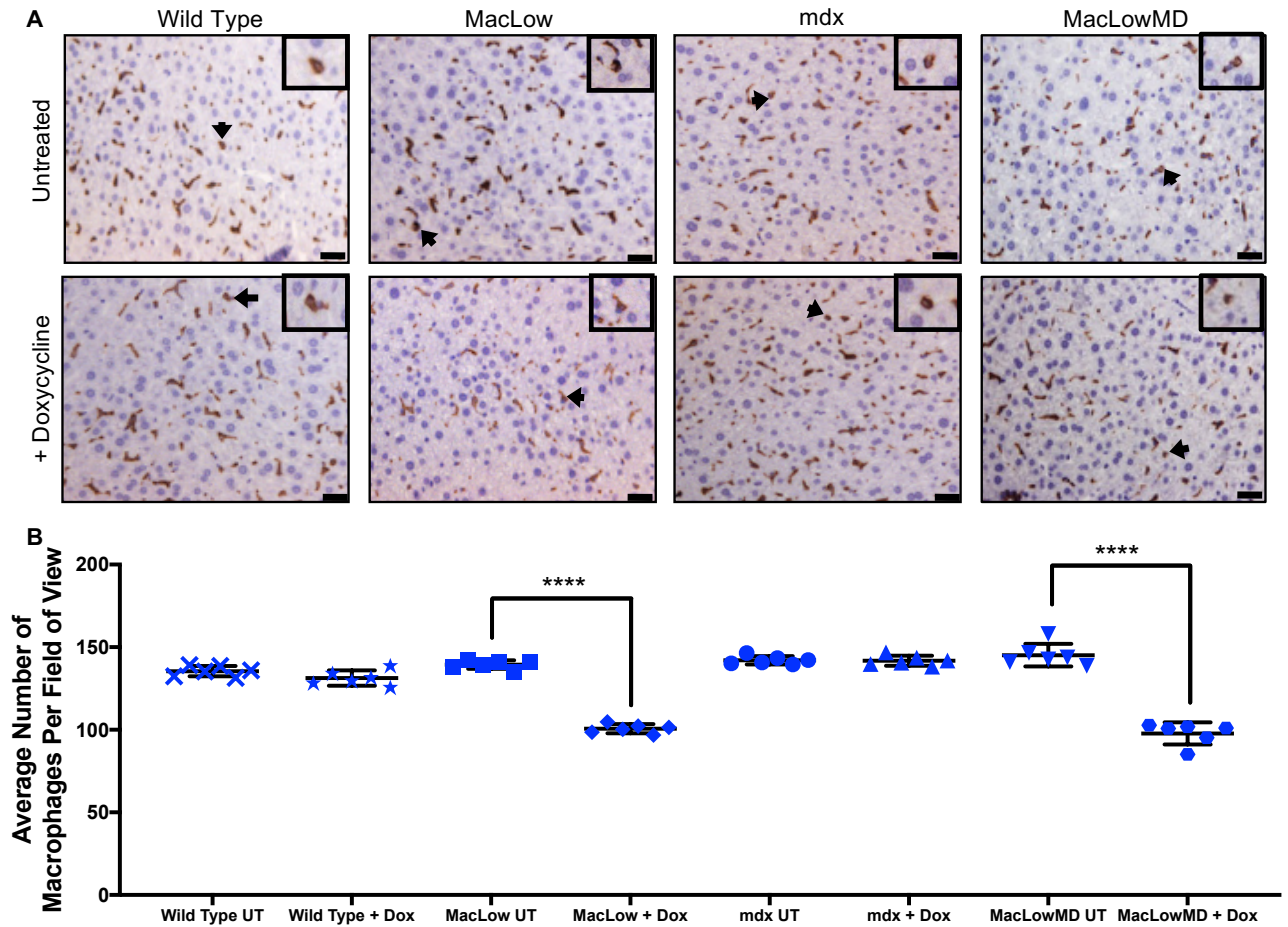


**Figure 3.2.1 Effect of six week doxycycline treatment on total macrophage numbers in liver.** Complete liver sections of n of 6 Wild type, MacLow and mdx and MacLowMD mice either untreated or doxycycline treated were stained for F4/80 and analysed. **A)** Representative images of F4/80 immunohistochemistry of formalin fixed liver. Arrows indicate examples of F4/80+ macrophages. **B)** Quantification of F4/80+ macrophages.

Macrophage morphology is indicated in inserts. Scale bar = 75µm. \*\*\*\* =  $p < 0.0001$ , (one way ANOVA). Data is expressed as mean  $\pm$  SEM.

### **3.2.2 Effect of Six Week Doxycycline Treatment on CD68 Positive Macrophages in Muscle**

The effect of six week doxycycline treatment on the number of CD68+ macrophages was assessed by immunofluorescent staining of frozen muscle sections. CD68+ macrophages were stained with Alexa Fluor647. These macrophages are identified by arrows in panel **A** of each figure, as well as enlarged panels. For each tissue analysed, all CD68+ macrophage counts were normalised to the average untreated value for that genotype (for example, MacLowMD + dox was normalised to MacLowMD UT) in order to allow comparison between genotypes and slightly different sized tissues.

#### **3.2.2.1 Tibialis Anterior**

Quantification of CD68+ macrophages revealed that, as expected, in non-diseased wild type and MacLow TA muscle there were no CD68+ macrophages (Figure 3.2.2.1 A). There were significantly more CD68+ macrophages in the diseased mdx and MacLowMD muscle than non-diseased wild type and MacLow TA muscle ( $p < 0.0001$ ). However, doxycycline treatment did not significantly affect numbers of CD68+ macrophages within TA muscle from any of the genotypes (**Figure 3.2.2.1. A and B**). Whilst this was expected in doxycycline treated mdx TA, it had not been anticipated in doxycycline treated MacLowMD TA, which has the potential for doxycycline inducible CD68+ macrophage depletion ( $0.99 \pm 0.034$  mdx + dox compared to  $0.94 \pm 0.03$  MacLowMD + dox,  $p = 0.25$ ).

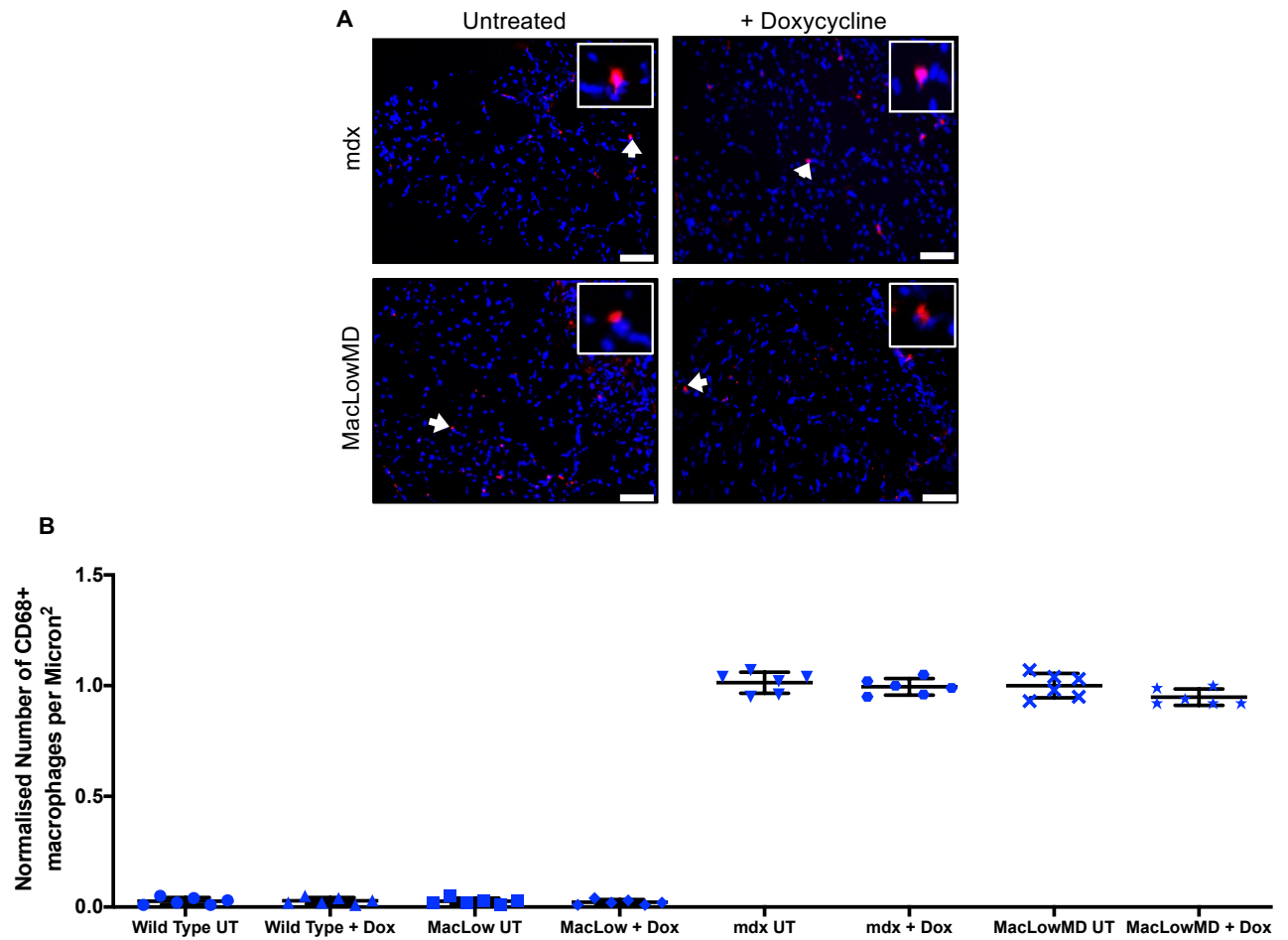


**Figure 3.2.2.1. Effect of six week doxycycline treatment on number of CD68+ macrophages in TA.** Complete TA sections were stained and analysed for n of 6 doxycycline treated MacLowMD and mdx mice. **A)** Representative images of CD68 immunofluorescent stain of frozen TA muscle. **B)** Quantification of number of CD68+ macrophages normalised to untreated controls.

Macrophage morphology is indicated in inserts. Scale bar = 40µm. Data is expressed as mean ± SEM.

### 3.2.2.2 Quadriceps

Similar to the results with TA muscle, results from quadricep indicated that there was no difference in the number of CD68+ macrophages between doxycycline treated mdx and MacLowMD tissue ( $1.007 \pm 0.03$  compared to  $1.02 \pm 0.02$ ,  $p$  0.81) (**Figure 3.2.2.2. A and B**).

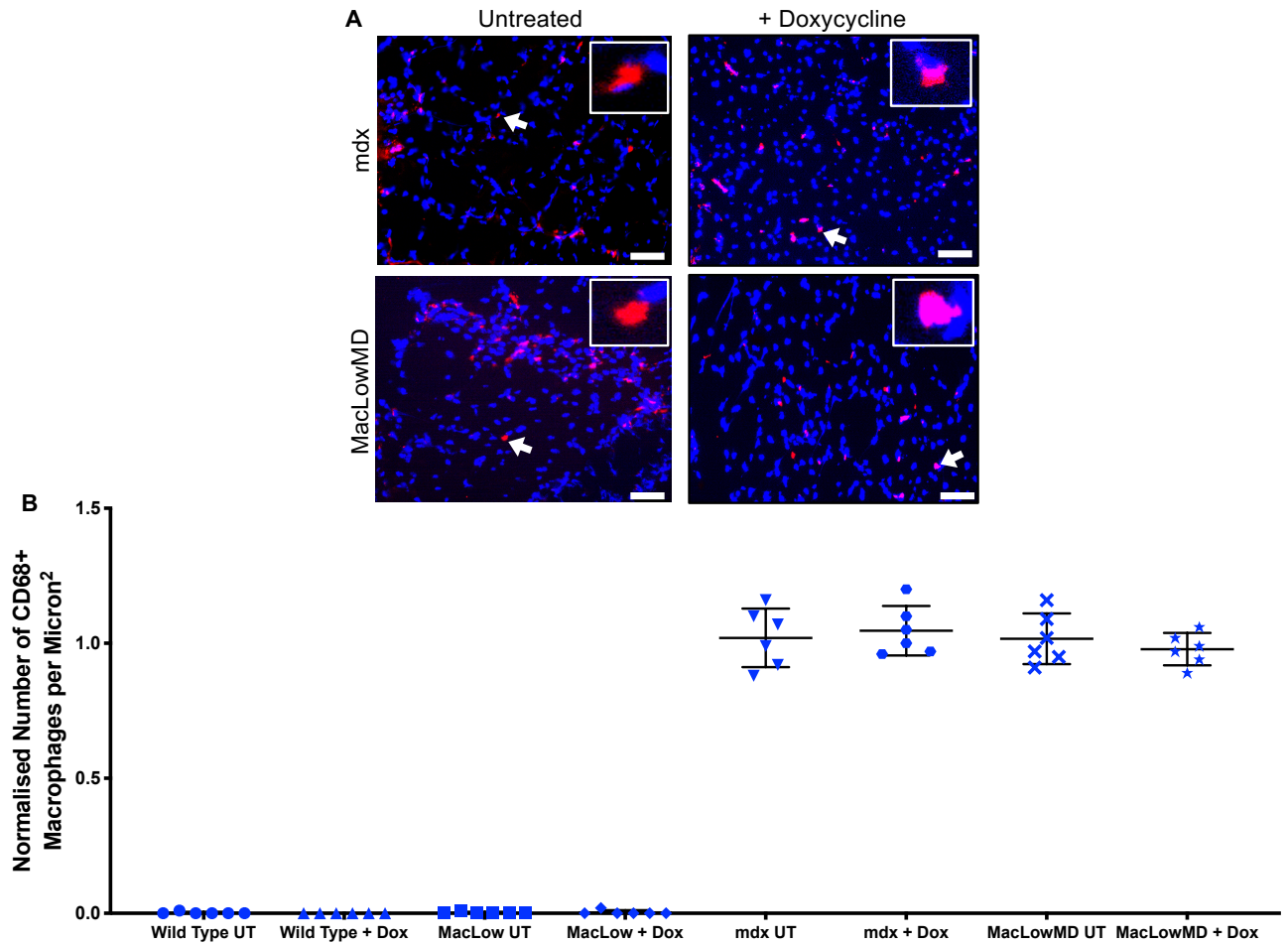


**Figure 3.2.2.2. Effect of six week doxycycline treatment on number of CD68+ macrophages in quadricep.** Complete quadricep sections were stained and analysed for n of 6 doxycycline treated MacLowMD and mdx mice. **A)** Representative images of CD68 immunofluorescent stain of frozen quadricep muscle. **B)** Quantification of number of CD68+ macrophages normalised to untreated controls. Macrophage morphology is indicated in inserts. Scale bar = 40µm. Data is expressed as mean ± SEM.

### 3.2.2.3 Diaphragm

Following six weeks doxycycline treatment quantification of CD68+ macrophages showed that, as expected, there were no CD68+ macrophages in non- diseased wild type and MacLow diaphragm muscle. Doxycycline treatment reduced the number of CD68 macrophages by 30% in MacLowMD diaphragm compared to doxycycline treated mdx diaphragm ( $0.96 \pm 0.03$  compared to  $0.66 \pm 0.02$ ,  $p < 0.01$ ) (**Figure 3.2.2.3. A and B**). Doxycycline treatment had no impact on the number of CD68+ macrophages in mdx diaphragm.

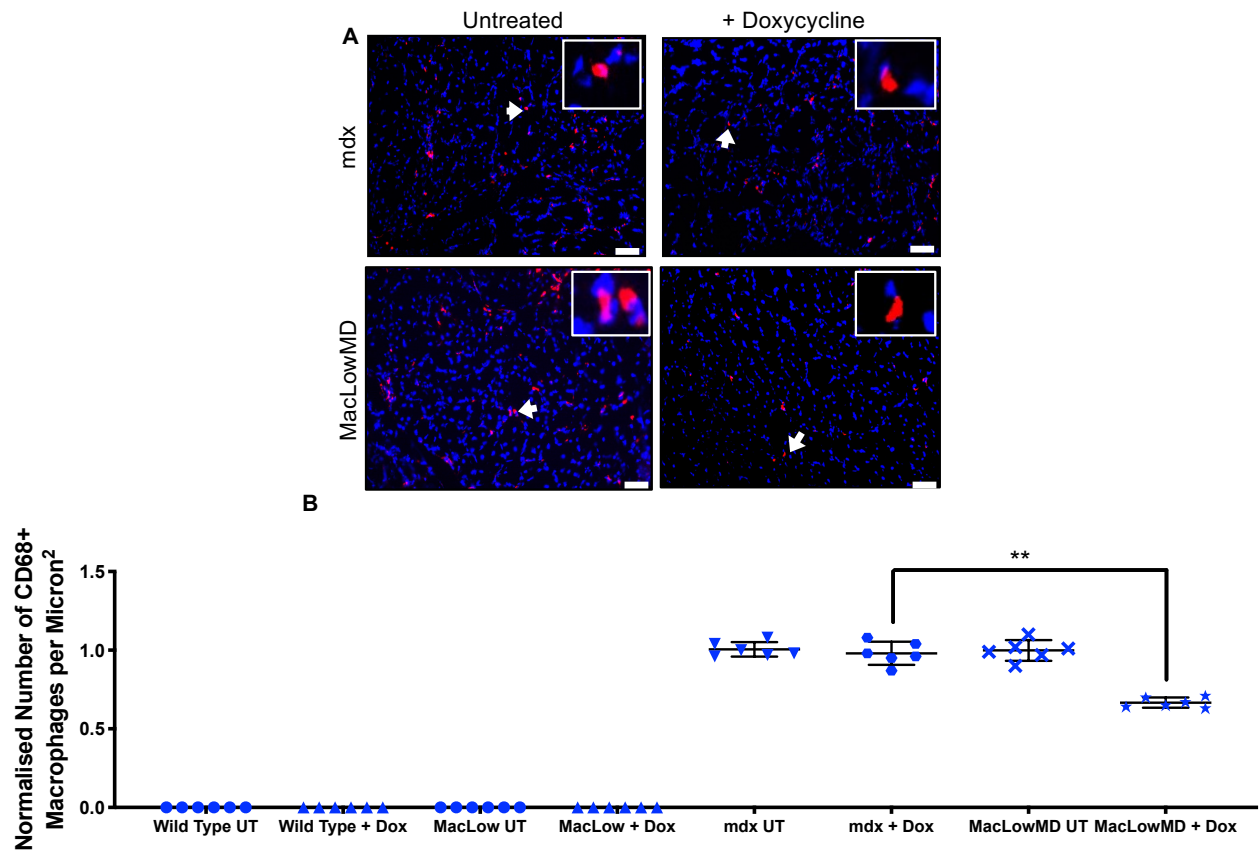


**Figure 3.2.2.3. Effect of six week doxycycline treatment on number of CD68+ macrophages in the diaphragm.** Complete diaphragm sections were stained and analysed for doxycycline treated n of 6 MacLowMD and mdx mice. **A)** Representative images of CD68 immunofluorescent stain of frozen diaphragm muscle. **B)** Quantification of number of CD68+ macrophages normalised to untreated controls. Macrophage morphology is indicated in inserts. Scale bar = 40µm. \*\* =  $p < 0.01$ , (unpaired T test). Data is expressed as mean ± SEM.

#### 3.2.2.4 Heart

Six week doxycycline treatment resulted in a 30% reduction in the number of CD68+ macrophages in MacLowMD doxycycline treated heart compared to doxycycline treated mdx heart muscle ( $0.71 \pm 0.01$  compared to  $1.02 \pm 0.01$ ,  $p < 0.001$ ) (**Figure 3.2.2.4. A and B**).

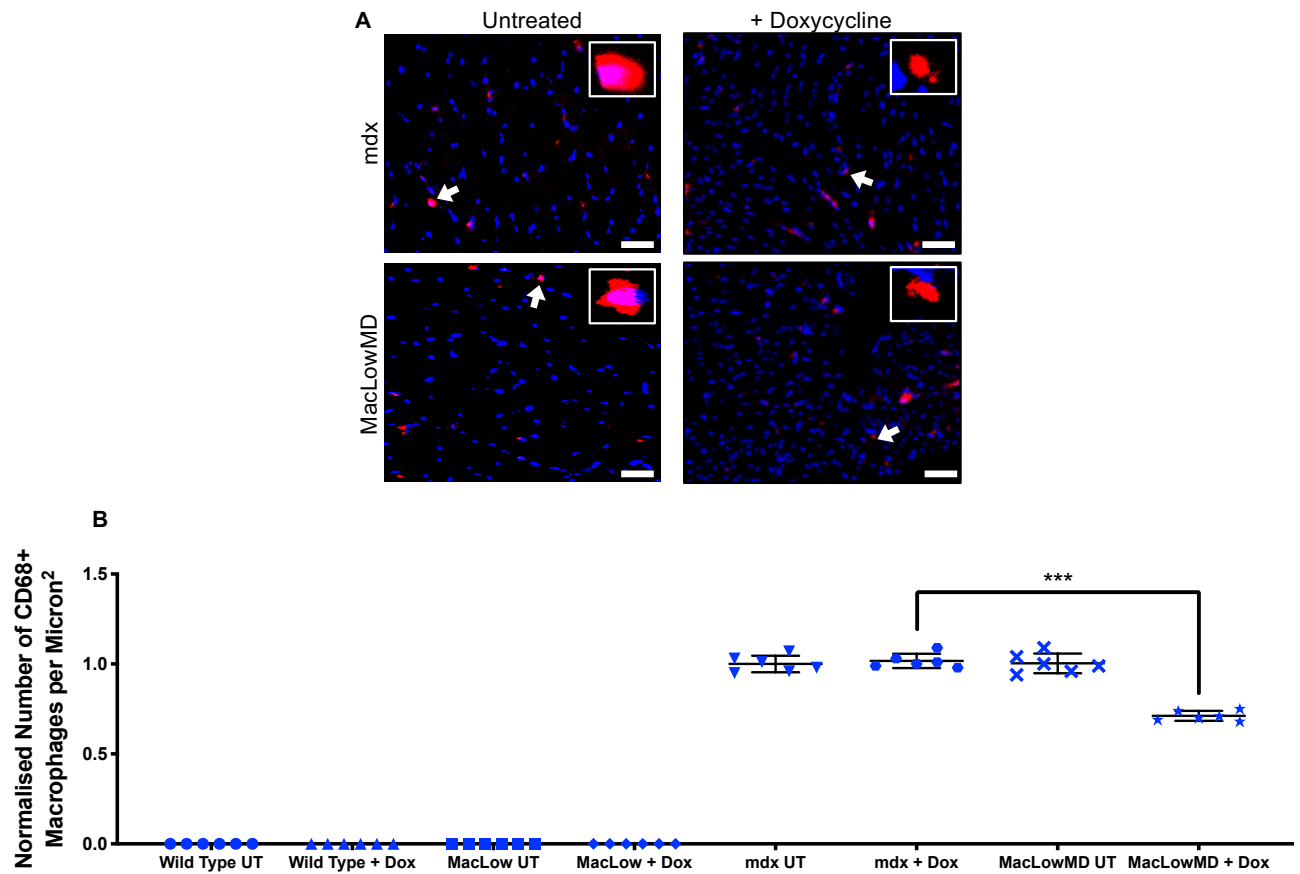


**Figure 3.2.2.4. Effect of six week doxycycline treatment on number of CD68+ macrophages in heart.** Complete heart sections were stained and analysed for n of 6 doxycycline treated MacLowMD and mdx mice. **A)** Representative images of CD68 immunofluorescent stain of frozen heart muscle. **B)** Quantification of number of CD68+ macrophages normalised to untreated controls. Macrophage morphology is indicated in inserts. Scale bar = 40µm. \*\*\* =  $p < 0.001$ , (unpaired T Test). Data is expressed as mean ± SEM.

### **3.2.3 Effect of Six Week Doxycycline Treatment on CD206 Positive Macrophages in Muscle**

The effect of six week doxycycline treatment on the number of CD206+ macrophages was assessed by immunofluorescent staining on frozen muscle sections. CD206+ macrophages were stained with Alexa Fluor 488 antibodies. CD206+ macrophages are indicated by arrows in panel **A** of each figure, as well as enlarged inserts. For each tissue analysed, all CD206+ macrophage counts were normalised to the average untreated value for that genotype (for example, MacLowMD + dox was normalised to MacLowMD UT).

#### **3.2.3.1 Tibialis Anterior**

As expected, quantification of CD206+ macrophages showed that in non-diseased wild type and MacLow TA muscle there were no CD206+ macrophages and significantly more CD206+ macrophages seen in diseased mdx and MacLowMD muscle ( $p < 0.0001$ ). Quantification of CD206+ macrophages showed that their numbers were increased by 40% in doxycycline treated MacLowMD compared to treated mdx TA muscle ( $1.4 \pm 0.08$  compared to  $1 \pm 0.02$ ,  $p < 0.01$ ) (**Figure 3.2.3.1. A and B**).

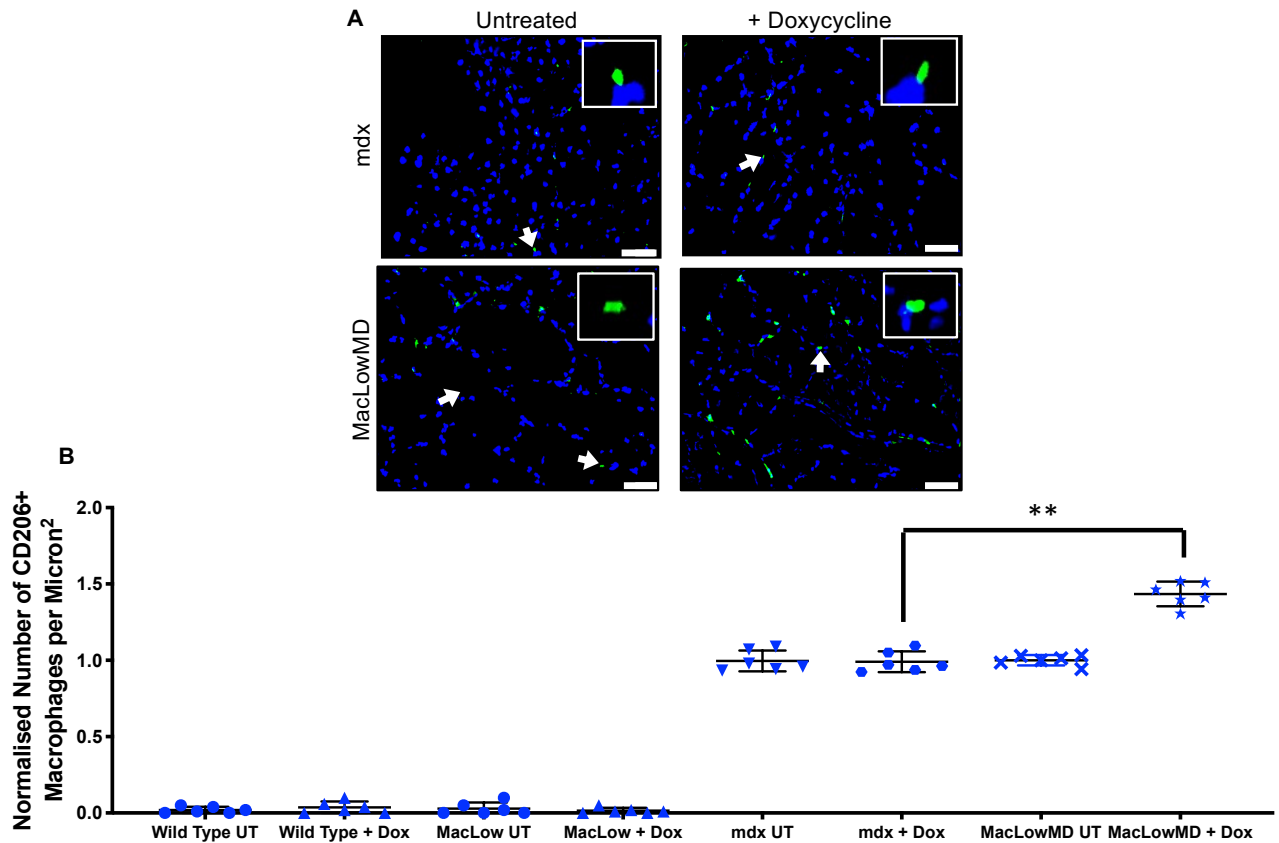


**Figure 3.2.3.1. Effect of six week doxycycline treatment on number of CD206 macrophages in TA.** Complete TA sections were stained and analysed for n of 6 doxycycline treated MacLowMD and mdx mice. **A)** Representative images of CD206 immunofluorescent stain of frozen TA muscle. **B)** Quantification of number of CD206+ macrophages normalised to untreated controls.

Macrophage morphology is indicated in inserts. Scale bar = 40 $\mu$ m. \*\* =  $p < 0.01$ , (unpaired T Test). Data is expressed as mean  $\pm$  SEM.

### 3.2.3.2 Quadriceps

Six week doxycycline treatment resulted in a 39% increase in the number of CD206+ macrophages in MacLowMD doxycycline treated quadriceps compared to doxycycline treated mdx quadriceps muscle ( $1.48 \pm 0.03$  compared to  $1.01 \pm 0.01$ ,  $p < 0.01$ ) (**Figure 3.2.3.2 A and B**).

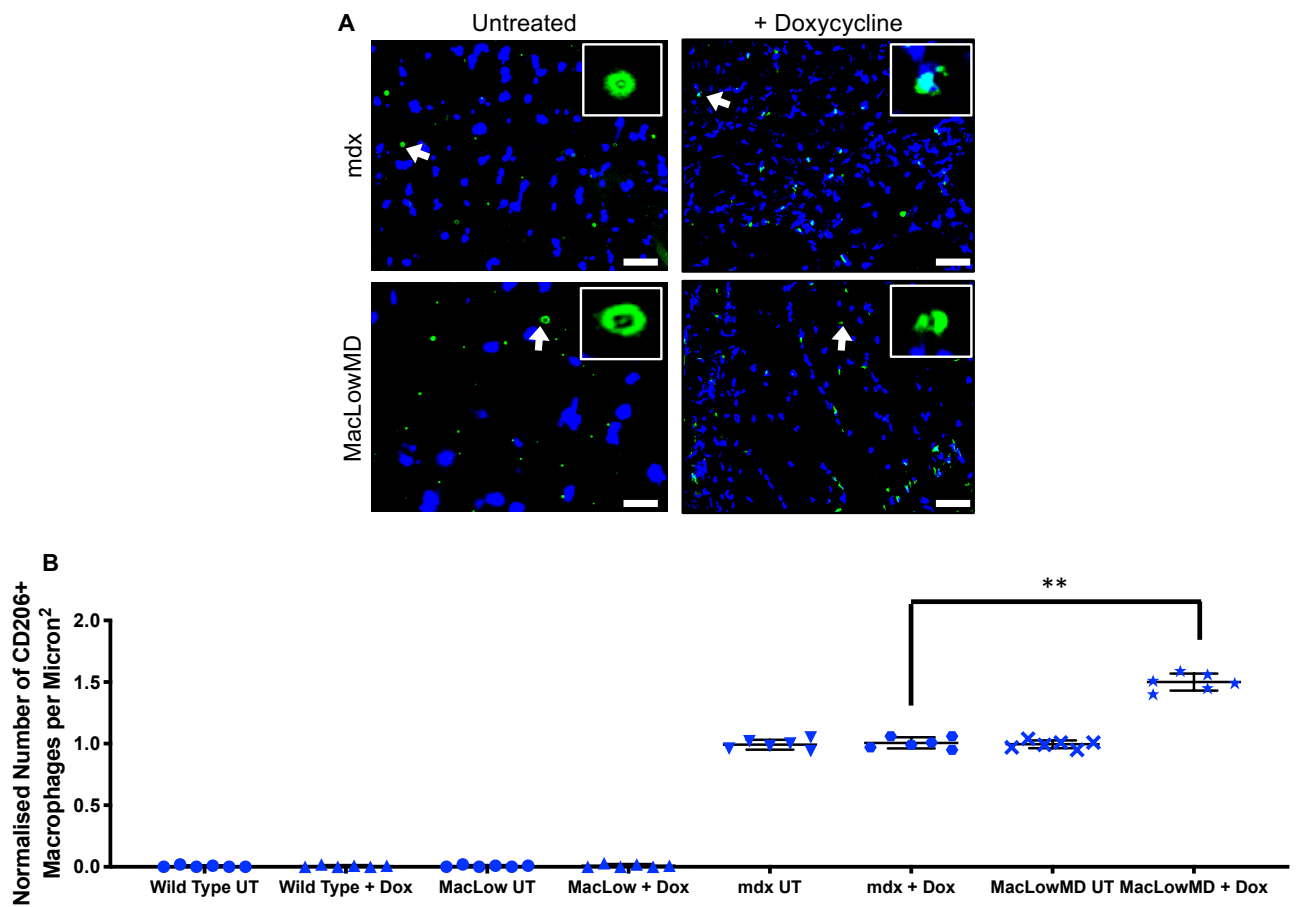


**Figure 3.2.3.2. Effect of six week doxycycline treatment on number of CD206 macrophages in quadricep.** Complete quadricep sections were stained and analysed for n of 6 doxycycline treated MacLowMD and mdx mice. **A)** Representative images of CD206 immunofluorescent stain of frozen quadricep muscle. **B)** Quantification of number of CD206+ macrophages normalised to untreated controls. Macrophage morphology is indicated in inserts. Scale bar = 40µm. \*\* =  $p < 0.01$ , (unpaired T Test). Data is expressed as mean ± SEM.

### 3.2.3.3 Diaphragm

Six week doxycycline treatment resulted in a 28% increase in the number of CD206+ macrophages in MacLowMD doxycycline treated diaphragm compared to doxycycline treated mdx diaphragm muscle ( $1.23 \pm 0.02$  compared to  $0.95 \pm 0.01$ ,  $p < 0.01$ ) (**Figure 3.2.3.3. A and B**).

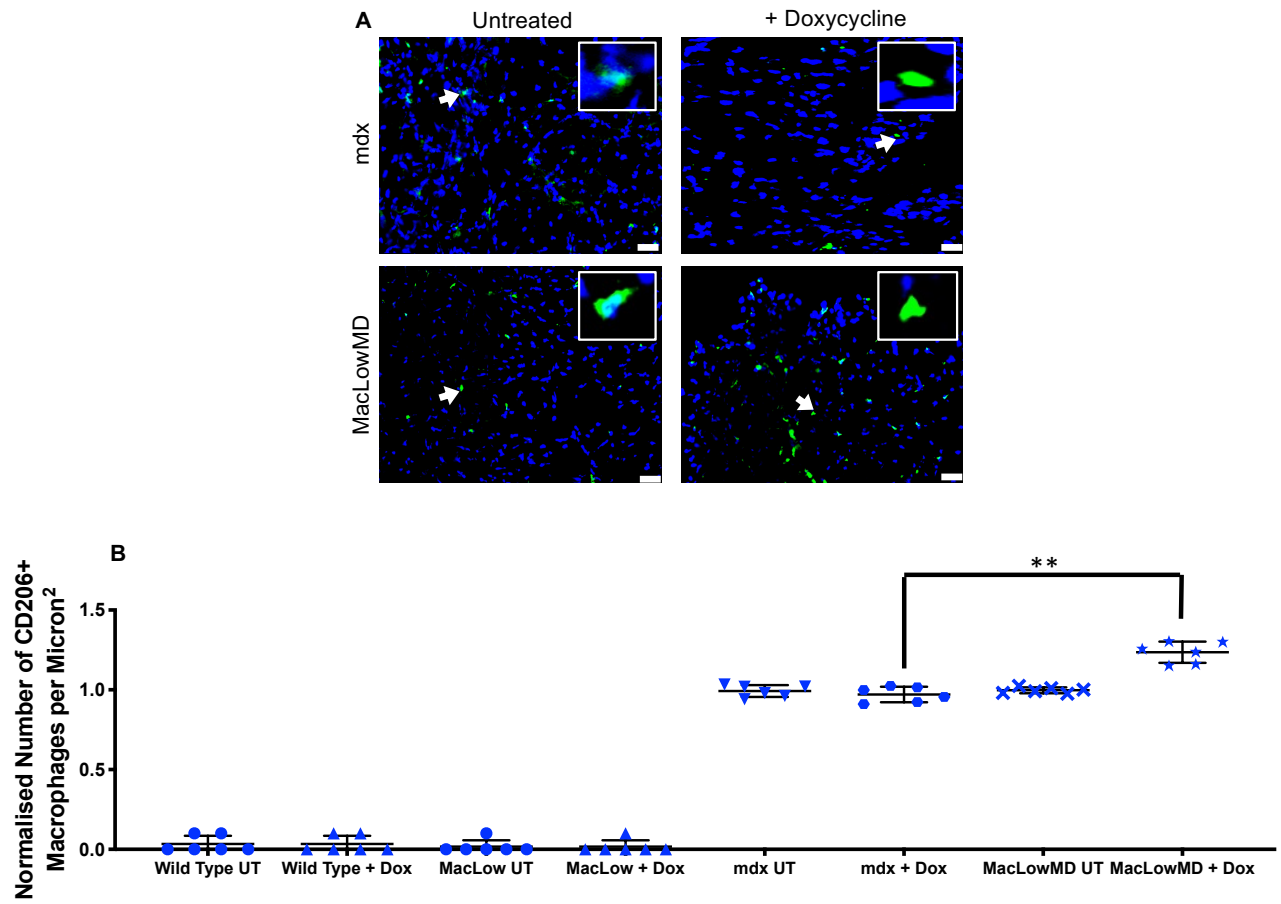


**Figure 3.2.3.3. Effect of six week doxycycline treatment on number of CD206 macrophages in diaphragm.** Complete diaphragm sections were stained and analysed for n of 6 doxycycline treated MacLowMD and mdx mice. **A)** Representative images of CD206 immunofluorescent stain of frozen diaphragm muscle. **B)** Quantification of number of CD206+ macrophages normalised to untreated controls. Macrophage morphology is indicated in inserts. Scale bar = 40 $\mu$ m. \*\* =  $p < 0.01$ , (unpaired T Test). Data is expressed as mean  $\pm$  SEM.

#### 3.2.3.4 Heart

Six week doxycycline treatment resulted in a 29% increase in the number of CD206+ macrophages in MacLowMD doxycycline treated heart compared to doxycycline treated mdx heart muscle ( $1.31 \pm 0.01$  compared to  $1.00 \pm 0.01$   $p < 0.001$ ) (**Figure 3.2.3.4. A and B**).

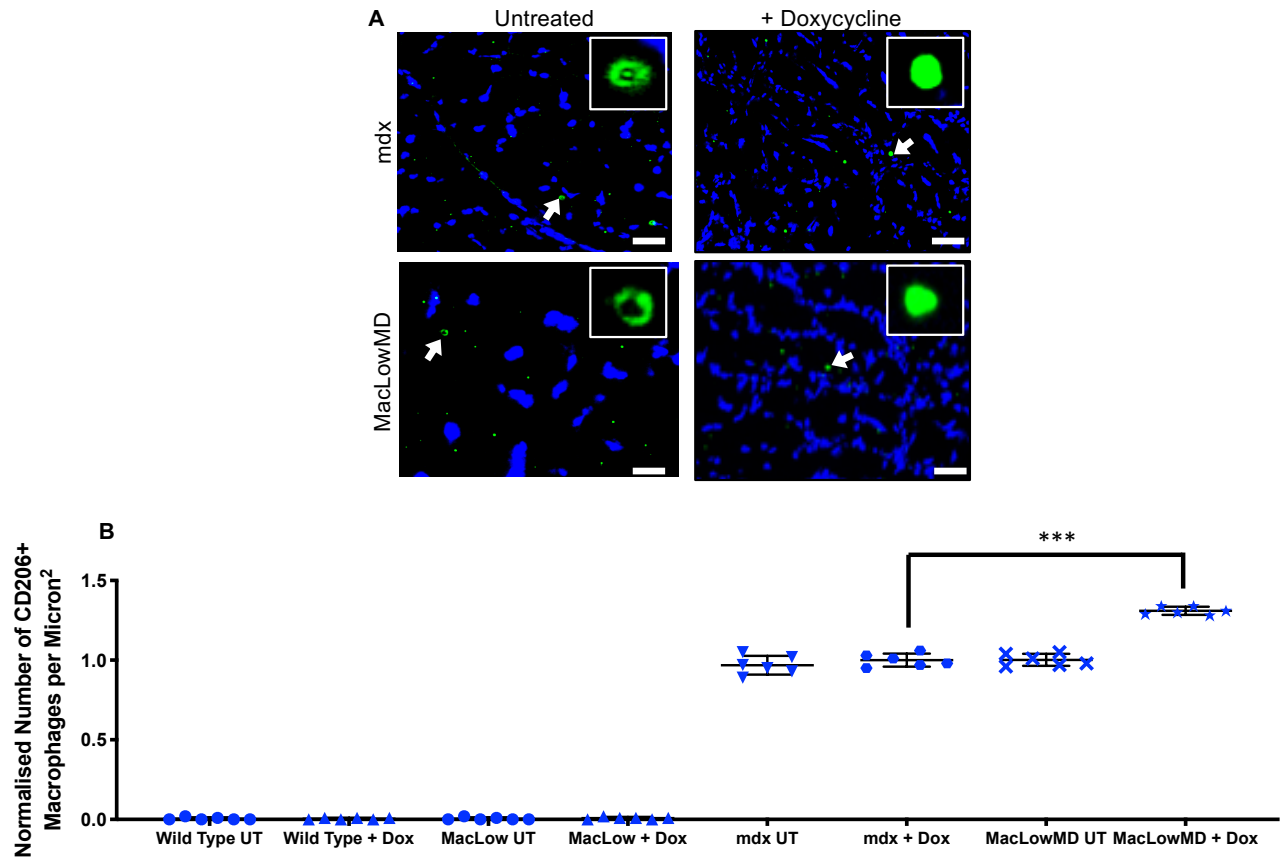


**Figure 3.2.3.3. Effect of six week doxycycline treatment on number of CD206 macrophages in heart.** Complete heart sections were stained and analysed for n of 6 doxycycline treated MacLowMD and mdx mice. **A)** Representative images of CD206 immunofluorescent stain of frozen heart muscle. **B)** Quantification of number of CD206+ macrophages normalised to untreated controls. Macrophage morphology is indicated in inserts. Scale bar = 40µm. \*\*\* =  $p < 0.001$ , (unpaired T Test). Data is expressed as mean ± SEM.

### **3.2.4 Effect of Six Week Doxycycline Treatment on CD163 Positive Macrophages in Muscle**

The impact of six week doxycycline treatment on the number of CD163+ macrophages was assessed by immunofluorescent staining on frozen muscle sections. CD163+ macrophages were stained with Alexa Fluor 488 fluorescence and are indicated by arrows in panel **A** of each figure, as well as enlarged panels. For each tissue analysed, all CD163+ macrophage counts were normalised to the average untreated value for that genotype (for example, MacLowMD + dox was normalised to MacLowMD UT).

#### **3.2.4.1 Tibialis Anterior**

Following six weeks doxycycline treatment quantification of CD163+ macrophages showed that, as expected, there were very few CD163+ macrophages seen in non- diseased wild type and MacLow TA muscle. There were significantly more CD163+ macrophages in the diseased mdx and MacLowMD TA ( $p < 0.0001$ ). Six week doxycycline treatment caused numbers of CD163+ macrophages to double in MacLowMD TA compared to treated mdx TA muscle ( $2.1 \pm 0.04$  compared to  $1 \pm 0.03$ ,  $p < 0.0001$ ). Doxycycline treatment had no impact on the number of CD163+ macrophages in mdx TA (**Figure 3.2.4.1. A and B**).

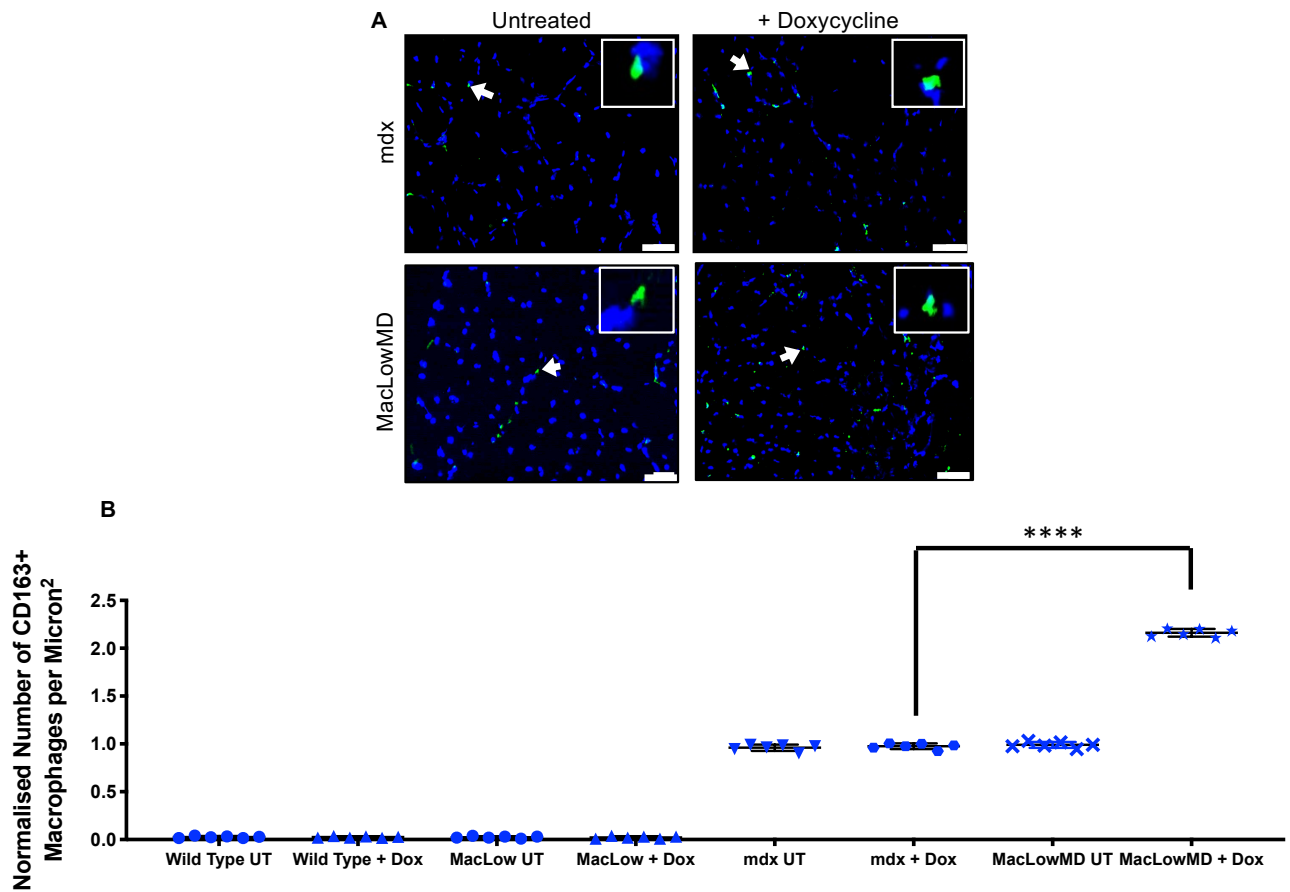


**Figure 3.2.4.1. Effect of six week doxycycline treatment on number of CD163 macrophages in TA.** Complete TA sections were stained and analysed for n of 6 doxycycline treated MacLowMD and mdx mice. **A)** Representative images of CD163 immunofluorescent stain of frozen TA muscle. **B)** Quantification of number of CD163+ macrophages normalised to untreated controls.

Macrophage morphology is indicated in inserts. Scale bar = 40 $\mu$ m. \*\*\*\* =  $p < 0.0001$ , (unpaired T test). Data is expressed as mean  $\pm$  SEM.

### 3.2.4.2 Quadriceps

Six week doxycycline treatment resulted in an 86% increase in the number of CD163+ macrophages in doxycycline treated MacLowMD quadriceps compared to treated mdx quadriceps muscle ( $1.93 \pm 0.03$  compared to  $1.01 \pm 0.02$ ,  $p < 0.001$ ) (**Figure 3.2.4.2. A and B**).

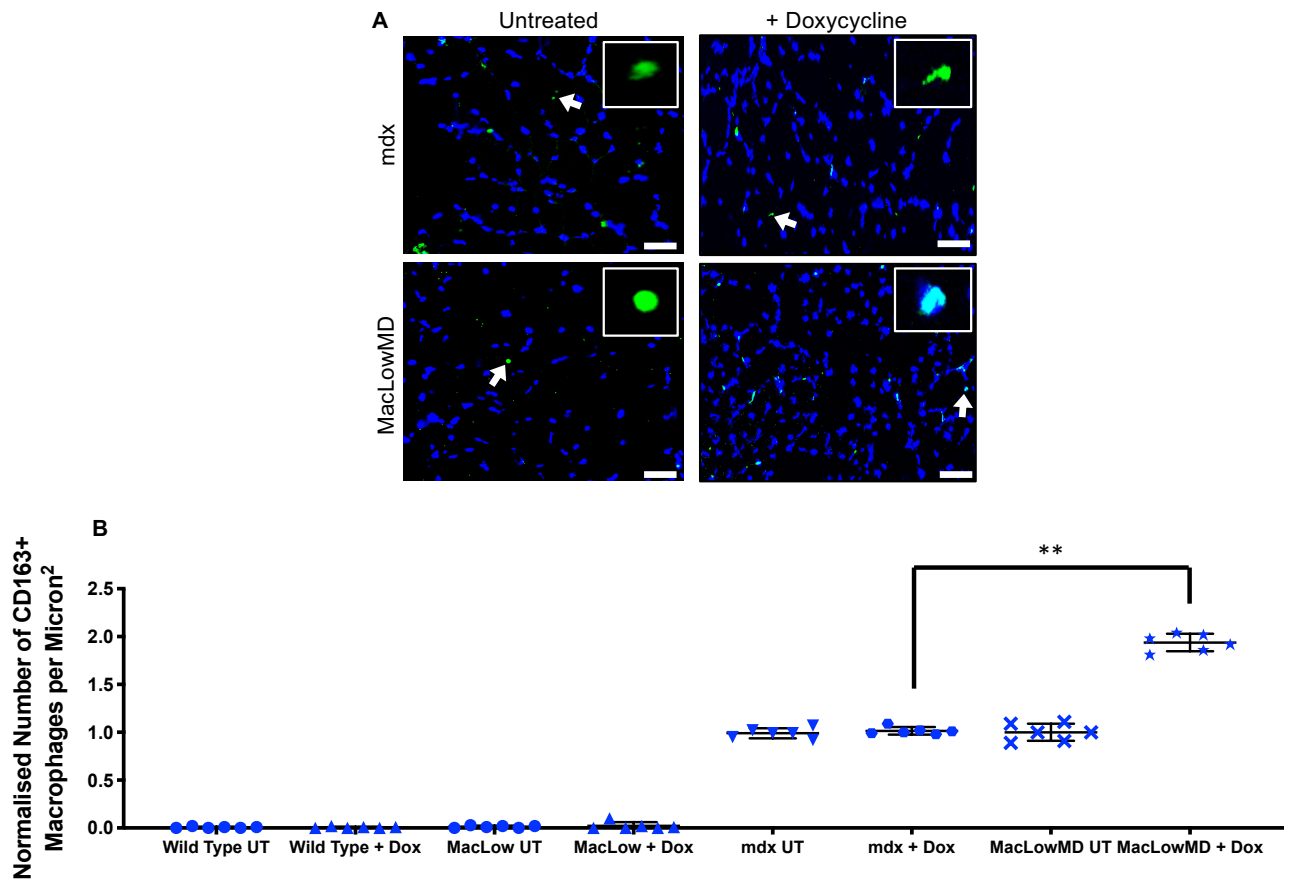


**Figure 3.2.4.2. Effect of six week doxycycline treatment on number of CD163 macrophages in quadriceps.** Complete quadriceps sections were stained and analysed for n of 6 doxycycline treated MacLowMD and mdx mice. **A)** Representative images of CD163 immunofluorescent stain of frozen quadriceps muscle. **B)** Quantification of number of CD163+ macrophages normalised to untreated controls. Macrophage morphology is indicated in inserts. Scale bar = 40µm. \*\*\* =  $p < 0.001$ , (unpaired T test). Data is expressed as mean  $\pm$  SEM.

### 3.2.4.3 Diaphragm

Six week doxycycline treatment resulted in a 59% increase in the number of CD163+ macrophages in doxycycline treated MacLowMD diaphragm compared to treated mdx diaphragm muscle ( $1.59 \pm 0.03$  compared to  $1.00 \pm 0.02$ ,  $p < 0.01$ ) (**Figure 3.2.4.3. A and B**).

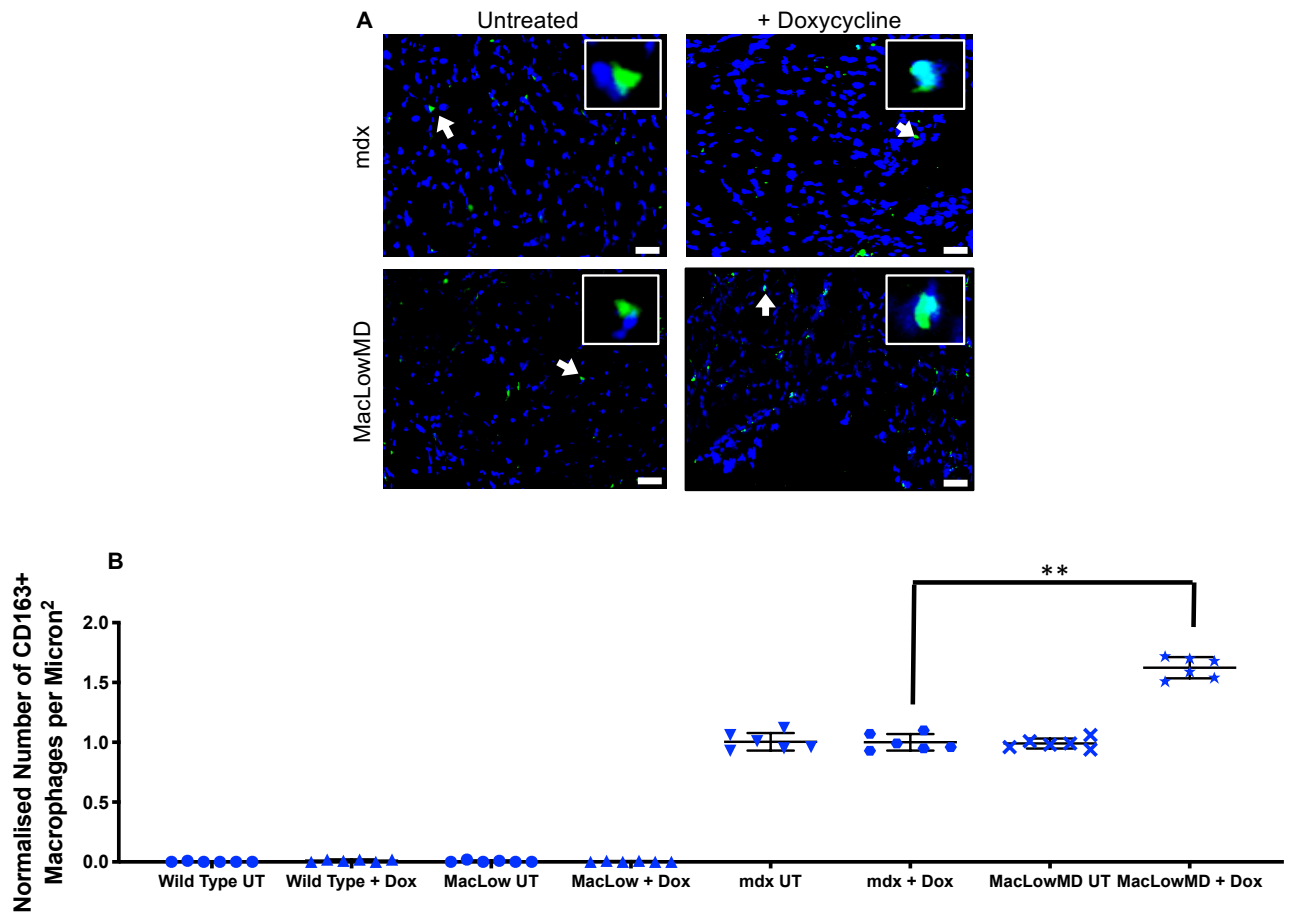


**Figure 3.2.4.3. Effect of six week doxycycline treatment on number of CD163 macrophages in diaphragm.** Complete diaphragm sections were stained and analysed for n of 6 doxycycline treated MacLowMD and mdx mice. **A)** Representative images of CD163 immunofluorescent stain of frozen diaphragm muscle. **B)** Quantification of number of CD163+ macrophages normalised to untreated controls. Macrophage morphology is indicated in inserts. Scale bar = 40µm. \*\* =  $p < 0.01$ , (unpaired T test). Data is expressed as mean ± SEM.

#### 3.2.4.4 Heart

Six week doxycycline treatment resulted in a 39% increase in the number of CD163+ macrophages in doxycycline treated MacLowMD heart compared to treated mdx heart muscle ( $1.41 \pm 0.01$  compared to  $1.01 \pm 0.01$ ,  $p < 0.001$ ) **(Figure 3.2.4.4. A and B).**

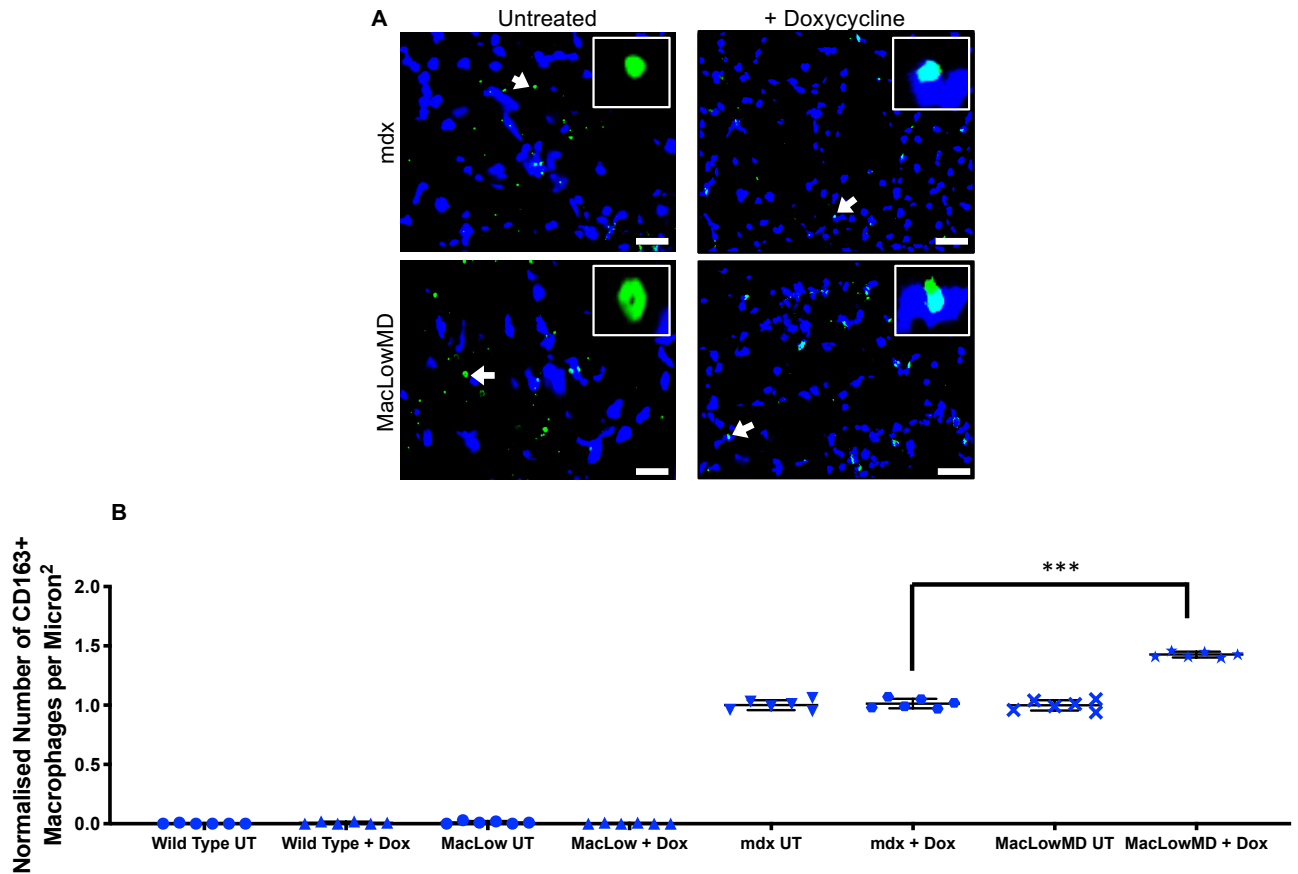


**Figure 3.2.4.4. Effect of six week doxycycline treatment on number of CD163 macrophages in heart.** Complete heart sections were stained and analysed for n of 6 doxycycline treated MacLowMD and mdx mice. **A)** Representative images of CD163 immunofluorescent stain of frozen heart muscle. **B)** Quantification of number of CD163+ macrophages normalised to untreated controls. Macrophage morphology is indicated in inserts. Scale bar = 40µm. \*\*\* =  $p < 0.001$ , (unpaired T test). Data is expressed as mean ± SEM.

### 3.3 Discussion

The aim of this chapter was to assess the effect of six week doxycycline treatment on the numbers of F4/80+ macrophages in liver, as well as the extent of CD68+ macrophage depletion and the impact on numbers of M2 CD206 and CD163 macrophages.

Following six weeks of doxycycline treatment a reduction in the number of F4/80+ cells was seen, however at a decreased level of 33% in MacLowMD liver compared to the previously observed reduction of 50% resulting from two weeks treatment (Miller *et al.*, unpublished). This decreased level of reduction between two week and six week doxycycline treatment was also observed in the number of CD68+ macrophages in diaphragm and heart muscle, which is consistent with the differences in the level of F4/80+ reduction.

Unexpectedly, six weeks doxycycline treatment had no significant impact on numbers of CD68+ macrophages within MacLowMD TA and quadricep muscle. However, a significant 30% reduction in numbers of CD68+ macrophages was observed in MacLowMD diaphragm and heart. This is a similar level of reduction as seen in F4/80+ macrophages in six week treated liver. M1 macrophages in mdx muscle deactivate as the disease progresses from the acute peak of pathology to the regenerative phase of the disease (Villalta *et al.*, 2009). As hindlimb muscles, including TA and quadriceps, are the first muscles affected in the mdx mouse (Villalta *et al.*, 2011b), it is possible that the majority of M1, CD68+ macrophages have been deactivated by the time the tissue has been harvested at ten weeks.

Six week doxycycline treatment had a significant effect on numbers of M2 macrophages, with numbers of CD163+ macrophages being doubled in doxycycline treated MacLowMD TA. As previously described in Section 3.1 of this chapter, macrophages are a plastic population with M2a, CD206+ macrophages competing with CD68+ macrophages for arginine (Villalta *et al.*, 2009). As CD68+ macrophages have been depleted, this allows CD206+ to have greater access to arginine and as such results in increased numbers of M2a macrophages. Furthermore, M2c, CD163+ macrophages deactivate M1 macrophages. Increased numbers of CD163+ macrophages observed throughout all tissue types would result in further reduction in numbers of CD68+ macrophages.

As expected, for all muscle macrophage markers there were negligible numbers of macrophages in non- diseased genotypes for all tissues (wild type and MacLow). Furthermore, for all muscle macrophage markers, as well as F4/80, doxycycline treatment had no effect on the number of macrophages in mdx and wild type muscles lacking the MacLow potential of inducible CD68+ macrophage depletion. This, along with results comparing doxycycline treated mdx to MacLowMD, indicates that any observed effects are occurring as a result of reduction of CD68+ macrophage numbers, rather than purely due to doxycycline treatment.

Findings in this chapter proved similar to those of Duffield *et al.*, 2015, who used diphtheria injection in order to deplete macrophages in transgenic

CD11b-DTR mice expressing diphtheria toxin receptor. Duffield *et al.*'s results showed a 48% reduction in number of F4/80+ macrophages in liver, close to the 33% reduction in F4/80+ cells in liver discussed in this chapter (Duffield *et al.*, 2015). Unlike the MacLowMD model, Duffield *et al.*'s model targeted all macrophages non-specifically. The specific nature of the MacLowMD model in targeting only CD68+ macrophages may potentially explain the discrepancy between findings in this chapter and Duffield *et al.* A greater discrepancy between numbers of F4/80+ macrophages is seen between the MacLowMD model and a number of other studies, including those by Mojumdar *et al.*, 2014 (57% reduction in number of F4/80+ macrophages in diaphragm) and Kawanishi *et al.*, 2016 (80% reduction in number of F4/80+ macrophages in gastrocnemius muscle) (Mojumdar *et al.*, 2014) (Kawanishi *et al.*, 2016).

A significant limitation of work performed in this chapter is the lack of a dual stain. Due to the plasticity of macrophages, and the potential for both M1 and M2 markers to be expressed at the same time, a dual stain would ideally have been included in this work. Dual stains would include either F4/80 and CD68, CD206 and CD163, in order to confirm both that stain is a macrophage cell, as well as level of current subtype; or between CD68 and CD206 or CD163 in order to ensure that the same macrophage is not being quantified incorrectly or multiple times, as well as allowing a clearer understanding into pro/ anti-inflammatory switch. As the results stand, they lack conviction in ensuring that macrophages stained are true CD68+ (M1) or true CD206+ / CD163+ (M2) macrophages. A further limitation of this chapter is the use of CD68 as a marker of M1 macrophages. A number of cytochemical studies showed that

low expression of CD68 was found in several cell types including umbilical cord mesenchymal stem cells (La Rocca, Anzalone and Farina, 2009), fibroblasts, endothelial cells (Gottfried *et al.*, 2008), and various tumour cell lines, as well as intimal smooth muscle cells of human arteries (Andreeva, Pugach and Orekhov, 1997). The specificity of CD68, both as a marker of M1 macrophages, and also a promotor in the MacLow model, must be questioned. Furthermore, CD68 tends to be a more common macrophage in human, rather than murine studies. A more appropriate, and more specific, murine M1 marker would be iNOS (Villalta *et al.*, 2011b).

In summary 6-week doxycycline treatment of MacLowMD mice resulted in varying degrees of CD68+ macrophage depletion in the four muscles studied to date. Interestingly, across all four muscles an increase in M2 macrophage numbers were seen. The potential for the use of the MacLow model to reduce muscle degeneration is heightened due to the observed increase in numbers of anti-inflammatory, repair phenotype, M2 macrophages following inducible CD68+ macrophage deletion.

The next stage of this project was to assess how the effect of CD68+ macrophage depletion on the balance of macrophage phenotype in muscle impacted on the extent of muscle damage. This is discussed in the next results chapter, Chapter 4.

## Chapter 4: The Impact of CD68+ Macrophage Depletion on The Level of Muscle Damage

---

### 4.1 Introduction

A number of previous studies have indicated that macrophage depletion results in a reduction in muscle fibre damage, indicating a primary role for macrophages in DMD pathogenesis (Wehling, Spencer and Tidball, 2001), (Kawanishi *et al.*, 2016). A 2001 study by Wehling *et al.* showed that the ablation of muscle macrophages from mdx mice through repeated intraperitoneal injections of anti-F4/80 antibodies resulted in a 75% reduction of muscle cell necrosis observed through immunofluorescent staining. (Wehling *et al.*, 2001). In 2016 Kawanishi *et al.* found that macrophage depletion by clodronate liposome injection led to a significant reduction in the number of muscle fibres stained positive following anti IgG antibody staining after exhaustive exercise in male C57BL/6J mice. Presence of IgG in the muscle fibre cytosol indicates the presence of muscle membrane lesions, signifying muscle fibre damage. Clodronate is phagocytosed by macrophages using liposome vehicles (Summan *et al.*, 2006). Clodronate accumulates intracellularly and irreversibly damages the macrophage causing it to die by apoptosis. This mechanism allows clodronate liposome mediated depletion of macrophages, as identified by histological analysis using pan- macrophage marker, F4/80.

As well as specifically studying muscle damage by using immunofluorescent staining, it is also possible to use biomarkers. Historically, the biomarker most commonly used for muscle damage was serum creatine kinase (CK). CK is normally located within the interior of muscle. Rupturing of the plasma membrane due to dystrophin deficiency results in CK leaking from the interior of muscle cells into the bloodstream (serum). This means that levels of CK can be used as a measure of muscle damage. However, CK levels vary in response to physical activity, age and muscle injury, and as such are not an appropriate biomarker for studying the severity of pathology or monitoring treatment efficiency (Gasper and Gilchrist, 2005).

A 2015 study by Rouillon *et al.* assessed the effect of using myomesin, particularly myomesin-3 (MYOM3), the myofibrillar structural protein, as a biomarker of muscle damage in DMD. Myomesin, much like CK, is a protein normally located in muscle that leaks into blood following rupturing of the muscle plasma membrane. Rouillon *et al.* found that MYOM3 as a biomarker showed less variability than CK in mdx mice, suggesting that MYOM3 is a more relevant biomarker for monitoring therapeutic outcome and pathology severity in DMD (Rouillon *et al.*, 2015).

Currently, there has been no previous investigation of the effect of specific depletion of CD68+ macrophages on muscle damage. The previous results chapter validated the MacLowMD model, showing a reduction in numbers of M1 macrophages across the diaphragm and heart, and an increase in numbers of M2 macrophages across all muscles studied.

In this chapter, the aim was to determine the impact of CD68+ macrophage depletion on muscle fibre damage.

This was achieved by:

1. IgG staining of muscle to quantify muscle fibre damage.
2. Quantification of MYOM3 blood serum levels by MYOM3 western blot.

As previously mentioned, presence of IgG in the muscle fibre cytosol indicates the presence of muscle membrane lesions, signifying muscle fibre damage. Muscle fibre damage was assessed in the muscle of MacLow-MD mice treated with doxycycline for either two or six weeks. For two week doxycycline treatment TA muscle was analysed, and for six week doxycycline treatment four muscle types- TA, diaphragm, quadriceps and heart, were used to study muscle fibre damage.

Western blot analysis of serum from six week doxycycline treated mice using the myomesin MYOM3 biomarker was also used as an indicator of muscle damage. Results from MYOM3 western blots are used as a second line for evidence, alongside IgG staining, for the impact of macrophage depletion on muscle damage.

## 4.2 Results

### 4.2.1 Effect of Two Week Doxycycline Treatment on Muscle Fibre Damage

The effect of two week doxycycline treatment of MacLowMD mice has previously been shown to lead to 50% CD68+ macrophage depletion (Miller *et al.*, unpublished). Mice from this study were culled at the age of 4 weeks, the initial stage where macrophages become involved in muscle damage. In section 4.2.1.1 of this chapter, the impact of two week doxycycline treatment on muscle fibre damage will be investigated. Due to tissue availability, only MacLowMD mice muscle is examined in this section.

#### 4.2.1.1 Tibialis Anterior

In order to assess the impact of two week doxycycline treatment on the level of muscle fibre damage frozen TA muscle sections were IgG immunofluorescent stained. Presence of IgG within the cytosol of damaged muscle fibres is indicated by green fluorescence (**Figure 4.2.1. A, arrows**).

Complete TA sections were stained and analysed for four doxycycline treated and four untreated MacLowMD samples. FIJI version 2 software was used to measure the cross-sectional area of damaged muscle fibres. The amount of fluorescence (e.g. presence of IgG) was calculated as a percentage of the total tissue.

Quantification of IgG staining revealed that following two week doxycycline treatment muscle fibre damage was significantly reduced by 69% when

comparing untreated MacLowMD ( $0.39 \pm 0.10$ ) with treated MacLowMD TA ( $0.12 \pm 0.01$ ) ( $p < 0.05$ ) (**Figure 4.2.1. B**). Muscles were of a comparable size between the two groups, average for treated MacLowMD TA was  $10472.63 \mu\text{m}^2$ , and untreated MacLowMD TA was  $10962 \mu\text{m}^2$ . It is important that muscles are of a comparable size because if muscle area was smaller then the percentage of IgG stained would be bigger and results would be skewed. Furthermore, DMD muscle has pockets of damage, further establishing the need for whole muscles of comparable sizes to be analysed.

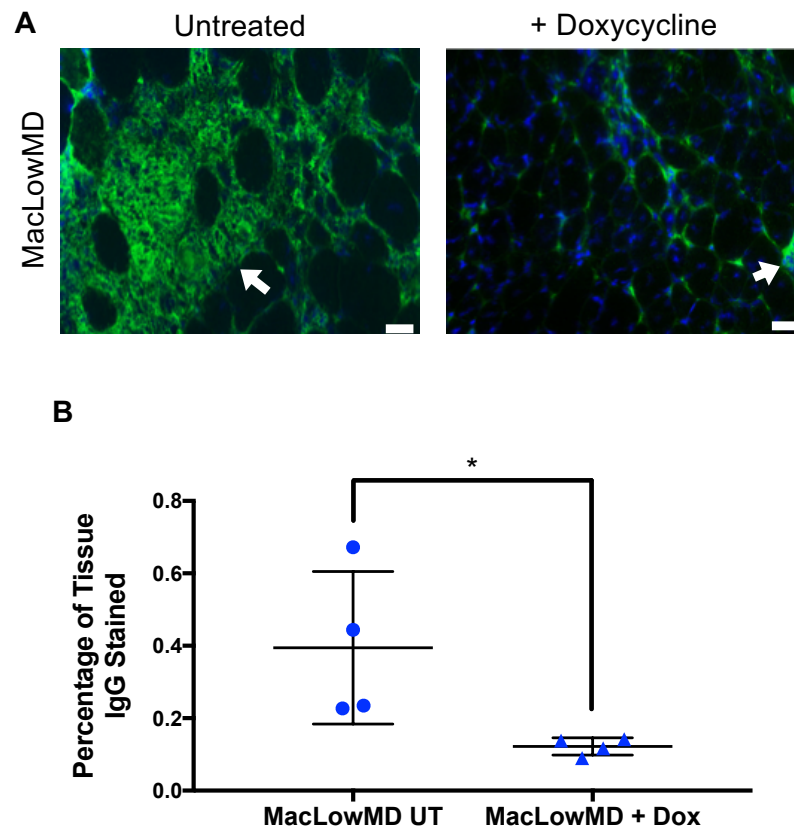


**Figure 4.2.1. Effect of two week doxycycline treatment on IgG staining in MacLowMD TA muscle.** Complete TA sections were stained and analysed n of 4 doxycycline untreated and treated MacLowMD mice. **A)** Representative images of IgG immunofluorescent stain of frozen TA muscle. Arrows indicate examples of IgG stained muscle fibres. **B)** Quantification of percentage of tissue IgG stained. Scale bar = 50µm. \* =  $p < 0.05$ , (unpaired T Test). Data is expressed as mean  $\pm$  SEM.

## **4.2.2 Effect of Six Week Doxycycline Treatment on Muscle Fibre Damage**

Results in this Chapter 4.2.2 will discuss the effect of six week doxycycline treatment on muscle fibre damage. Results aimed to understand the impact of depleting CD68+ macrophages on the level of muscle damage.

### **4.2.2.1 Tibialis Anterior**

Complete TA sections were stained and analysed for three doxycycline treated and untreated MacLowMD, mdx, MacLow and wild type samples. Findings in this and further results chapters focus on comparisons between doxycycline treated mdx and doxycycline treated MacLowMD muscle. This allows us to ensure that any effects are occurring due to the MacLowMD model and CD68+ macrophage depletion in diseased tissue.

A complete IgG stained TA section can be seen in Chapter 8.1 Appendix I.

Quantification of IgG staining revealed that, as expected, in non- diseased wild type and MacLow TA muscle there was no muscle fibre damage. There was significantly more IgG staining in the diseased mdx and MacLowMD compared to healthy MacLow and wild type muscle (0% in MacLow and wild type muscle compared to 0.23% mdx untreated, 0.23% mdx treated, 0.22% MacLowMD untreated and 0.12% MacLowMD treated,  $p < 0.0001$ ). Doxycycline treatment had no impact on the amount of IgG staining in mdx TA (0.23% mdx untreated compared to 0.23% mdx treated) confirming that doxycycline treatment alone does not result in muscle damage. Results showed that the amount of IgG staining was reduced by 47% in treated MacLowMD TA compared to treated

mdx TA ( $0.12 \pm 0.01$  compared to  $0.23 \pm 0.006$ ,  $p < 0.01$ ) (**Figure 4.2.2.1. A & B**). Muscles were of a comparable size between the two groups, average for treated mdx TA was  $11809.5 \mu\text{m}^2$ , and treated MacLowMD TA was  $12006 \mu\text{m}^2$ .

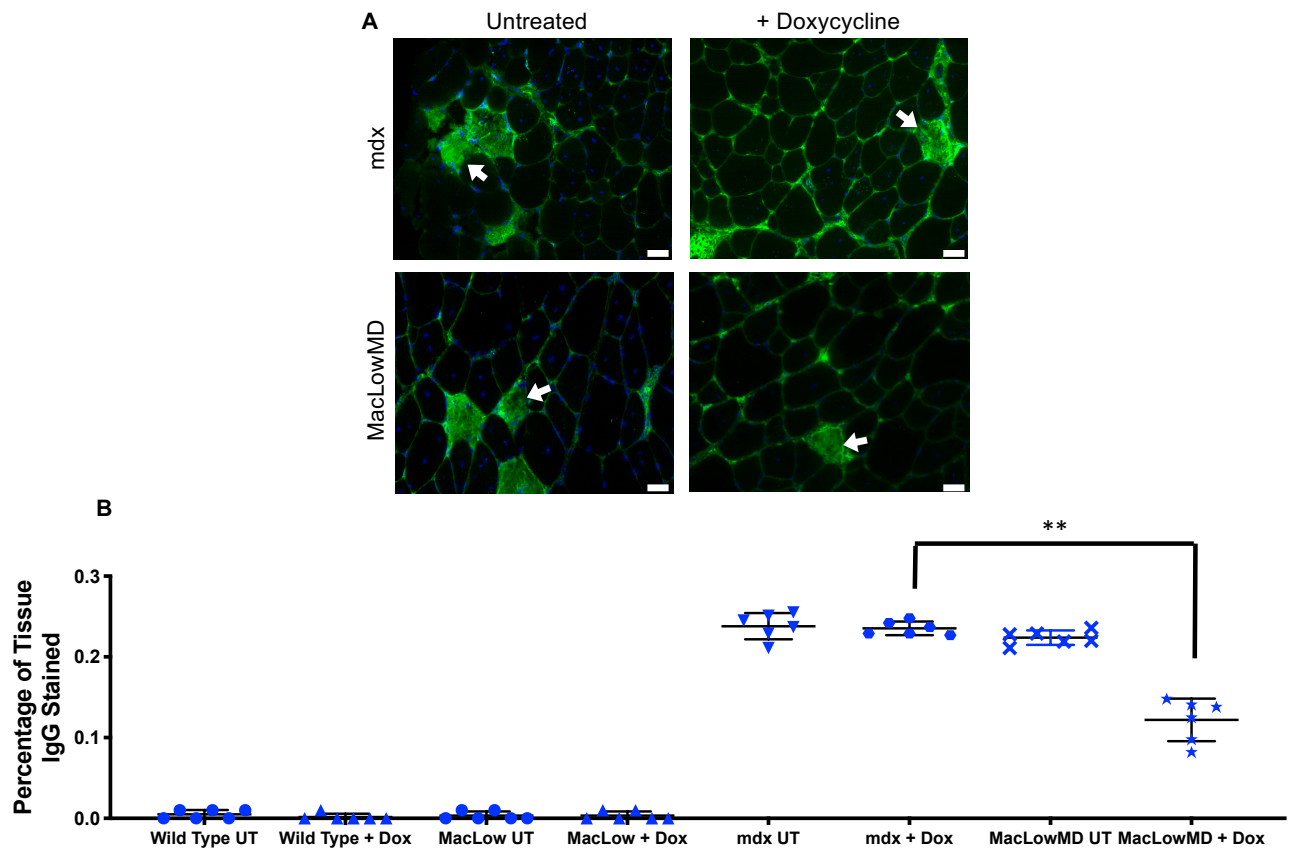


**Figure 4.2.2.1. Effect of six week doxycycline treatment on IgG staining in MacLowMD and mdx TA muscle.** Complete TA sections were stained and analysed for n of 6 doxycycline treated MacLowMD and mdx mice. **A)** Representative images of IgG immunofluorescent stain of frozen TA muscle. Arrows indicate examples of IgG stained muscle fibres. **B)** Quantification of percentage of tissue IgG stained. Scale bar = 50µm. \* =  $p < 0.01$ , (unpaired T Test). Data is expressed as mean  $\pm$  SEM.

#### 4.2.2.2 Quadriceps

Quantification of IgG staining revealed that, as expected, in non-diseased wild type and MacLow quadricep muscle there was no muscle fibre damage. There was significantly more IgG staining in the diseased mdx and MacLowMD compared to healthy MacLow and wild type quadricep muscle (0% in MacLow and wild type muscle compared to 0.95% mdx untreated, 0.97% mdx treated, 0.99% MacLowMD untreated and 0.53% MacLowMD treated) ( $p < 0.0001$ ). Doxycycline treatment had no impact on the amount of IgG staining in mdx quadricep (0.95% mdx untreated compared to 0.97% mdx treated). Results showed that the amount of IgG staining was reduced by 45% in treated MacLowMD quadricep compared to treated mdx quadricep ( $0.97 \pm 0.002$  compared to  $0.53 \pm 0.04$ ,  $p < 0.01$ ) (**Figure 4.2.2.2. A and B**). Muscles were of a comparable size between the two groups, average area for treated mdx quadriceps was  $4176\mu\text{m}^2$ , and treated MacLowMD quadriceps was  $3993\mu\text{m}^2$ .

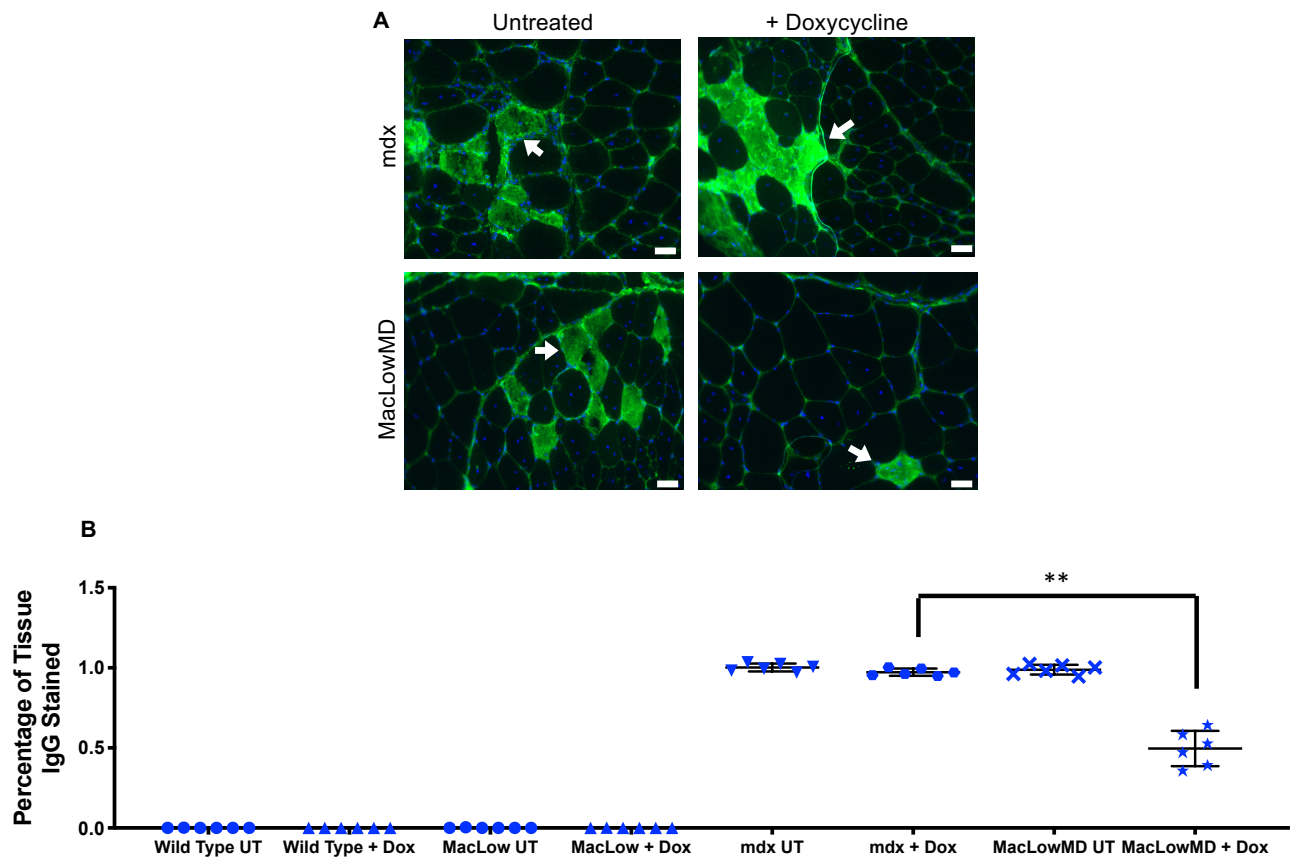


**Figure 4.2.2.2. Effect of six week doxycycline treatment on IgG staining in MacLowMD and mdx quadriceps.** Complete quadriceps sections were stained and analysed for n of 6 doxycycline treated MacLowMD and mdx mice. **A)** Representative images of IgG immunofluorescent stain of frozen quadriceps muscle. Arrows indicate examples of IgG stained muscle fibres. **B)** Quantification of percentage of tissue IgG stained.

Scale bar = 50µm. \*\* =  $p < 0.01$ , (unpaired T Test). Data is expressed as mean ± SEM.

#### 4.2.2.3 Diaphragm

As anticipated, quantification of IgG staining showed that in non-diseased wild type and MacLow diaphragm muscle there was no muscle fibre damage. Significantly more IgG staining was seen in diseased mdx and MacLowMD muscle (0% in MacLow and wild type muscle compared to 1.29% mdx untreated, 1.33% mdx treated, 1.28% MacLowMD untreated and 0.86% MacLowMD treated) ( $p < 0.0001$ ). Six week doxycycline treatment had no impact on the amount of IgG staining in mdx diaphragm (1.29% mdx untreated, 1.33% mdx treated). Quantification of IgG staining showed that muscle fibre damage was reduced by 35% in doxycycline treated MacLowMD compared to treated mdx diaphragm muscle ( $0.86 \pm 0.01$  compared to  $1.32 \pm 0.02$ ,  $p < 0.01$ ) (**Figure 4.2.2.3. A and B**). Muscles were of a comparable size between the two groups, average area for treated mdx diaphragm was  $6823.5\mu\text{m}^2$ , and treated MacLowMD diaphragm was  $7187.5\mu\text{m}^2$ .

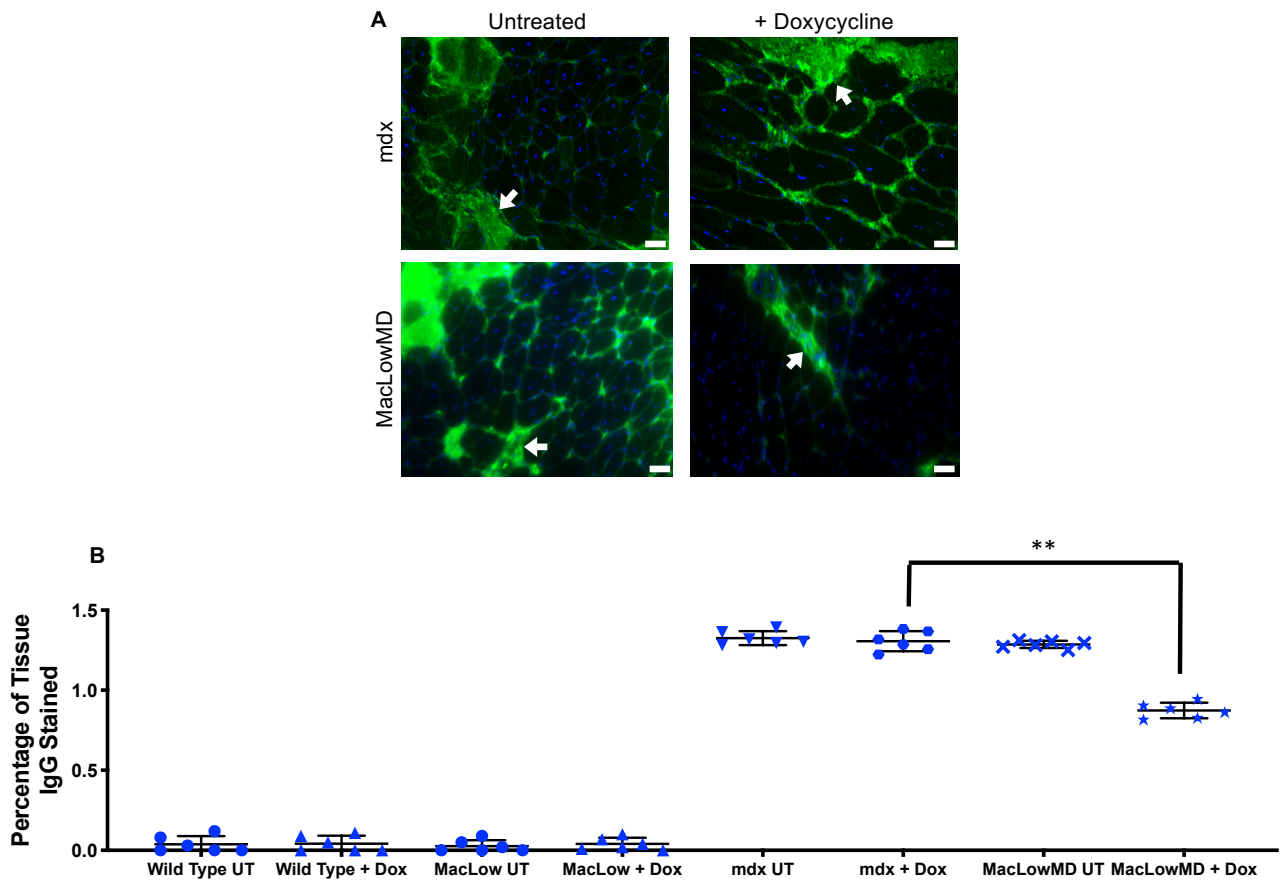


**Figure 4.2.2.3. Effect of six week doxycycline treatment on IgG staining in MacLowMD and mdx diaphragm.** Complete diaphragm sections were stained and analysed for n of 6 doxycycline treated MacLowMD and mdx mice. **A)** Representative images of IgG immunofluorescent stain of frozen diaphragm muscle. Arrows indicate examples of IgG stained muscle fibres. **B)** Quantification of percentage of tissue IgG stained.

Scale bar = 50µm. \* =  $p < 0.05$ , (unpaired T Test). Data is expressed as mean  $\pm$  SEM.

#### 4.2.2.4 Heart

As anticipated, quantification of IgG staining showed that in non-diseased wild type and MacLow heart muscle there was no muscle fibre damage. Significantly more IgG staining was seen in diseased mdx and MacLowMD muscle (0% in MacLow and wild type muscle compared to 0.88% mdx untreated, 0.86% mdx treated, 0.87% MacLowMD untreated and 0.59% MacLowMD treated) ( $p < 0.0001$ ). Six week doxycycline treatment had no impact on the amount of IgG staining in mdx heart (0.88% mdx untreated compared to 0.86% mdx treated). Quantification of IgG staining showed that muscle fibre damage was reduced by 31% in doxycycline treated MacLowMD compared to treated mdx heart muscle ( $0.86 \pm 0.02$  compared to  $0.59 \pm 0.02$ ,  $p < 0.05$ ) (**Figure 4.2.2.4. A and B**). Muscles were of a comparable size between the two groups, average area for treated mdx heart was  $2349\mu\text{m}^2$  and treated MacLowMD heart was  $1913.5\mu\text{m}^2$ .

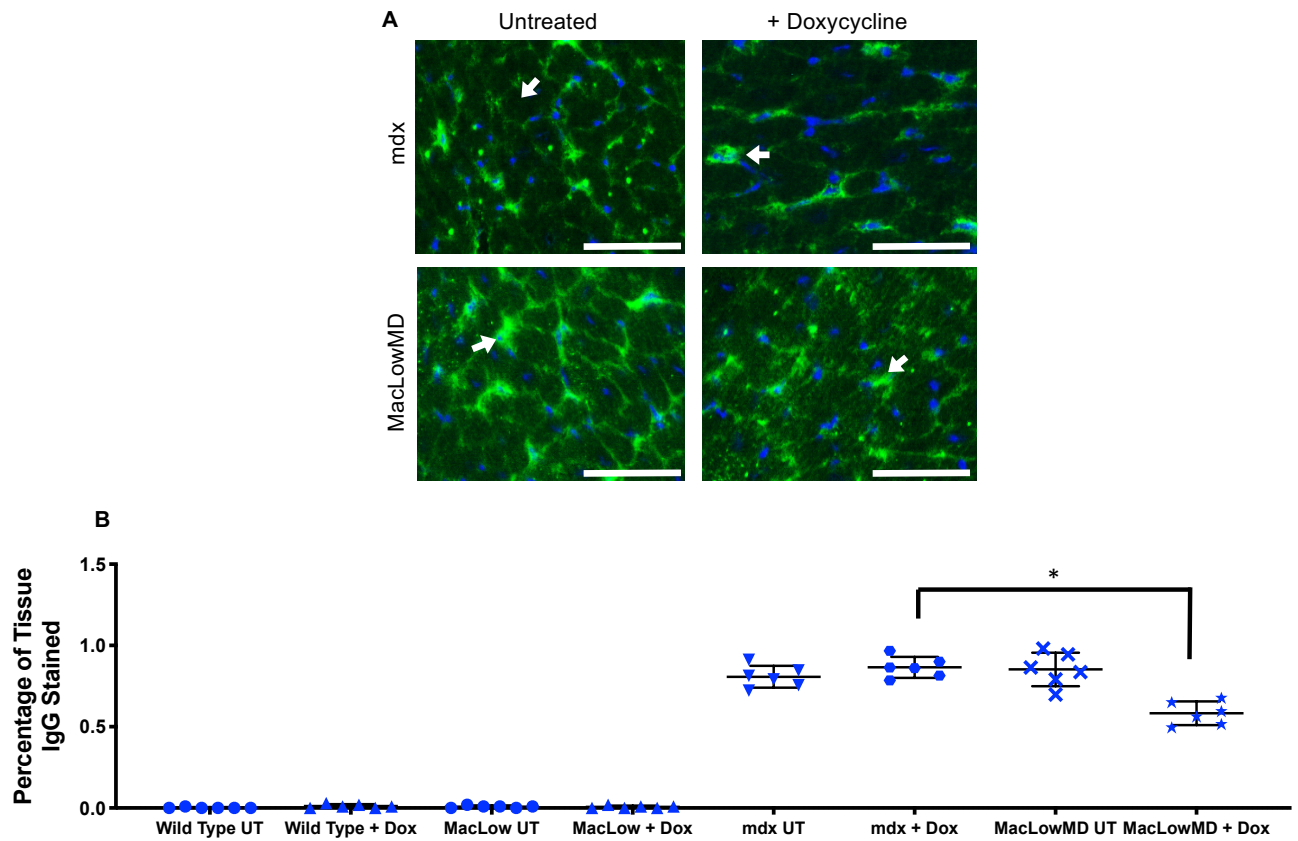


**Figure 4.2.2.4. Effect of six week doxycycline treatment on IgG staining in MacLowMD and mdx heart.** Complete heart sections were stained and analysed for n of 6 doxycycline treated MacLowMD and mdx mice. **A)** Representative images of IgG immunofluorescent stain of frozen heart muscle. Arrows indicate examples of IgG stained muscle fibres. **B)** Quantification of percentage of tissue IgG stained. Scale bar = 50µm. \* =  $p < 0.05$ , (unpaired T Test). Data is expressed as mean ± SEM.

Percentage of IgG stained tissue are summarised in Table 4.3.1

<b>Two Week Doxycycline Treatment Tissue Percent IgG Stained</b>				
	<b>Disease and no macrophage depletion</b>		<b>Disease and CD68+ macrophage depletion</b>	
	<b>MacLowMD UT</b>		<b>MacLowMD + dox</b>	
<b>TA</b>	0.39%		0.12%	
<b>Six Week Doxycycline Treatment Tissue Percent IgG Stained</b>				
	<b>Healthy</b>		<b>Disease</b>	<b>Disease and CD68+ macrophage depletion</b>
	<b>Wild type + dox</b>	<b>MacLow + dox</b>	<b>mdx + dox</b>	<b>MacLowMD + dox</b>
<b>TA</b>	0%	0%	0.23%	0.12%
<b>Quadriceps</b>	0%	0%	0.97%	0.53%
<b>Diaphragm</b>	0%	0%	1.33%	0.86%
<b>Heart</b>	0%	0%	0.86%	0.59%

**Table 4.2.2.1 Summary of percentage of IgG stained tissue for two and six week doxycycline treatment.**

### **4.2.3 Effect of Six Week Doxycycline Treatment on Myomesin Blood Serum Levels**

The impact of six week doxycycline treatment and CD68+ macrophage depletion on the amount of muscle damage was also assessed by determining the levels of the DMD biomarker myomesin (MYOM3) in blood serum by western blot analysis. MYOM3 has two isoforms, one of 130 kDa and one of 162 kDa. Levels of MYOM3 were normalised to the housekeeping gene, GAPDH. This corrects for small, unavoidable sample- to- sample and lane- to- lane variability as level of GAPDH is expected to be consistent throughout all samples (11882413 (Shibuya and Ikewaki, 2002)).

MYOM3 western blots were performed on blood serum from three doxycycline treated and untreated MacLowMD, mdx, MacLow and wild type samples.

Following six week doxycycline treatment MYOM3 western blots showed that, as expected, there was no myomesin in non- diseased MacLow and wild type serum (0.00 mean pixel value for MacLow and wild type serum). The two isoforms of MYOM3 were expressed in the serum of diseased mdx and MacLowMD (**Figure 4.2.3. A and B**). There was no change in the amount of either isoforms of MYOM3 between mdx and MacLowMD serum treated with doxycycline for six weeks (**Figure 4.2.3. C and D**).

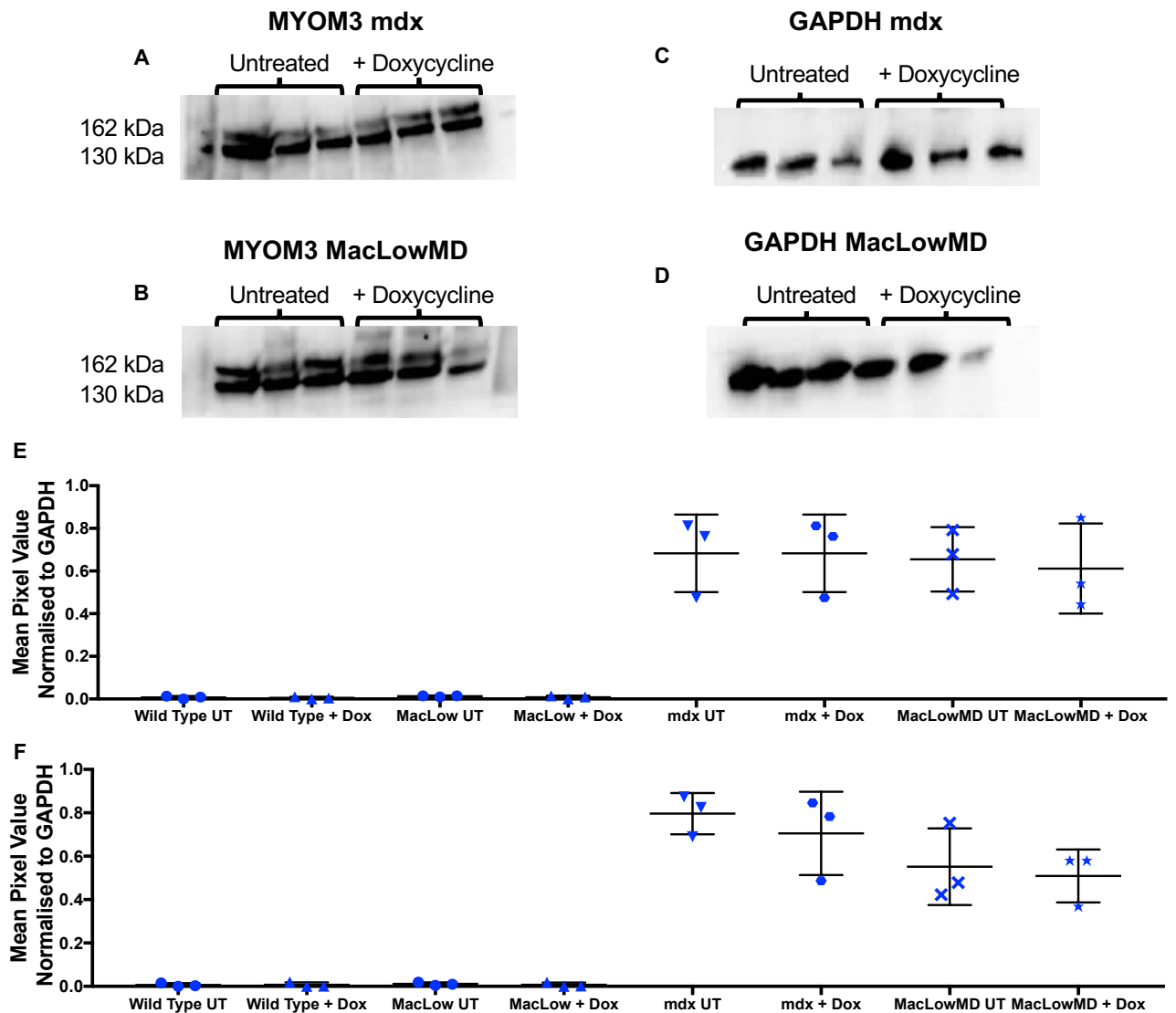


**Figure 4.2.3. Effect of six week doxycycline treatment on myomesin blood levels in MacLowMD and mdx mice.** Levels of MYMO3 were quantified for 3 doxycycline treated MacLowMD and mdx mice. **A.** MYOM3 western blot for n of 3 doxycycline treated and untreated mdx blood serum samples. **B.** MYOM3 western blot for n of 3 doxycycline treated and untreated MacLowMD blood serum samples. **C.** GAPDH western blot for n of 3 doxycycline treated and untreated mdx blood serum samples. **D.** GAPDH western blot for n of 3 doxycycline treated and untreated MacLowMD blood serum samples. **E)** Quantification of levels of MYOM3 130 kDa isoform in blood serum. **F)** Quantification of levels of MYOM3 162 kDa isoform in blood serum.

Unpaired T Test. Data is expressed as mean  $\pm$  SEM.

Samples were visualised using a G:Box Chemiluminescent Image Visualiser (Syngene, Cambridge, UK) and quantified using Genetools software (Version 4.3.8).

### 4.3 Discussion

Previous studies have shown that macrophage depletion has resulted in a reduction in muscle damage in mdx mice. However, prior work has not detailed the effects on muscle damage of specifically depleting a specific macrophage subpopulation. This chapter details the effects of specific CD68+ macrophage depletion on the extent of muscle damage in MacLowMD mice.

As seen in Table 4.2.2.1 in six week doxycycline treatment healthy wild type and MacLow muscles show 0% IgG staining. IgG staining was highest in the diseased mice with an intact macrophage population. A significant decrease in the percentage of IgG stained tissue, and thus muscle fibre damage, is seen in all doxycycline treated MacLowMD tissue in both the two week and six week study.

Due to tissue availability, two week doxycycline treatment studies only allowed comparisons in MacLowMD muscle, which was not ideal as only the effects on doxycycline treatment were seen. Findings in six week doxycycline results focus on comparisons between mdx and MacLowMD doxycycline treated muscle. This ensures that any changes being observed are due to CD68+ macrophage depletion and allows the true effects of the MacLowMD model to be seen.

Following two week doxycycline treatment a 69% reduction in the percentage of IgG immunofluorescent staining and muscle fibre damage was seen in TA muscle. Six week doxycycline treatment also resulted in a reduction in the

percentage of IgG immunofluorescent staining being seen in TA muscle, however at 47% was much less than the 69% reduction in muscle damage seen in two week doxycycline treatment. The difference in muscle damage observed between the two ages it is likely due to less measurable damage being seen in six weeks study due it being towards the stage of peak regeneration.

Results in Chapter 3 show that hindlimb muscles, TA and quadriceps, show no change in the number of CD68+ macrophages following six week doxycycline treatment. However, both these skeletal muscles have a greater increase in numbers of both CD206 and CD163 positive M2 macrophages studied than either the diaphragm or heart (47% in TA, 45% in quadriceps compared to 35% in diaphragm and 31% in heart). Unlike TA and quadriceps, CD68+ macrophages in diaphragm and heart were reduced by 30%. However, whilst numbers of CD206 and CD163+ macrophages were increased, it was not to as greater extent and TA and quadriceps. This indicates that upregulation of M2, anti- inflammatory repair macrophages may have a greater contribution to reduction in muscle damage than the depletion of M1, pro- inflammatory macrophages, with greatest reduction in muscle damage being seen in TA and quadriceps, the two muscles with the greater increase in numbers of M2 macrophages.

Perhaps somewhat unexpectedly, unlike results from IgG immunofluorescent staining, MYOM3 western blots indicated that there was no difference in the amount of muscle damage in six week doxycycline treated blood serum. The

percentage of damaged tissue is low throughout all muscle types studied, with the maximum being 1.33% in mdx treated heart (Figure 4.2.2.4). It is possible that this level of damage was too small to allow a difference in MYOM3 in blood serum to be seen. Rouillon *et al.*, 2015, found that MYOM3 protein is less sensitive to low levels of muscle fibre damage.

It is important to question the comparability of IgG stain and MYOM3 blood serum. IgG staining allows low level muscle damage to be seen on a fibre- by- fibre basis. However, MYMO3 western blots allow muscle damage to be seen on a less specific level, instead investigating complete muscle damage throughout the whole animal, indicating that small changes would be less likely to be detected. A serum assay is often considered advantageous over looking at a section of each muscle as there is less bias i.e. muscles being studied are required to be of comparable sizes, etc (Rouillon *et al.*, 2015).

For both IgG immunofluorescent staining and MYOM3 western blots there was no indicator of muscle damage in non- diseased genotypes for all tissues (wild type and MacLow).

Findings in this chapter indicate that reduction in number of CD68+ macrophages, and interestingly and increase in M2 macrophages, results in a reduction in muscle damage at fibre level. However, the potential for CD68+ macrophage depletion as a possible DMD patient treatment is limited by the lack of observed reduction in MYOM3 blood serum levels, as this indicates

that the extent of improvement in muscle damage was insufficient to reduce the amount of MYMO3 released into blood.

The next phase of this project was to understand the impact of CD68+ macrophage depletion on the regenerative capacity of muscle, as well as establishing whether the reduction in muscle fibre damage described in this chapter occurs as a result of impacting the regenerative ability of the muscle.

# Chapter 5: The Impact of CD68+ Macrophage Depletion on The Regenerative Capacity of Muscle

---

## 5.1 Introduction

In a healthy individual, specific phases of muscle regeneration occur after muscle damage, caused by injury, disease or old age (Karalaki *et al.*, 2009). Following muscle damage, the muscle tissue degenerates, becomes necrotic and there is an infiltration of immune cells, predominated by macrophages (Musaro, 2014). M1, CD68+ macrophages remove debris and release proinflammatory cytokines. M2, CD206+ and CD163+ macrophages release anti-inflammatory cytokines and activate muscle stem cells, known as satellite cells (Musaro, 2014) thereby, promoting tissue repair and regeneration. This immune response is vital to allow functional regeneration and muscle growth (Karalaki *et al.*, 2009).

Patients with DMD, as well as mdx mice, lack the dystrophin protein, the role of which is to stabilise the sarcolemma of muscle fibres. Due to the lack of dystrophin, muscle fibres in DMD patients are naturally weak and vulnerable to damage. As a result, muscle fibres undergo continuous cycles of damage and inflammation, which results in fibres losing the ability to correctly regenerate and repair over time and muscle, worsening muscle damage (Pessina and Muñoz-Cánoves, 2016). In DMD, during the inflammatory phase of muscle damage, a build-up of inflammatory cells, predominantly macrophages, occurs within the muscle.

If macrophage depletion results in a reduced capacity of muscle to regenerate, muscle will be unable to repair and damage will continue to build up within the muscle, not allowing healthy muscle to be regenerated and as a result, worsening muscle degeneration. This, obviously, is not a good outcome for patients.

Prior studies have targeted all macrophages. It is possible that targeting all populations of macrophages may be the cause of the negative effects on regeneration these groups observed. CD68+ macrophages are proinflammatory and exacerbate inflammation, CD206+ and CD163+ macrophages promote muscle repair and regeneration. As such, depletion of M2 macrophages would result in reduced capacity of muscle to regenerate. The MacLow model used in this study is assumed to specifically depletes CD68+ macrophages and does not affect numbers of M2 macrophages. In fact, as described in Chapter 3, numbers of CD206+ and CD163+ macrophages were increased. The balance of cytokines that induce CD68+, CD206+ and CD163+ macrophages is investigated in this chapter.

This chapter aims to ascertain the effects of CD68+, M1 macrophage depletion on muscle fibre regeneration in the mdx mouse model of DMD. CD68+ macrophages release proinflammatory cytokines which further exacerbates tissue damage. The ideal outcome of the MacLowMD model is to dampen down pro- inflammatory macrophages specifically without affecting M2, regenerating macrophages.

The reduced capacity of muscles to regenerate in DMD patients is associated with fibrosis. As previously mentioned, patients with DMD have naturally weak muscles due to the lack of dystrophin and are in a constant cycle of damage and repair. Over time, as the regenerative capacity of muscles is reduced, damaged muscle is replaced by fat and fibrotic tissue (Pessina and Muñoz-Cánoves, 2016). In fact, fibrosis is a hallmark pathological feature found in muscle biopsies from patients with DMD (Zhou and Lu, 2010) and is defined as unregulated, excessive deposition of extracellular matrix (ECM) components within tissue (Pessina and Muñoz-Cánoves, 2016). This results in scarring and thickening of the effected tissue. In DMD, fibrosis directly causes muscle dysfunction and contributes to the lethality of DMD (Pessina and Muñoz-Cánoves, 2016).

Macrophage plasticity is readily apparent in tissue repair and fibrosis, resulting in macrophages playing both a pro and anti- fibrotic role at various stages of tissue repair.

A 2014 study by Beljaars *et al.* studied CCL4 chronically damaged human and mouse livers. Mice received twice-weekly intraperitoneal injections of CCL4 for 4 or 8 weeks. The toxicity of CCL4 has classically been used to induce liver lesion and liver fibrosis (Dong *et al.*, 2016). Beljaars *et al.* found that a higher number of CD68+ macrophages were found in fibrotic livers compared to healthy livers and were found concentrated in scars during advanced fibrosis (Beljaars *et al.*, 2014). Liver stained for both CD68+ and CD206+

macrophages indicated that double-positive cells were more frequent in fibrotic liver than in normal livers (Beljaars *et al.*, 2014). The ability of macrophages, particularly M2 macrophages, to produce and activate the pro-fibrotic cytokine, TGF $\beta$ 1, has been attributed to their pro-fibrotic function (Murray *et al.*, 2014). Interestingly, TGF $\beta$ 1 has also been shown to have a role in macrophage necroptosis (24497535 (Wong *et al.*, 2014)).

Conversely, a 2016 study by Borthwick *et al.* used transgenic mice expressing the CD11b-diphtheria toxin receptor to deplete CD11b<sup>+</sup> (a pan macrophage marker) at a number of time points in three models of type-2 cytokine-driven lung disease (Borthwick *et al.*, 2016). Depletion of CD11b<sup>+</sup> macrophages caused a significant reduction in fibrosis in the maintenance and resolution phases of disease.

The hypothesis of this chapter is that a reduction in the number of CD68<sup>+</sup> macrophage will not impair the regenerative capacity of muscles and will reduce the level of muscle fibrosis. Furthermore, it is hypothesised that MacLowMD mice will show reduced expression of M1 inducing cytokines, as well as increased expression of M2 inducing cytokines.

This hypothesis was tested by:

1. Laminin staining and feret's minimum diameter measurements to allow muscle fibre size to be established. If regeneration is not affected, it is expected that there will be no difference in size of muscle fibres in doxycycline treated MacLowMD compared to treated mdx muscle.

Laminin staining to quantify the percentage of regenerating muscle fibres. If regeneration is not affected, it is expected that the percentage of regenerating fibres will not differ in doxycycline treated MacLowMD compared to treated mdx muscle. Laminin staining to quantify to total number of muscle fibres. If regenerating is not affected, it is expected that the total number of fibres will not differ in doxycycline treated MacLowMD compared to treated mdx muscle.

2. Collagen staining to quantify the percentage of fibrotic tissue. If fibrosis is not affected, it is expected that the percentage of collagen staining will not differ in doxycycline treated MacLowMD compared to treated mdx muscle.
3. qPCR of cytokines that induce CD68+ (TNF $\alpha$ ), CD206+ (IL4) and CD163+ macrophages (IL10). As CD68+ macrophages are selectively depleted, it is expected that MacLowMD muscle is to show reduced expression of TNF  $\alpha$ . As indicated in Chapter 3, an increase in M2 macrophages are seen in MacLowMD muscle. As such, increased expression of IL4 and IL10 is expected to be seen.

When testing the effect of six week doxycycline treatment, tests one to four described above was performed in three distinct muscles: Tibialis Anterior (TA); diaphragm and quadriceps. Heart was not included in analysis as no central nucleation is shown in cardiac muscle fibres. MacLowMD and mdx samples were diseased, whilst MacLow and wild type samples had no disease. MacLowMD and MacLow samples were capable of inducing CD68+ macrophage depletion with doxycycline administration, whilst mdx and wild

type were not. Due to tissue availability, in Chapter 5.2.1 and 5.2.2 only allowed comparisons in MacLowMD muscle, which was not ideal as only the effects of doxycycline treatment coupled with a reduction in macrophage numbers could be observed. Genotypes used in the six week doxycycline study allowed comparisons between mdx and MacLowMD doxycycline treated muscle to be made. This ensures that any changes being observed are due to CD68+ macrophage depletion, rather than purely doxycycline treatment. This enables the true effects of the MacLowMD model to be seen. Due to tissue availability, Chapter 5.2.5 only allowed comparisons between doxycycline treated mdx and MacLowMD TA and diaphragm muscle.

## 5.2 Results

### **5.2.1 Effect of Two Week Doxycycline Treatment on the Regenerative Capacity of Muscle Fibres and Total Fibre Number**

Previous findings from our laboratory indicated that two week doxycycline treatment resulted in a reduction in the number of regenerating fibres (fibres with central nuclei) in MacLowMD TA (data shown in Chapter 1.7). Feret's minimum diameter measurements would indicate if regeneration was reduced as a result of an impairment of the regenerative capacity of muscle. If muscle regeneration was being impaired, smaller fibres would be seen in doxycycline treated MacLowMD TA.

Complete frozen TA sections were laminin stained (**Figure 5.2.1A**). Feret's minimum diameter measurements were obtained by manually drawing around fibres using FIJI Version 2 software. Regenerating fibres were indicated by centralised nuclei. If regeneration was being delayed smaller muscle fibres be seen.

Feret's minimum diameter measurements revealed that the 50% decrease in CD68+ macrophages previously observed by our laboratory (unpublished) resulted in no statistically significant difference in regenerating muscle fibre size between treated MacLowMD TA muscle compared to untreated TA muscle for the total number of fibres in each section ( $p = 0.99$ ) (**Figure 5.2.1. B**).

A large variation in muscle fibre size is seen in DMD patients and muscle of the mdx mouse (Watkins and Cullen, 1982). If an increased variation in muscle fibre sizes was seen in doxycycline treated MacLowMD TA, CD68+ macrophage depletion would be making muscle pathology worse. However, results from the total fibres (**Figure 5.2.1. C**) further indicate that a 50% decrease in CD68+ macrophages resulted in no statistically significant difference in muscle fibre size between treated MacLowMD TA muscle compared to untreated TA muscle ( $p = 0.99$ ).

The total number of muscle fibres within treated MacLowMD TA muscle and untreated TA muscle was quantified in order to understand whether the 33% decrease in numbers of regenerating fibres previously observed in our laboratory (unpublished) occurred due to a reduction in muscle fibre numbers. Furthermore, results allow it to be determined whether a 50% reduction in CD68+ macrophage numbers affects the total number of muscle fibres when the muscle is at the stage of peak necrosis.

Laminin staining and manual quantification indicated no difference in the total number of muscle fibres in doxycycline treated and untreated MacLowMD TA muscle ( $874 \pm 106.7$  compared to  $852.3 \pm 145.4$ ,  $p= 0.91$  respectively) (**Figure 5.2.1.**).

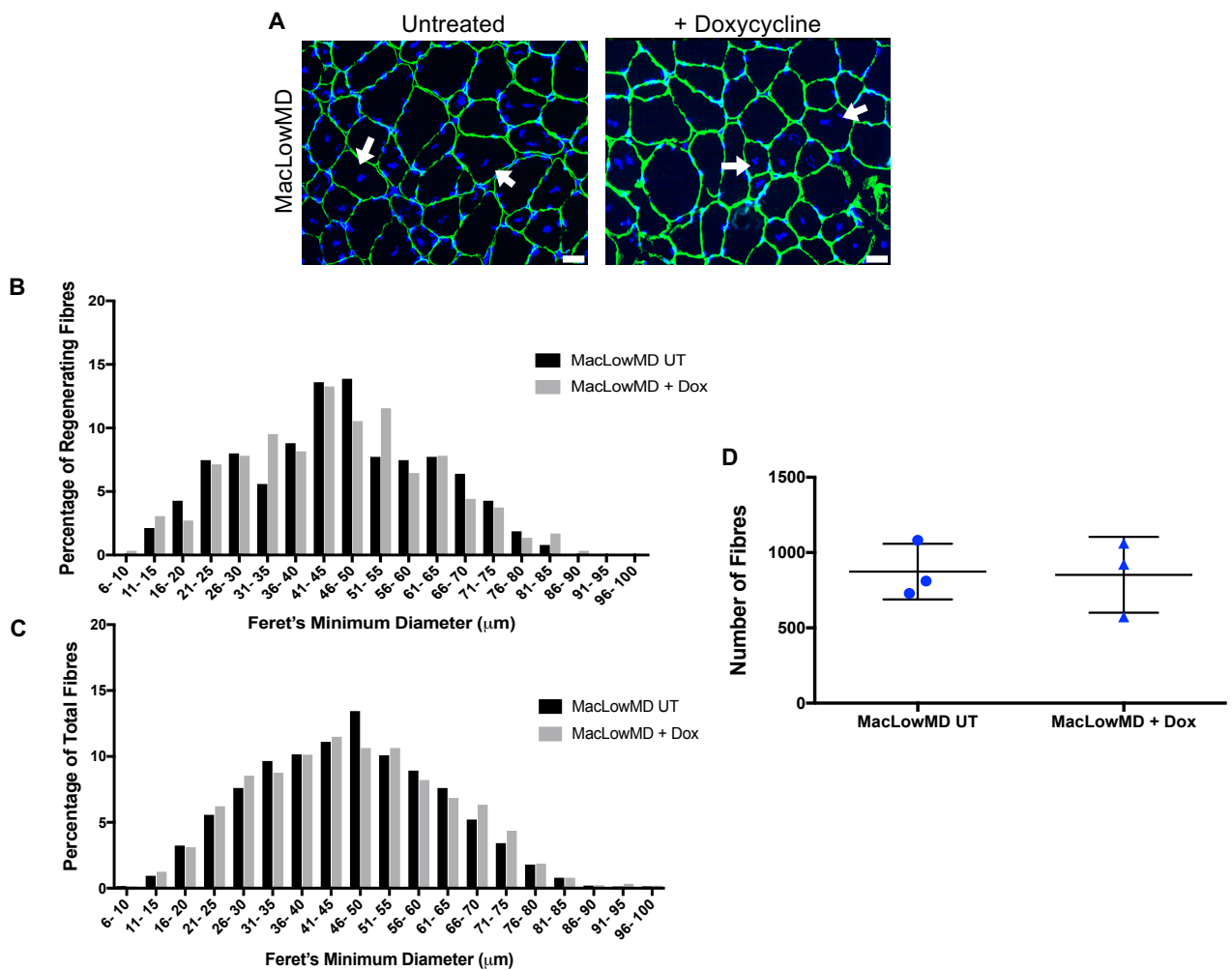


**Figure 5.2.1. Effect of two week doxycycline treatment on fibre regenerative capacity and number of fibres in MacLowMD TA muscle.** Complete TA sections were stained and analysed for doxycycline treated and untreated MacLowMD mice. **A)** Representative images of laminin immunofluorescent stain of frozen TA muscle. Arrows indicate centrally nucleated regenerating muscle fibres. **B)** Feret's minimum diameter measurements for regenerating fibres. **C)** Feret's minimum diameter measurements for all fibres. **D)** Total fibre number for doxycycline treated and untreated MacLowMD mice.  $n = 3$ , Scale bar =  $50\mu\text{m}$ . Paired T test. Data is expressed as mean  $\pm$  SEM.

## **5.2.2 Effect of Six Week Doxycycline Treatment on the Percentage of Regenerating Muscle Fibres**

The percentage of fibres with centrally located nuclei, i.e. regenerating fibres, was quantified to understand how it was affected by CD68+ macrophage depletion. The number of regenerating fibres was calculated as a percentage of total fibre number.

### **5.2.2.1 Tibialis Anterior Muscle**

Laminin staining and calculation of percentage of regenerating fibres indicated that there was no difference between the percentage of regenerating fibres in doxycycline treated mdx and MacLowMD TA muscle ( $51.09 \pm 2.811$  compared to  $52.49 \pm 2.377$ ,  $p= 0.72$ ) (**Figure 5.2.2.1**). Thus, six week doxycycline treatment had no impact on the percentage of regenerating TA muscle fibres.

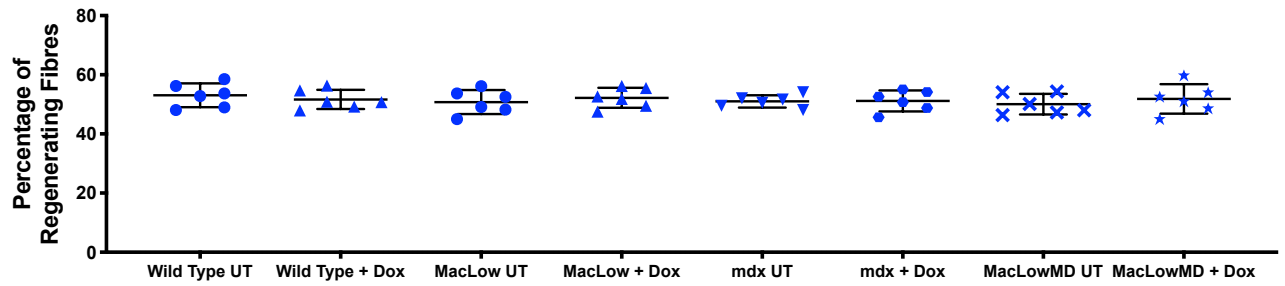


**Figure 5.2.2.1. Effect of six week doxycycline treatment on the percentage of regenerating TA muscle fibres.** Complete TA sections were stained and percentage of regenerated calculated for n of 6 doxycycline treated mdx and MacLowMD mice. Central nucleation quantified as a marker of regeneration. Unpaired T Test. Data is expressed as mean  $\pm$  SEM.

### 5.2.2.2 Quadriceps

Laminin staining and calculation of percentage of regenerating fibres indicated that there was no difference between the percentage of regenerating fibres in doxycycline treated mdx and MacLowMD quadricep muscle ( $49.27 \pm 3.07$  compared to  $47.46 \pm 2.49$ ,  $p= 0.67$ ) (**Figure 5.2.2.2**). Thus, six week doxycycline treatment had no impact on the percentage of regenerating quadricep muscle fibres.

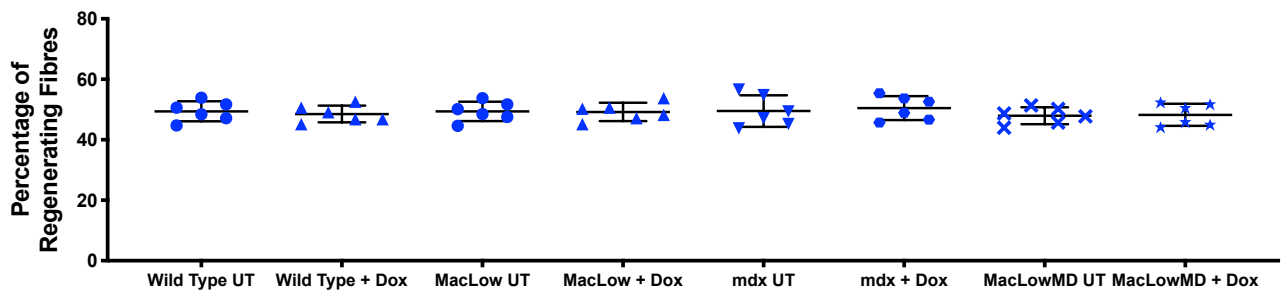


**Figure 5.2.2.2. Effect of six week doxycycline treatment on the percentage of regenerating quadricep muscle fibres.** Complete quadricep sections were stained and percentage of regenerated calculated for n of 6 doxycycline treated mdx and MacLowMD mice. Central nucleation quantified as a marker of regeneration. Unpaired T Test. Data is expressed as mean  $\pm$  SEM.

### 5.2.2.3 Diaphragm

Laminin staining and percentage calculations revealed that there was no significant difference in the percentage of regenerating fibres between doxycycline treated mdx and MacLowMD diaphragm muscle ( $50.7 \pm 3.446$  compared to  $49.56 \pm 1.551$ ,  $p=0.77$ ) (**Figure 5.2.2.3.**). This demonstrates that 33% CD68+ macrophage depletion (Chapter 3.2.2.) had no impact on the percentage of regenerating fibres in diaphragm muscle.

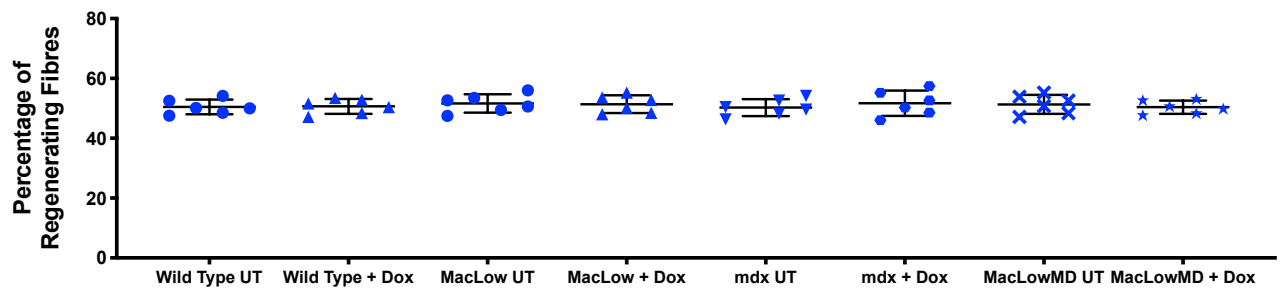


**Figure 5.2.2.3. Effect of six week doxycycline treatment on the percentage of regenerating diaphragm muscle fibres.** Complete diaphragm sections were stained and percentage of regenerated calculated for n of 6 doxycycline treated mdx and MacLowMD mice. Central nucleation quantified as a marker of regeneration. Unpaired T Test. Data is expressed as mean ± SEM.

### **5.2.3 Effect of Six Week Doxycycline Treatment on the Regenerative Capacity of Muscle Fibres and Total Fibre Number**

The previous section, 5.2.1, studied the effect of CD68+ macrophage depletion on the regenerative capacity of muscle fibres at the stage of peak muscle necrosis. In this section, mice were treated for six weeks with doxycycline and tissue taken at the stage of peak regeneration (when animals were ten weeks old). We are making the assumption that the presence of smaller regenerating muscle fibres are an indication of delayed regeneration (Tidball and Wehling-Henricks, 2007, Wang *et al.*, 2014, and Lui *et al.*, 2017). It is important to mention that another argument suggest that small regenerating muscle fibres are also a marker of regeneration following muscle damage (Tedesco *et al.*, 2010). Results in Chapter 5.2.2 show that, in all muscle types, there is no effect of CD68+ macrophage depletion on the percentage of regenerating fibres. This chapter will assess the CD68+ macrophage depletion on the regenerative capacity of muscle fibres.

#### **5.2.3.1 Tibialis Anterior Muscle**

Complete TA sections were stained with anti-laminin antibodies to enable delineation of individual muscle fibres (**Figure 5.2.3.1. A**).

A complete laminin stained TA section can be seen in Chapter 8.2 Appendix II.

Feret's minimum diameter measurements revealed that there was no statistically significant difference in the size of regenerating fibres between

doxycycline treated mdx TA and MacLowMD TA muscle for the total number of fibres in each section ( $p = >0.99$ ) (**Figure 5.2.3.1. B**). If regeneration was being delayed a greater number of smaller regenerating fibres would be seen.

Healthy fibres are very uniform in size and shape. Diseased muscle has a large variation in muscle fibre sizes. Results from the total fibre analysis (**Figure 5.2.3.1. C**) further indicate that that there was no statistically significant difference in the size of all fibres- both regenerating and non-regenerating, between treated mdx TA muscle compared to treated MacLowMD TA muscle ( $p = 0.99$ ).

There was no difference between the size of doxycycline treated mdx and MacLowMD TA and untreated mdx and MacLowMD TA

This indicates, as hypothesised, that muscle fibre regenerative capacity is not impaired or delayed in six week doxycycline treated MacLowMD TA muscle compared to untreated MacLowMD TA muscle.

As in Chapter 5.2.2, the total number of muscle fibres, both regenerating and non-regenerating, were quantified in order to see if CD68+ macrophage depletion resulted in loss of muscle fibres.

Laminin staining and manual quantification of total fibres showed that there was no significant difference in the total number of muscle fibres between doxycycline treated mdx and MacLowMD TA muscle ( $721.7 \pm 38.33$  compared

to  $701.6 \pm 21.14$ ,  $p= 0.70$ ) (**Figure 5.2.3.1 D**). Thus, six week doxycycline treatment had no impact on the total number of muscle fibres in TA.

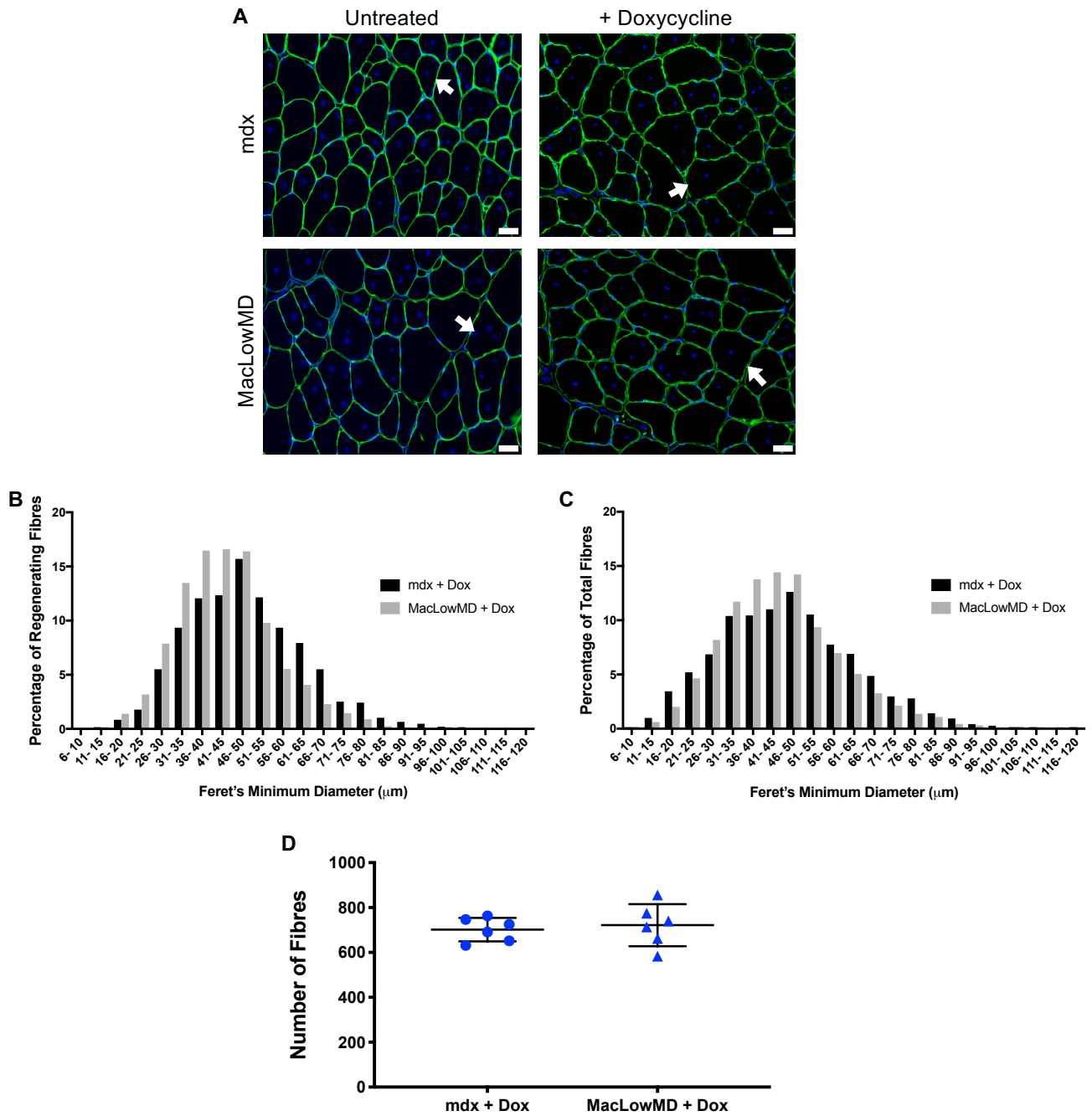


**Figure 5.2.3.1. Effect of six week doxycycline treatment on fibre regenerative capacity and total fibre number in mdx and MacLowMD TA muscle.** Complete TA sections were stained and analysed for n of 6 doxycycline treated mdx and MacLowMD mice. **A)** Representative images of laminin immunofluorescent stain of frozen TA muscle. Arrows indicate centrally nucleated regenerating muscle fibres. Scale bar =  $50\mu\text{m}$ . **B)** Feret's minimum diameter measurements for regenerating fibres. Paired T test. **C)** Feret's minimum diameter measurements for total fibres. Paired T Test. **D)** Total fibre number for n of 6 doxycycline treated MacLowMD and mdx mice. Unpaired T test. Data is expressed as mean  $\pm$  SEM.

### 5.2.3.2 Quadriceps

Complete quadricep sections were laminin immunofluorescent stained (**Figure 5.2.3.2. A**).

Feret's minimum diameter measurements revealed that there was no statistically significant difference in regenerating muscle fibre size between doxycycline treated mdx quadricep and MacLowMD quadricep muscle for the total number of fibres in each section ( $p = 0.87$ ) (**Figure 5.2.3.2. B**). If regeneration was being delayed a greater number of smaller fibres would be seen.

Disease pathology is indicated by an increase in smaller, thinner fibres, where in healthy muscle fibres are very uniform in size and shape. Results from the total fibres (**Figure 5.2.3.2. C**) further indicate that that there was no statistically significant difference in the size of all fibres- both regenerating and non- regenerating, between treated mdx quadriceps muscle compared to treated MacLowMD TA muscle ( $p = 0.79$ ).

This indicates that muscle fibre regenerative capacity is not impaired or delayed in six week doxycycline treated MacLowMD quadricep muscle.

There was no difference between the size of doxycycline treated mdx and MacLowMD quadricep and untreated mdx and MacLowMD TA.

Laminin staining and manual quantification of total fibres showed that there was no significant difference in the total number of muscle fibres between doxycycline treated mdx and MacLowMD quadricep muscle ( $386.7 \pm 10.34$  compared to  $351 \pm 14.31$ ,  $p= 0.11$ ) (**Figure 5.2.3.2**). Thus, six week doxycycline treatment had no impact on the total number of muscle fibres in quadriceps.

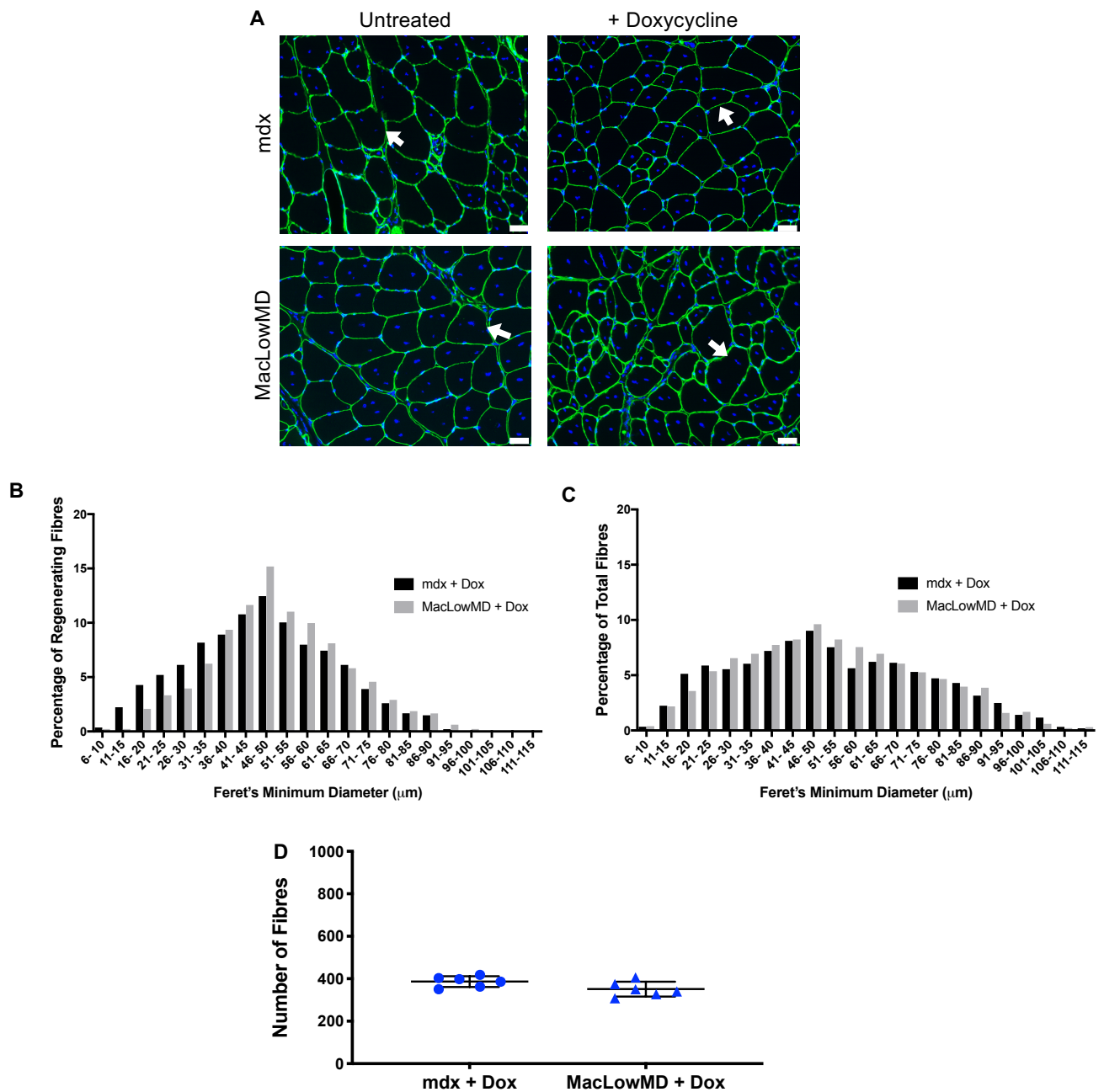


**Figure 5.2.3.2. Effect of six week doxycycline treatment on fibre regenerative capacity and total fibre number in mdx and MacLowMD quadricep muscle.**

Complete quadricep sections were stained and analysed for n of 6 doxycycline treated mdx and MacLowMD mice. **A)** Representative images of laminin immunofluorescent stain of frozen quadricep muscle. Arrows indicate centrally nucleated regenerating muscle fibres. Scale bar =  $50\mu\text{m}$ . **B)** Feret's minimum diameter measurements for regenerating fibres. Paired T test **C)** Feret's minimum diameter measurements for total fibres. Paired T test. **D)** Total fibre number for n of 6 doxycycline treated MacLowMD and mdx mice. Unpaired T test. Data is expressed as mean  $\pm$  SEM.

### 5.2.3.3 Diaphragm

Complete diaphragm sections were laminin stained as described in Chapter 5.2.3.1 (**Figure 5.2.3.3. A**).

As previously detailed in Chapter 3.2.2.2, six week doxycycline treatment resulted in a 33% reduction in the number of CD68+ macrophages in MacLowMD diaphragm (Figure 2.2.3). Feret's minimum diameter measurements showed that a 33% decrease in CD68+ macrophages had no effect on regenerating muscle fibre size, and thus regenerative capacity, between mdx treated diaphragm compared to MacLowMD diaphragm muscle for the regenerating fibres in each section ( $p = 0.99$ ) (**Figure 5.2.3.3. B**).

Feret's diameter measurements for total muscle fibres (**Figure 5.2.3.3. C**) indicate that a 33% reduction in CD68+ macrophages resulted in no statistically significant difference in muscle fibre size, between treated MacLowMD diaphragm muscle compared to mdx diaphragm muscle ( $p = 0.99$ ).

This indicates that 33% reduction in CD68+ macrophages in six week doxycycline treated diaphragm does not impair or delay the regenerative capacity of the diaphragm.

There was no difference between the size of doxycycline treated mdx and MacLowMD TA and untreated mdx and MacLowMD diaphragm.

Manual quantification of total muscle fibres indicated that there was no difference in the total number of muscle fibres in doxycycline treated mdx and MacLowMD diaphragm muscle ( $404.0 \pm 45.11$  compared to  $482 \pm 15.86$ ,  $p=0.33$ ) (**Figure 5.2.3.3.**). Thus, 33% CD68+ macrophage depletion (Chapter 3.2.2.2) had no impact on the total number of muscle fibres in diaphragm.

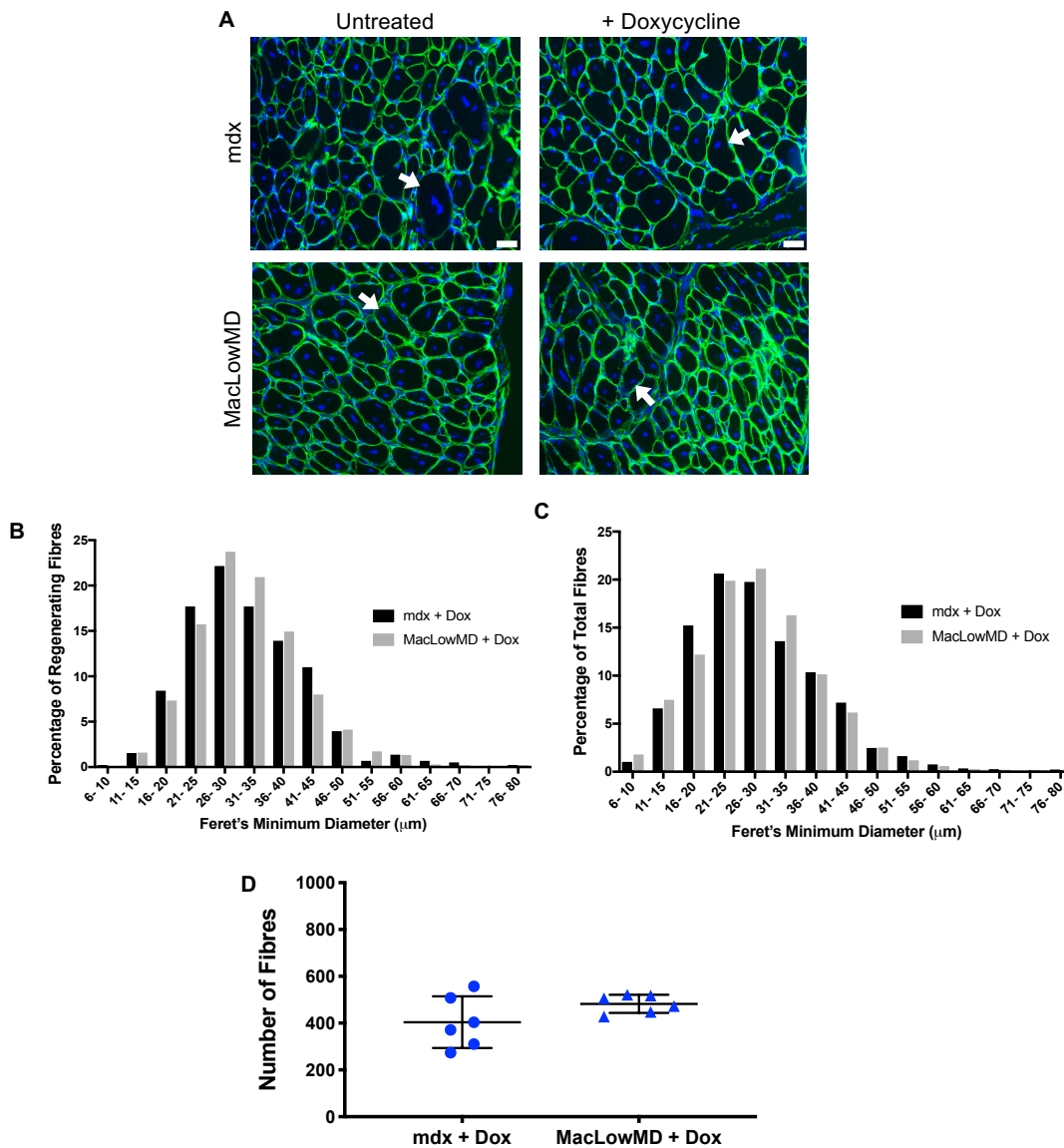


**Figure 5.2.3.3. Effect of six week doxycycline treatment on fibre regenerative capacity and total fibre number in mdx and MacLowMD diaphragm muscle.** Complete diaphragm sections were stained and analysed for n of 6 doxycycline treated mdx and MacLowMD mice. **A)** Representative images of laminin immunofluorescent stain of frozen diaphragm muscle. Arrows indicate centrally nucleated regenerating muscle fibres. Scale bar =  $50\mu\text{m}$ . **B)** Feret's minimum diameter measurements for regenerating fibres. Paired T test. **C)** Feret's minimum diameter measurements for total fibres. Paired T test. **D)** Total fibre number for n of 6 doxycycline treated MacLowMD and mdx mice. Unpaired T test. Data is expressed as mean  $\pm$  SEM.

#### **5.2.4 Effect of Six Week Doxycycline Treatment on the Level of Fibrosis**

Fibrosis, the unregulated excessive deposition of extracellular matrix (ECM) components tissue, is a primary pathological feature of DMD. Collagen is one of the primary components of the ECM that accumulates around damaged tissue during fibrosis. Therefore, collagen staining was used as an indicator of fibrosis in this section with the aim of understanding the impact of specific CD68+ macrophage depletion on the level of tissue fibrosis.

##### **5.2.4.1 Tibialis Anterior Muscle**

Collagen staining (**Figure 5.2.4.1A**) and calculation of percentage of fibrotic tissue revealed that there was no significant difference between the percentage of fibrotic tissue in doxycycline treated mdx TA muscle and MacLowMD TA muscle ( $0.04 \pm 0.0007$  compared to  $0.03 \pm 0.001$ ,  $p= 0.07$ ) (**Figure 5.2.4.1B**). The level of fibrosis was negligible in both doxycycline treated and untreated MacLowMD and mdx TA muscle ( $p < 0.0001$ ). This was the case across all muscle types studied. Furthermore, there was significantly less collagen staining in wild type TA muscle than diseased TA muscle (**Figure 5.2.4.1A**). This demonstrates that six week doxycycline treatment had no impact on the percentage of fibrotic TA muscle fibres.

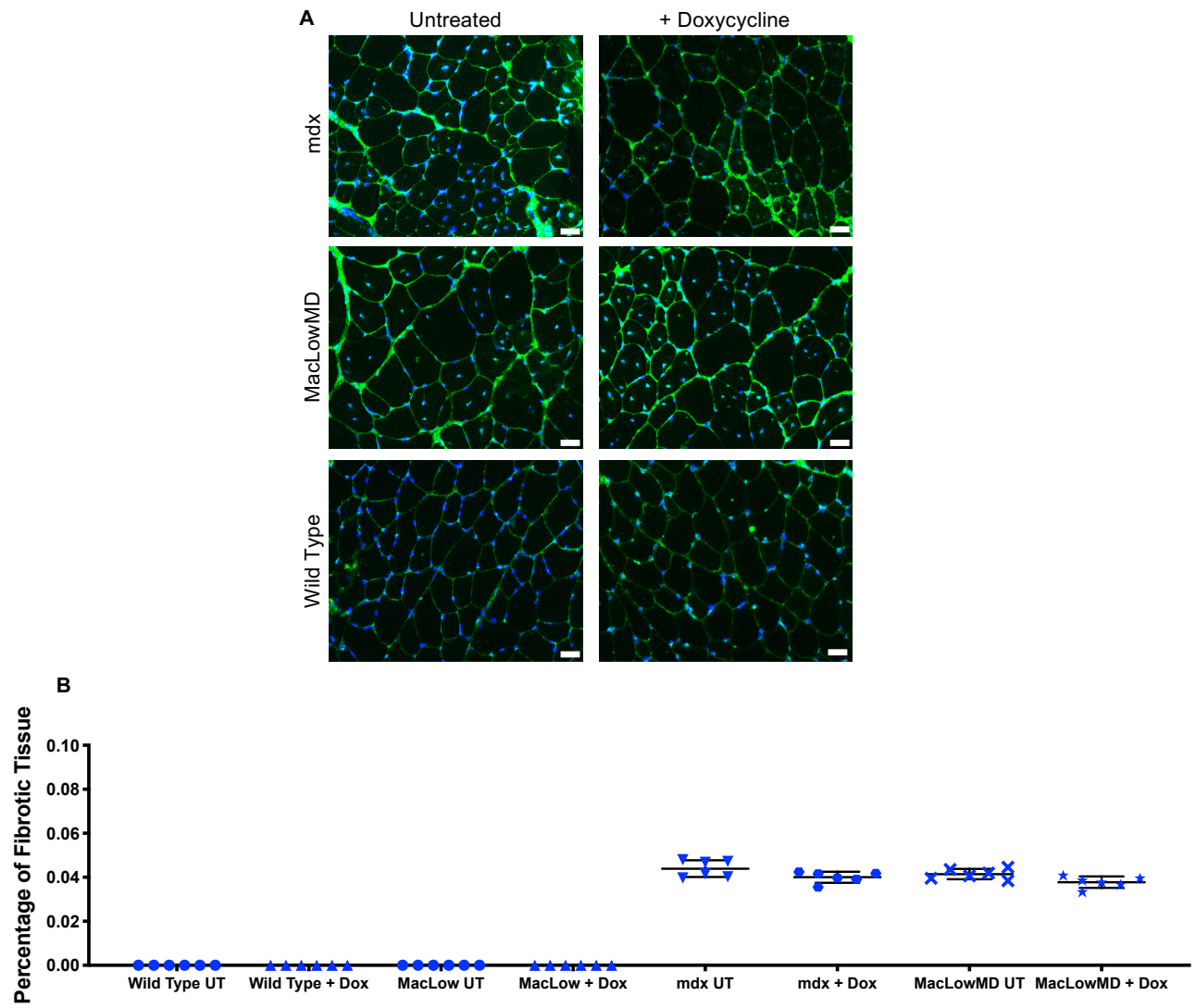


**Figure 5.2.4.1. Effect of six week doxycycline treatment on the percentage of fibrotic TA tissue.** Complete TA sections were collagen stained, and percentage of fibrotic tissue calculated for n of 6 doxycycline treated mdx and MacLowMD mice.

Scale bar = 50 $\mu$ m. Unpaired T Test. Data is expressed as mean  $\pm$  SEM.

#### 5.2.4.2 Quadriceps

Collagen staining (**Figure 5.2.4.2 A**) and calculation of percentage of fibrotic tissue revealed that there was no significant difference between the percentage of fibrotic tissue in doxycycline treated mdx and MacLowMD quadricep muscle ( $0.0387 \pm 0.0094$ , compared to  $0.0377 \pm 0.0012$ ,  $p= 0.97$ ) (**Figure 5.2.4.2 B**). This demonstrates that six week doxycycline treatment had no impact on the percentage of fibrotic quadricep muscle fibres. The level of fibrosis was negligible in both doxycycline treated and untreated MacLowMD and mdx quadriceps muscle. Furthermore, there was significantly less collagen staining in wild type quadriceps muscle than diseased quadriceps muscle (**Figure 5.2.4.2A**).

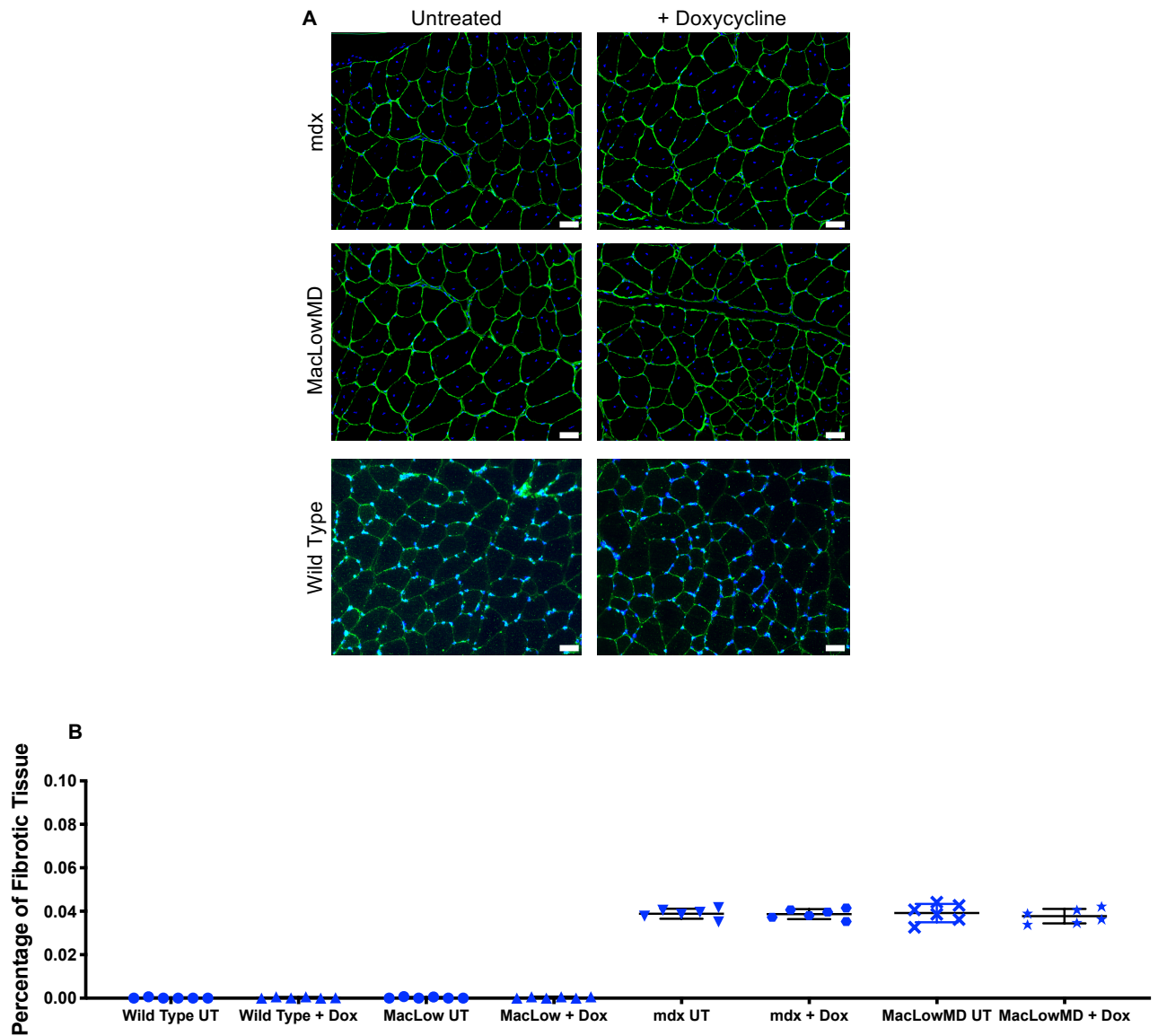


**Figure 5.2.4.2. Effect of six week doxycycline treatment on the percentage of fibrotic quadriceps tissue.** Complete quadriceps sections were collagen stained, and percentage of fibrotic tissue calculated for n of 6 doxycycline treated mdx and MacLowMD mice.

Scale bar = 50 $\mu$ m. Unpaired T Test. Data is expressed as mean  $\pm$  SEM.

#### 5.2.4.3 Diaphragm

Collagen staining and fibrotic tissue percentage calculations revealed that there was no significant difference in the percentage of tissue fibrosis between doxycycline treated mdx and MacLowMD diaphragm muscle ( $0.076 \pm 0.003$ , compared to  $0.072 \pm 0.003$ ,  $p=0.45$ ). (**Figure 5.2.4.3.**) This demonstrates that 33% CD68+ macrophage depletion (Chapter 3.2.2.2) had no impact on the percentage of fibrotic tissue in diaphragm muscle. Despite this, diaphragm is the only muscle in the study with any areas of albeit minimal fibrotic tissue. There was also significantly less collagen staining in wild type diaphragm muscle than diseased diaphragm muscle. (**Figure 5.2.4.3A**)

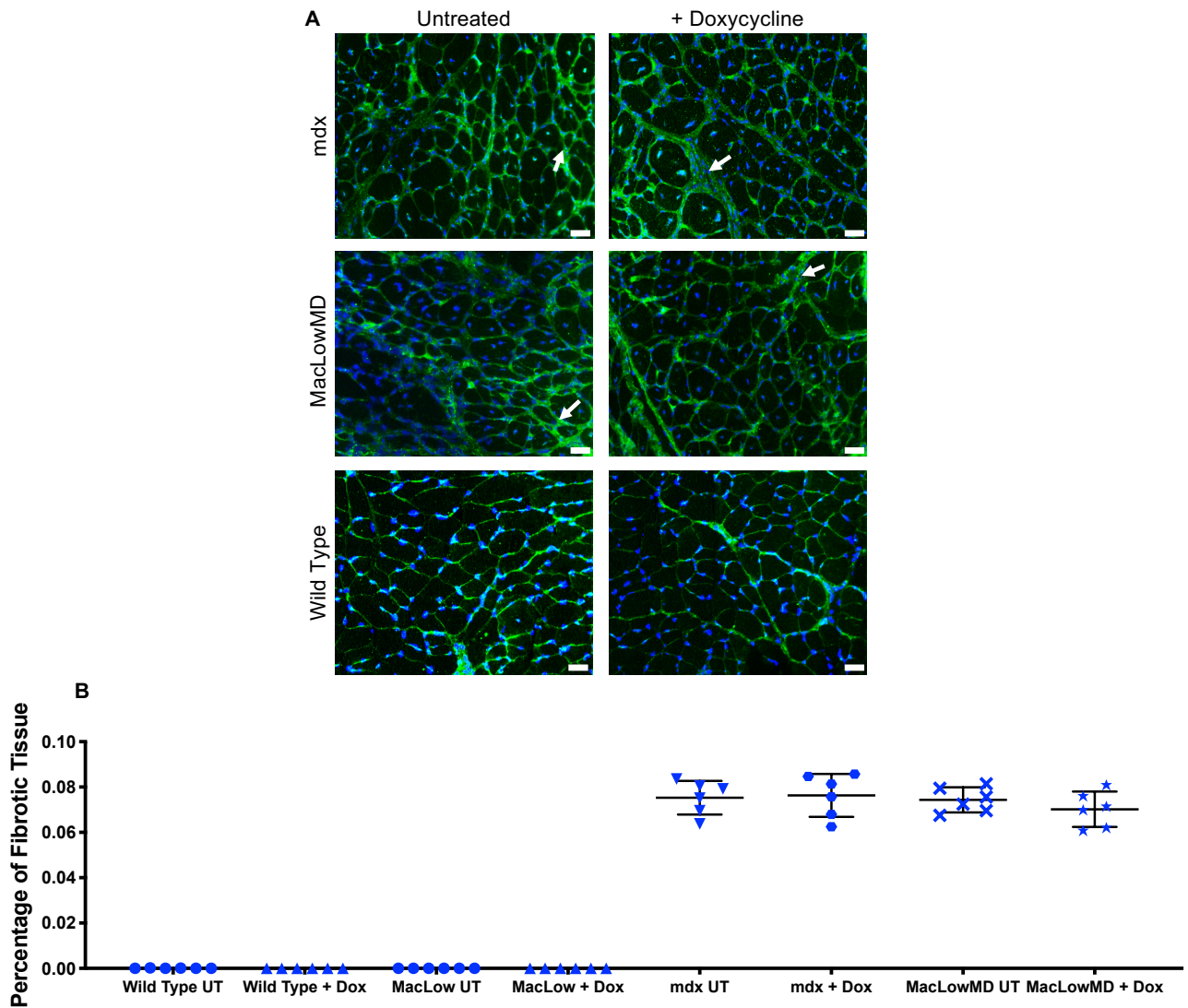


**Figure 5.2.4.3 Effect of six week doxycycline treatment on the percentage of diaphragm fibrotic tissue.** Complete diaphragm sections were collagen stained, and percentage of fibrotic tissue calculated for n of 6 doxycycline treated mdx and MacLowMD mice.

Arrows indicate areas of fibrosis. Scale bar = 50 $\mu$ m. Unpaired T Test. Data is expressed as mean  $\pm$  SEM.

#### 5.2.4.4 Heart

Collagen staining and fibrotic tissue percentage calculations revealed that there was no significant difference in the percentage of tissue fibrosis between doxycycline treated mdx and MacLowMD heart muscle ( $0.074 \pm 0.003$  compared to  $0.073 \pm 0.002$ ,  $p=0.93$ ). (**Figure 5.2.4.4.**) This demonstrates that 30% CD68+ macrophage depletion (Chapter 3.2.2.4) had no impact on the percentage of fibrotic tissue in heart muscle. The level of fibrosis was negligible in both doxycycline treated and untreated MacLowMD and mdx heart muscle. Furthermore, there was significantly less collagen staining in wild type heart muscle than diseased heart muscle (**Figure 5.2.4.4A**).

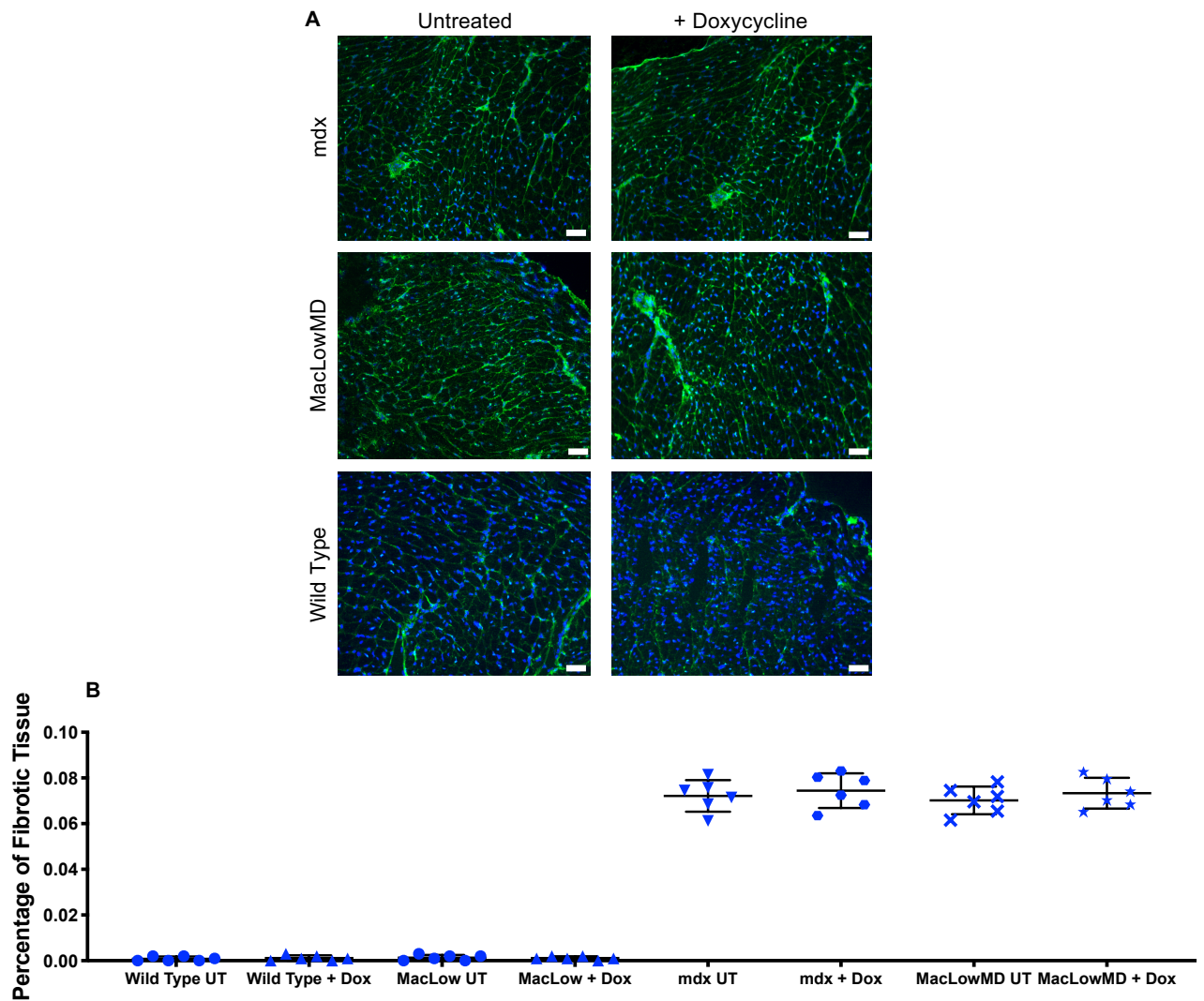


**Figure 5.2.4.4. Effect of six week doxycycline treatment on the percentage of fibrotic heart tissue.** Complete heart sections were collagen stained, and percentage of fibrotic tissue calculated for n of 6 doxycycline treated mdx and MacLowMD mice.

Scale bar = 50µm. Unpaired T Test. Data is expressed as mean ± SEM.

### **5.2.5 Effect of Six Week Doxycycline Treatment on the Expression of Proinflammatory and Anti-inflammatory Cytokines**

The impact of six week doxycycline treatment and CD68+ macrophage depletion on the expression of proinflammatory and anti-inflammatory cytokines in TA and diaphragm was also assessed using qPCR. TNF $\alpha$  is responsible for inducing proinflammatory CD68+ macrophages, IL4 induces anti-inflammatory CD206+ macrophages and IL10 both induces anti-inflammatory CD163+ macrophages, as well as downregulating proinflammatory CD68+ macrophages.

Delta cycle threshold ( $\Delta$ CT) values were calculated by normalising target templates to GAPDH housekeeping gene. Delta delta CT values and fold changes were then calculated. qPCRs were performed on doxycycline treated mdx and MacLowMD TA and diaphragm tissue.

Following six week doxycycline treatment qPCRs showed that, in both TA and diaphragm, there was no significant difference in the expression of TNF $\alpha$  between mdx and MacLowMD (1.62 compared to 1.19 in TA and 1.15 compared to 1.00 in diaphragm). This demonstrates that six week doxycycline treatment, and 33% reduction in CD68+ macrophages in diaphragm (Chapter 3.2.2.2), had no impact on the expression in TNF $\alpha$  (**Figure 5.2.5**). Expression of IL4 and was expressed at such a low level it was undetermined in both mdx and MacLowMD TA and diaphragm. Expression of IL10 was also undetermined in diaphragm. There was no significant difference in the

expression of IL10 between mdx and MacLowMD TA muscle (1.24 compared to 1.75) (**Figure 5.2.5**).

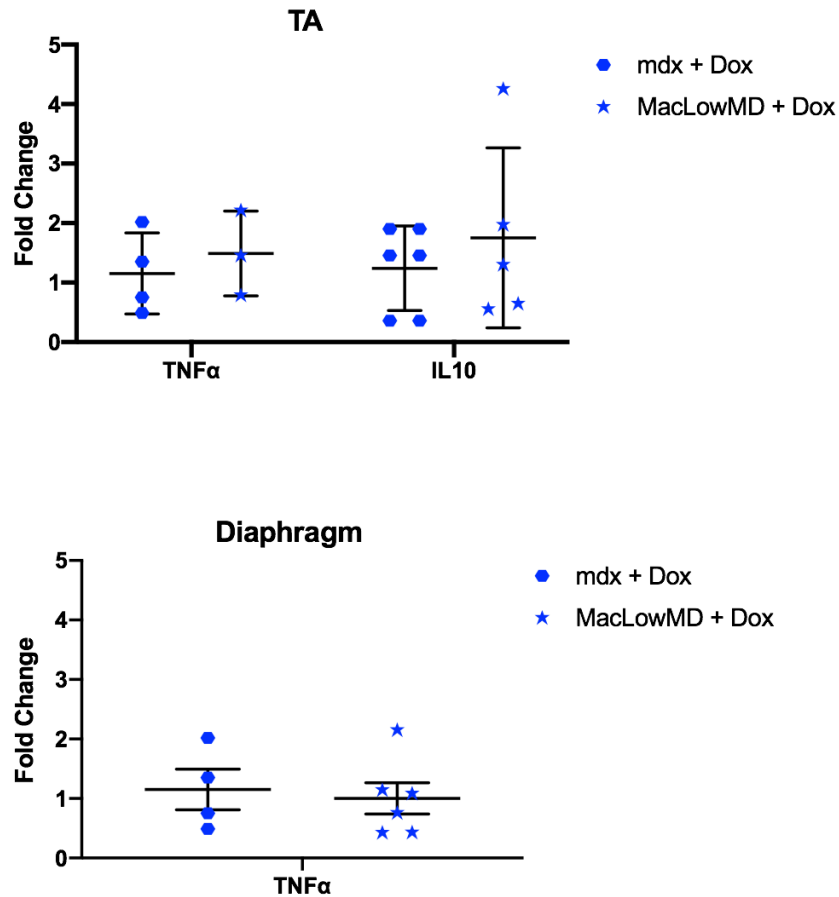


**Figure 5.2.5 Effect of Six Week Doxycycline Treatment on the Expression of Proinflammatory and Anti-inflammatory Cytokines in TA and Diaphragm muscle.** RNA was extracted from and n of 6 TA and diaphragm muscle and reversed transcribed to cDNA before being amplified using qPCR. GAPDH was used as a housekeeping gene with data expressed relative to this. Unpaired T Test. Data is expressed as mean  $\pm$  SEM. qPCR was ran using an Applied Biosystems 7900HT Real- Time PCR Machine (Applied Biosystems, California, USA) and data obtained using SDS software (Version 2.4).

### 5.3 Discussion

Previous studies have shown that macrophage depletion has resulted in a reduced regenerative capacity of muscle. However, no prior studies have investigated the impact of depletion of a specific subpopulation of macrophages on muscle regeneration. First, it was determined if regeneration was impaired or delayed; second, it was determined if regenerating fibres were being depleted or if total fibre count is affected.

Regenerative capacity of muscle was studied at two time points- mice treated for two weeks with doxycycline and culled at the age of six weeks, the age of peak necrosis; and mice treated for six weeks with doxycycline and culled at the age of ten weeks, the age where disease phenotype is moving towards peak regeneration. This is confirmed in Chapter 4, where level of muscle damage is lower in mice treated for six weeks with doxycycline than mice treated for two weeks with doxycycline, indicating that muscle is beginning to regenerate.

MacLowMD mice treated with doxycycline for two weeks showed no impairment or delay in regeneration, as well as no change in the total number of muscle fibres compared to untreated MacLowMD mice, as shown by the lack of any significant shift in muscle fibre size in doxycycline treated MacLowMD mice. Previous studies from our laboratory indicate that two week doxycycline resulted in a 50% reduction in the number of CD68+ macrophages, as well as a 33% reduction in the number of regenerating fibres. Results in chapter 4.2.1.1 indicate a 69% reduction in muscle damage. As the

regenerative capacity of muscle was not impaired following two week doxycycline treatment, this indicates that the observed reduction in muscle damage and reduction in regeneration is likely to be due to a reduction in disease pathology and an increase in M2 macrophages. This suggests that we are seeing a 33% reduction in regeneration due to a 69% reduction in muscle damage, indicating that two week doxycycline treated MacLowMD muscle is healthier and as such, does not need to regenerate as much as untreated MacLowMD muscle.

MacLowMD mice treated with doxycycline for six weeks show no impairment or delay in regeneration, no depletion of regenerating fibres, as well as no change in the total number of muscle fibres compared to untreated mdx mice. Combining these results indicate that six week doxycycline treatment and CD68+ macrophage depletion (33% in diaphragm and 30% in heart) has no negative impact on the regenerative capacity of muscle. However, it is important to acknowledge that the percentage of regenerating fibres is much higher than expected in doxycycline treated and untreated Wild Type and MacLow muscle. This high starting point may potentially be a reason why no difference in percentage of regenerating fibres is seen.

Interestingly, no impact on regenerative capacity of muscle was seen in six week treated TA and quadricep muscle. As previously mentioned in Chapter 3.2.2.1, there was no change in the numbers of CD68+ macrophages following six week doxycycline treatment in both TA and quadricep. Lui *et al*, 2017, detailed that unlike M1 (CD68+) macrophages, M2 (CD206+, CD163+)

macrophages can reduce effects the inflammatory response and promote myoblast fusion and the growth of muscle cells (Liu *et al.*, 2017). Furthermore, M2 macrophages are capable of activation of satellite cells to further promote muscle regeneration (Rigamonti *et al.*, 2014). These results assist in the explanation of the lack of effect on regenerative capacity of TA and quadricep MacLowMD muscle. As detailed in Chapter 3, sections 3.2.3.1 and 3.2.4.1, numbers of CD206+ and CD163+ macrophages are upregulated in six week doxycycline treated MacLowMD TA and quadricep muscle. Therefore, the increase in the number of M2 macrophages observed in Chapter 3 may counteract the damaging effects of M1 macrophages in muscle regeneration and results in negative capacity of TA and quadricep muscle not being impaired. This situation is recapitulated in diaphragm and heart muscle, as whilst CD68+ macrophages are depleted by 33% and 30% respectively, numbers of CD206+ and CD163+ macrophages were also increased. Surprisingly, despite an observed increase in CD206+ and CD163+ macrophages in TA and quadricep, no reduction in CD68+ macrophage was observed. Due macrophage polarity, as well as a lack of a dual stain, there is potential that the same macrophages are being quantified multiple times.

Findings have shown that, whilst CD68+ macrophage depletion had no effect on the level of fibrosis in all muscles, the percentage of fibrotic tissue in diaphragm (average 0.076%) and heart (average 0.075%) is higher than that in TA (average 0.035%) and quadriceps (average 0.038%). This is consistent with previous studies findings, including a 2015 study by Gutpell, Hrinivich and Hoffman that found that fibrosis was present in muscles of young mice, and

the amount of fibrosis in the diaphragm of twelve weeks old mdx was significantly higher than the amount of fibrosis in both TA and quadriceps, as indicated in **Figure 5.3.1**. (Gutpell, Hrinivich and Hoffman, 2015).



**Figure 5.3.1. Comparison of histopathology of twelve weeks-old muscles.** Muscle from mdx diaphragm, quadriceps, soleus, tibialis anterior and gastrocnemius muscles for Gutpell *et al's.*, 2015 study. Collagen staining is shown in blue.

However, results in the present study show that there were very low levels of fibrosis in all tissues at this age, except a minimal amount in diaphragm. This is confirmed by comparison with the wild type controls for each tissue. Previous research has shown that extensive areas of fibrotic tissue are seen in the diaphragm of mdx mice from the age of twelve weeks (Gosselin and Williams, 2006). Mice in my study were sacrificed at ten weeks of age, and therefore prior to significant development of fibrotic tissue, particularly in the diaphragm. In order to improve fibrosis results, a potential improvement would be to use Masson's Trichrome stain, which has increased clarity and specificity than collagen immunofluorescence (Mao *et al.*, 2016).

Results from qPCRs showed no difference between the expression of TNF $\alpha$  in doxycycline treated mdx and MacLowMD TA and diaphragm tissue, as well as in IL10 in doxycycline treated mdx and MacLowMD TA muscle. These findings are opposed to Tidball and Villalta, 2010, who suggested that release

of anti-inflammatory cytokines, such as IL10, would cause levels of CD68+ macrophages to be reduced (Tidball and Villalta, 2010). Despite a previously observed reduction in CD68+ macrophages in diaphragm, and an increase in CD163+ macrophages in both TA and diaphragm, qPCRs showed no change in expression in proinflammatory or anti-inflammatory cytokines was. However, qPCRs showed each cytokine studied was expressed at such a low level that any true impact on expression cannot be solidly assessed, particularly IL4, which was undetectable in both TA and diaphragm tissue.

Findings from both the two week and six doxycycline studies were not consistent with those from Tidball and Wehling-Henricks, 2007, Wang *et al.*, 2014, and Lui *et al.*, 2017, who both found that macrophage depletion resulted in an impairment in the regenerative capacity of muscle following macrophage depletion. However, whilst all these previous studies targeted all macrophages, both M1 and M2, this study specifically depleted CD68+ macrophages. M1, CD68+ macrophages are proinflammatory and exacerbate inflammation, but M2, CD206+ and CD163+ macrophages promote muscle repair and regeneration. As such, avoiding depleting M2 macrophages, as the MacLowMD model allows, avoids losing the beneficial, regenerative capacity M2 macrophages allow.

In the four muscles studied to date, no change was found in the regenerative capacity of the muscle, and consequently in the level of fibrosis. Regardless of the level of CD68+ depletion this is novel for a macrophage depletion model, as all other models resulted in regeneration being impaired, as indicated by a

reduction in the number of centrally nucleated fibres. This strengthens the potential for use of the MacLowMD model in wider disease research.

## Chapter 6: General Discussion and Future Work

---

### 6.1 Discussion

In the work presented in this thesis I have utilised the MacLow model of inducible macrophage depletion to investigate the role of macrophages in three main areas-

1. The impact of CD68+ macrophage depletion on macrophage phenotype in muscle.
2. The impact of CD68+ macrophage depletion on the level of muscle damage.
3. The impact of CD68+ macrophage depletion on the regenerative capacity of muscle.

The data I have collected supports the hypothesis that depleting CD68+ macrophages numbers will result in improved disease pathology in the MacLowMD mice. Reducing numbers of CD68+ macrophages by 30% resulted in a reduction in muscle fibre damage by as much as 35%. This emphasises the role of CD68+ macrophages in DMD disease severity.

The two major findings in this study are the observed increase in numbers of M2 macrophages and the lack of impact of the regenerative capacity of muscles.

The MacLow model is unique in its potential to target a specific subset of macrophages. Chapter 3 demonstrates that six week doxycycline treatment and reduction of numbers of CD68+ macrophages resulted in an increase in numbers of M2 (CD163+ and CD206+), macrophages. This was observed across all muscle types examined- TA, quadriceps, diaphragm and heart. These findings indicate at the age of ten weeks there is a varied level of reduction of numbers of CD68+ macrophages being depleted between each muscle studied. Due to macrophage plasticity a reduction in numbers of CD68+ macrophages must have occurred to drive the observed increased numbers of M2 macrophages. At the age of ten weeks, mdx muscle phenotype is moving towards the stage of peak repair, which occurs at the age of twelve weeks (Villalta *et al.*, 2011b). In both diaphragm and heart, despite the beginnings of a shift towards repair, there is a continued presence of high numbers of pro-inflammatory CD68+ macrophages, likely due to these muscles being the most severely affected in the mdx mouse (Anderson *et al.*, 1998). This means that, unlike less affected hindlimb muscles, there remains high numbers of CD68+ macrophages to be reduced by the MacLow phenotype. This explains both the inconsistency between reduction of numbers of CD68+ macrophages being depleted between diaphragm and heart and hindlimb muscles, but also the smaller increase in M2 macrophages in diaphragm and heart. As there remains greater numbers of M1 macrophages, fewer have progressed towards the M2 phenotype (Villalta *et al.*, 2009). In the case of hindlimb muscles, TA and quadriceps, despite a significant increase in both CD163+ and CD206+ macrophages, a reduction in numbers of CD68+ macrophages was not observed at the age of ten weeks.

Unlike diaphragm and heart, hindlimb muscles are not as severely affected in the mdx model. There is less muscle necrosis, which means that numbers of CD68+ macrophages do not remain as high in hindlimb muscles at the age of ten weeks as in diaphragm and heart. However, following two weeks doxycycline treatment, where necrosis, and numbers of CD68+ macrophages were higher in hindlimb muscles, a 50% reduction in numbers of CD68+ macrophages was seen in six week old TA muscle (unpublished). At the age of ten weeks, CD68+ macrophages in hindlimb muscle have been depleted to a baseline level of a 1.06 ratio in M1: M2 macrophages (Famenini *et al.*, 2017). As such, there is no observed reduction of CD68+ macrophages at this age. Not only does this explain the discrepancy in numbers of CD68+ macrophages depleted between hindlimb muscles and diaphragm and heart, but also explains the higher numbers of M2 macrophages observed in hindlimb muscles.

The plasticity of macrophages and the observed M1 decrease- M2 increase pattern seen in this study is in accordance with findings from previous studies by Villalta *et al.*, 2011 (Villalta *et al.*, 2011b). In this study, Villalta *et al.* isolated macrophages from mdx mice. The group stimulated macrophages with IL10 and found that the expression of CD68 was decreased and M2 markers CD163 and CD206 were increased (Villalta *et al.*, 2011b). Whilst, unlike this study, Villalta *et al.*'s study was *ex vivo* (using macrophage cells isolated from mdx mice), their results support the balance of M1- M2 macrophage polarisation.

However, this study's findings are an incremental increase in knowledge as it is novel to observe this following targeted M1, CD68+ macrophage depletion in DMD. It is possible that following CD68+ macrophage depletion in MacLow mice, plasticity of surviving macrophages allows them to progress to the alternative activation state to clear up the cell debris and dead cells (Weisser, van Rooijen and Sly, 2012). Interestingly, across all four muscles an increase in M2 macrophage numbers was seen. This is very important when considering the bigger picture, as anti-inflammatory, repair phenotype M2 macrophages are increased, this increases the potential for the use of the MacLow model to reduce muscle degeneration and the severity of the mdx disease phenotype. However, increased numbers of M2 macrophages have the potential to be detrimental. A previous 2015 study by Wang *et al.* have shown that M2, specifically CD206+ M2a, macrophages are highly involved in the promotion of fibrosis (Wang *et al.*, 2015). Wang *et al.* utilised a muscle-specific Neuronal Nitric Oxide Synthase (nNOS) transgene in mice to prevent age-related increases in M2a macrophages. Bone marrow from mice with the nNOS transgene was subsequently transplanted into young and old mice, and TA, quadriceps and soleus muscles were collected 8 months later. Wang found no indication of increased collagen accumulation and fibrosis in muscles from young mice (aged 8 weeks). This is consistent with findings from this study, despite mice being on a different background (Wang *et al.*, 2015). However, Wang *et al.* observed that old mice showed fewer M2a macrophages and less accumulation of collagen and fibrosis, thus indicating the role of M2a macrophages in muscle fibrosis (Wang *et al.*, 2015). Whilst no increase in fibrosis was observed in my study, it is important to consider this

potential limitation for future trails in aged mice, or even potential in human DMD treatment.

A hugely important, and novel, finding from my study is that specific CD68+ macrophage depletion has no negative impact on the potential of muscles to regenerate. This has a huge implication of the use of the model in future research into further degenerative muscle disorders. Previous studies which have targeted macrophage populations indiscriminately (Tidball and Wehling-Henricks, 2007), (Wang *et al.*, 2014a) and (Liu *et al.*, 2017), all found that the regenerative capacity of muscles was diminished. This resulted in a number of side effects, specifically poor health of animals, and poor longevity of these models. It is important to establish that the aforementioned studies did not target macrophages in the same way as my study. Wehling- Hendricks used anti- F4/80 intraperitoneal injections, Wang *et al.* used transgenic mice expressing the CD11b-diphtheria toxin receptor and Kawanishi *et al.* used intraperitoneal injections of clodronate- containing liposomes. Furthermore, these studies all targeted macrophages non-discriminately, targeting both M1 and M2 macrophage phenotypes. A comparison of previous macrophage depletion models to the MacLowMD model is detailed in Table 6.1.1.

	<b>Method of Macrophage Depletion</b>	<b>Macrophage Population Targeted</b>	<b>Macrophage Depletion Level</b>	<b>Effects on Muscle</b>	<b>Issues with Health/ Longevity</b>
<b>Kawanishi et al., 2016</b>	Intraperitoneal injection of clodronate encapsulated liposome.  Male C57BL/6J male aged 9 weeks.	Non-specific.	80% reduction in number of F4/80+ macrophages in gastrocnemius muscle.	Reduced muscle damage following treadmill exercise.	None described.
<b>Duffield et al., 2005</b>	Transgenic models expressing diphtheria toxin receptor. Macrophage depletion induced by diphtheria injection.  CD11b-DTR mice aged 12 weeks treated for 2 weeks.	Non-specific.	48% reduction in number of F4/80+ macrophages in liver.	Reduced scarring and fewer myofibroblasts during advanced liver fibrosis.	Limited longevity.
<b>Burnett et al., 2004</b>	Transgenic MaFIA mice expressing a drug inducible suicide gene which allowed the systemic and reversible elimination of macrophages	Non-specific.	Fas-mediated apoptosis of 70-95% of macrophages in the vast majority of tissues.	None described.	Several abnormalities displayed including splenomegaly, lymphadenopathy, and thymic atrophy. Mice unable to survive more than 7 days post treatment
<b>Wehling et al., 2001</b>	Repeated intraperitoneal injections of anti-F4/80 in mdx mice from the age of 1- 4 weeks.	Non-specific.	90% reduction in numbers of circulating macrophages.	75% reduction of muscle cell necrosis.	Limited longevity.
<b>Mojumdar et al., 2014</b>	Genetic and pharmacological ablation of CC cytokine receptor 2 in mdx-CCR2 mice.	Non-specific.	57% reduction in number of F4/80+ macrophages in diaphragm.	Reduced central nucleation, increased regenerating fibre size, increasing the force-generating capacity of the diaphragm	None described.
<b>Giordano et al., 2015</b>	Genetic ablation of TLR4 in 6 week old TLR4-deficient mdx mice (mdx-TLR4 <sup>-/-</sup> ).	Non-specific.	71% decrease in F4/80+ macrophages in diaphragm.	Reduction in expression of pro-inflammatory genes, reduction in macrophage infiltration, muscle macrophages shifted to a more anti- inflammatory phenotype	None described.

<b>Wang et al., 2014</b>	Diphtheria toxin intra- peritoneal injections in 4 to 6 month old transgenic mice expressing the CD11b-diphtheria toxin receptor.	Non- specific	Depletion of blood circulating F4/80+ macrophages and F4/80+ macrophages in spleen.	Smaller regenerating fibres compared to control mice	Impaired/ delayed muscle fibre regeneration.
<b>MacLowMD</b>	Transgenic mouse model capable of inducible CD68+ macrophage depletion crossed with mdx mice.	CD68+ macrophage specific.	<b>33% reduction of F4/80+ macrophages in liver. 30% in CD68+ macrophages in diaphragm and heart. Increase in CD163+ and CD206+ macrophages in TA, quadriceps, diaphragm and heart.</b>	<b>Reduction in muscle fibre damage in TA, quadriceps, diaphragm and heart. No negative impairment in regeneration.</b>	<b>None.</b>

**Table 6.1.1. Comparison of previous macrophage depletion models.**

My results have indicated that there was no effect on the regenerative capacity of MacLow muscles in all muscles and timepoints studied to date. This is novel for a macrophage depletion model. This strengthens the potential for use of the MacLow model in wider disease research, specifically in diseases where macrophages have a significant role. For example, use of the MacLow model may have significant use in Rheumatoid Arthritis, where pro-inflammatory CD68+ macrophages exacerbate joint inflammation (Li, Hsu and Mountz, 2012). Furthermore, the lack of effect on regeneration seen in MacLow and MacLowMD muscle has even greater implications in DMD patients. As regeneration is not being reduced, damaged muscle can be repaired, resulting in a greater amount of healthy muscle in patients.

The fields of DMD and immunology lack sophisticated genetic models that allow the inducible and selective deletion of macrophages to study the role of

these cells in disease progression, muscle damage and muscle regeneration. In this thesis I show using the MacLowMD model is successful in depleting CD68+ macrophages in a specific, controlled manner, without having a detrimental effect on the health and longevity of animals. Not only does this have huge implications for further research into the immunological component of DMD, but also for future research into diseases where macrophages are known to undertake a role.

It is important to mention, although animal models have significantly enriched our understanding of the pathological processes involved muscle damage and DMD, the conclusions drawn in this study may not be fully translatable into human diseases. As previously mentioned in my Introduction Chapter (Chapter 1), there are a number of limitations of the mdx model. Whilst the inflammatory response of the mdx mouse mirrors that of human (Abdel-Salam, Abdel-Meguid and Korraa, 2009), in mdx mice utrophin upregulation restores the integrity of plasma membranes and spares some level of muscle degeneration, meaning that the level of muscle degeneration notably less in mdx mice than humans with DMD (Love *et al.*, 1989). Recently, a model with shortened telomeres, the mdx4cv/mTRG2 mouse model of DMD, was developed which more closely recapitulates both the skeletal muscle as well as the cardiac DMD phenotypes than the traditional mdx mouse (Yucel *et al.*, 2018). By utilising this improved DMD model and crossing it with our MacLow model, this would humanize my results more and increase the translatability of my findings for human benefit.

A further limitation could be with the design of the MacLow model. The MacLow model relies heavily upon diphtheria toxin A in the transgene, as well as doxycycline in order to induce CD68+ macrophage depletion. Both diphtheria toxin and doxycycline have previously been shown to have a negative effect on muscle. Diphtheria toxin has been shown to inhibit protein synthesis in guinea pig heart and muscle tissue (Bowman, Imhoff and Bonventre, 1970)) and doxycycline has been shown to inhibit muscle cell proliferation and migration in male Sprague-Dawley rats (Bendeck *et al.*, 2002). It is possible that the negative effects of diphtheria toxin and doxycycline are masking any true effects of the MacLow model on macrophage phenotype, muscle damage and muscle regeneration.

A final limitation of this study is the lack of a dual stain. Due to macrophage plasticity, it is hard to ensure that CD68, CD206 and CD163 stain are specifically being quantified for pro/ anti-inflammatory macrophages. As such, not only is it hard to ensure that macrophages aren't being quantified multiple times for each marker, but also understanding of the impact of pro/ anti-inflammatory phenotype switch is limited.

## **6.2 Future Work**

I believe that, in the future, there is huge scope for further work to follow on from my findings. Future work would focus on three main areas:

- The impact of the MacLowMD model and CD68+ macrophage depletion on cytokine expression.

- The impact of the MacLowMD model and CD68+ macrophage depletion on muscle strength and mobility.
- The identification of potential druggable targets.

### 6.2.1. The Impact of the MacLowMD Model and CD68+ Macrophage Depletion on Cytokine Expression

My findings identified that the depletion of CD68+ macrophages in MacLowMD mice affected the numbers of M2 macrophages invading damaged muscle. In the future I would be keen to investigate the impact of this altered macrophage phenotype on cytokine production. Not only could this help to further explain the observed increase in numbers of M2 macrophages, but it could also result in the identification of additional therapeutic targets. I would hypothesis that in doxycycline treated MacLowMD mice I would observe higher expression of cytokines responsible for inducing M2 macrophages, as well as a decreased expression of cytokines responsible for the induction of M1, CD68+ macrophages, when compared to cytokine expression in doxycycline treated mdx mice.

In order to understand the effect of CD68+ macrophage depletion I would perform a flow cytometry application know as a Cytometric Bead Array on blood and muscle samples from six week doxycycline treated and untreated mdx and MacLowMD animals (BD Biosciences, 2018). Each bead in the cytometric bead array will have a unique fluorescence intensity and is coated with a specific capture antibody and reporter molecule. A combination of different cytometric beads would be mixed with muscle tissue or blood

samples, along with a mixture of antibodies for the cytokines I would study. Cytometric Bead Array would allow us to quantify the expression of up to 30 proteins simultaneously (BD Biosciences, 2018). The samples would then be ran on a flow cytometer. Analysis software would gate on each individual bead population and determines the median fluorescence intensity for each protein in the array, allowing their expression levels to be quantified (BD Biosciences, 2018). Cytometric Bead Array would be advantageous over western blot as it would allow multiple proteins to be quantified from one sample (Castillo and MacCallum, 2012). The cytokines I would quantify include  $TNF\alpha$  and IL6, which are involved in the induction of M1 macrophages, as well as IL4, IL13, IL1R and IL10, which are involved in the induction of M2 macrophages. Particular interest would be taken in the effects of CD68+ macrophage depletion on the expression of IL10, as not only does IL10 induce M2 macrophages, but also works to downregulate pro-inflammatory M1 macrophages (Villalta *et al.*, 2011b). The impact of CD68+ macrophage depletion on the expression of IL10 may be key in identifying the cause of the increased numbers of M2 macrophages seen throughout my study.

In my study I used Real Time PCR in order to attempt to understand the relationship between macrophage phenotype and cytokine expression. In these PCRs, I studied cDNA obtained from whole tissues (TA and diaphragm). However, as discussed in Chapter 5.3, levels of cytokine expression were largely too low to be detected. In order to address this, along with Cytometric Bead Arrays, I would perform in situ hybridisation (ISH). ISH allows for more direct and precise localisation of a specific nucleic acid within a histologic

section using a complementary strand of nucleic acid with a reporter molecule attached. Visualisation of the reporter molecule would allow localisation of cytokines of interest within the tissue. ISH would allow macrophage specific reporting (CD68, CD206 and CD163), along with colocalization of cytokines of interest (IL10, IL4, etc), allowing direct expression of cytokines within tissues to be identified. I would hypothesise higher reporting of cytokines involved in the expression of CD206+ and CD163+, M2 macrophages, as well lower reporting of cytokines involved in the expression of CD68+, M1 macrophages.

### 6.2.2 The Impact of the MacLowMD Model and CD68+ Macrophage Depletion on Muscle Strength and Mobility

As previously mentioned, one of the key findings of my study is the observed increase in M2 macrophages following specific reduction in numbers of CD68+ macrophages in the MacLowMD model. However, in my study I was unable to understand the extent of increased M2 macrophage numbers of the observed relative reduction in muscle damage. In order to understand the extent of the role of the increased numbers of M2 macrophages on the observed improvements in muscle damage in MacLowMD mice I would increase the numbers of M2 macrophages to see if a similar effect on muscle damage and regeneration is established. I hypothesise that I would find a reduction in muscle damage and an increase in muscle regeneration following upregulation of M2 macrophages. This would be done through the use of gold nanoparticles as described in a recent 2018 study by Raimondo *et al.* (Raimondo and Mooney, 2018). In this study muscle injury was induced in C57BL6/J mice by ischemic injury of TA muscle induced by femoral artery/vein

ligation. Two days following injury, mice were given TA intramuscular injections of IL4-conjugated gold nanoparticles. IL4 has previously been established as a marker of CD206+ macrophages (Villalta *et al.*, 2009). Gold nanoparticles were synthesized by hydroquinone reduction of gold onto citrate-stabilized seed particles. IL4 was conjugated to the gold surface via thiol-gold bonds and electrostatic interactions. Raimondo *et al.* showed that treatment with IL4-conjugated gold nanoparticles led to a twofold increase in the percentage of macrophages expressing the M2 phenotype compared with mice treated with the vehicle alone (Raimondo and Mooney, 2018). In my future work, I would inject hindlimb, diaphragm and cardiac muscle of mdx mice with the IL4-conjugated gold nanoparticles designed by Raimondo *et al.* in order to upregulate M2 macrophages. This would allow me to understand if the reduction in MacLowMD muscle damage found in my study occurred due to the observed increase in numbers of M2 macrophages. I would continue treatment for six weeks, in order to mirror treatment time in my current study, and then harvest muscle tissue. Similar analysis as described throughout this report would take place on tissue harvested (level of muscle damage and regeneration potential). One limitation of this method is that IL4 upregulation is transient, with Raimondo *et al.* observing a return of macrophage phenotype to pre-injection levels 14 days post-nanoparticle injection.

It would also be interesting to determine whether the effects of CD68+ macrophage depletion in the MacLow model impacts on muscle strength and physiological function. In order to be translatable to patient benefit, it is essential that the model has the potential to improve muscle strength, mobility

and, ultimately, quality of life. It has previously been established that mdx muscle has a lower maximal specific force than healthy muscle and has shown a dramatic force drop after lengthening contractions, indicating the impaired physiological function of mdx muscle (Gregorevic, Plant and Lynch, 2004). To identify if CD68+ macrophage depletion resulted in an improvement in muscle strength and physiological function, it could be possible to test MacLowMD mice for their susceptibility to mechanical stress by measuring the extent of force drop following successive lengthening contraction (Sharp, Bye-a-Jee and Wells, 2011). I would hypothesise that, due to the reduced muscle damage observed in my study, that MacLowMD mice with CD68+ macrophage depletion would have a greater level of resistance to the effects of mechanical stress than mdx mice. In order to measure force drop mice would be anaesthetised and the distal tendon of the TA muscle was dissected from surrounding tissue. TA muscle contractions were elicited by stimulating the distal part of the tendon via bipolar platinum electrodes. Optimal muscle length ( $L_0$ ) would be determined by gradually stretching the TA muscle using micromanipulators until the maximum isometric twitch force was achieved. Once the  $L_0$  is established, lengthening contraction would allow the susceptibility of TA muscles to contraction-induced injury to be assessed. TA muscle would be stimulated by 150 Hz for 7 seconds. After stimulation the muscle was lengthened by 10% of  $L_0$  (Sharp, Bye-a-Jee and Wells, 2011). This cycle would be repeated for 10 minutes before the muscles would be dissected and histologically analysed for markers of muscle strength. It would be believed that the reduced muscle fibre damage that I have observed in MacLowMD tissue in my study would result in an increased maximum specific

force than mdx mice. Force drop measurements have previously been used to successfully indicate an improved resistance to contraction-induced injury in Dag1<sup>Y890F/Y890F</sup> / mdx mice compared to control mdx mice (Miller *et al.*, 2012). Dag1<sup>Y890F/Y890F</sup> / mdx mice possess clear restoration of components of the dystrophin glycoprotein complex.

The effect of CD68+ macrophage depletion on muscle strength could also be tested using comparisons of forelimb grip strength measurement at the start of each treatment period and subsequent measurements throughout treatment using a Grip Strength meter (Spurney *et al.*, 2009). This procedure would test the impact of CD68+ macrophage depletion on MacLowMD muscle and dystrophic pathology and would further detail the potential from therapeutic use of the MacLow model, due to the potential benefits on muscle strength. I would hypothesise that due to the reduced muscle damage previously observed in my study, MacLowMD mice would have greater muscle strength and less exercise induced damage than mice without CD68+ macrophage depletion. I would also study the effect of CD68+ macrophage depletion following exercise induced damage on six week doxycycline treated MacLowMD mice. A number of previous studies, including a recent study by Gaiad *et al.*, 2017, have investigated the impact of exercise on myofiber damage of mdx mice (Gaiad *et al.*, 2017). Following the work performed by Gaiad *et al.*, I would use a treadmill to allow exercise induced damage, specifically following the 'TREAT-NMD' recommended protocol "Use of treadmill and wheel exercise for impact on mdx mice phenotype" (TREAT-NMD, 2015). Mouse exercise regimen would consist of 30 minute treadmill

running at a speed of 12 m/minute, twice weekly for four weeks. The treadmill would remain at 0% incline throughout the study. If mice became fatigued the treadmill speed would be reduced to 6 m/minute for 2 minutes, before speed being increased once more (De Jong and Borm, 2008). It would be expected that treadmill exercise would exacerbate disease pathology.

### 6.2.3 The Identification of Potential Druggable Targets

In order to drive my research toward patient benefit I would determine the effects of CD68+ macrophage depletion on changes in gene expression. This would allow potential druggable targets for the development of pharmacological intervention to be identified. cDNA would be generated from RNA taken from treated and untreated MacLowMD and mdx muscle and used in a Qiagen Skeletal Muscle Myogenesis and Myopathy gene focussed PCR array (Goulding *et al.*, 2014). This array contains 370 key genes involved in muscle function, differentiation and disease-related processes and would allow use to identify any differential gene expression induced by CD68+ cell depletion. Differences in expression would then be validated by RT-PCR, before being taken forward for therapy development.

To allow my research to become translatable for human benefit I would develop an IL10-conjugated gold nanoparticle for intramuscular injection, (Raimondo and Mooney, 2018) in order to increase the expression of muscular IL10. IL10 would be chosen because, as previously described, not only does it downregulate M1, CD68+ macrophages, but also upregulates M2 macrophages, thus closely replicating findings from this study. Use of IL10

conjugated gold nanoparticles would first be tested in mice, however it has the potential to offer a therapy to be developed and tested in humans, with the M2 macrophage upregulation and reduction in muscle fibre damage, without the impaired the capacity of muscles to regenerate, observed in my study, to be recapitulated in humans for patient benefit. As seen in my findings, this would be able to occur in limb muscles, as well as the most severely affected muscles- diaphragm and heart.

In short, the present project provided evidence that reducing numbers of proinflammatory CD68+ macrophages will result in improved disease pathology. Furthermore, the importance of M2 macrophages in the reduction of negative disease pathology has been further highlighted. Finally, it was found that the MacLow model did not impair the regenerative capacity of muscle, thus establishing the MacLow and MacLowMD models as sophisticated models for future DMD and immunology research. Future research in to the impact of the MacLowMD model and CD68+ macrophage deletion on cytokine expression and muscle strength, as well as the identification of possible druggable targets, would allow findings from this study to further have a potential therapeutic translation for DMD patient benefit.

## Chapter 7: Bibliography

---

ABDEL-SALAM, E., ABDEL-MEGUID, I. AND KORRAA, S. S. 2009. Markers of degeneration and regeneration in Duchenne muscular dystrophy. *Acta Myol*, 28(3), pp. 94-100.

AMEEN, V. AND ROBSON, L. G. 2010. Experimental models of duchenne muscular dystrophy: relationship with cardiovascular disease. *Open Cardiovasc Med J*, 4, pp. 265-77.

AMOASII, L., HILDYARD, J. C. W., LI, H., SANCHEZ-ORTIZ, E., MIREAULT, A., CABALLERO, D., HARRON, R., STATHOPOULOU, T. R., MASSEY, C., SHELTON, J. M., BASSEL-DUBY, R., PIERCY, R. J. AND OLSON, E. N. 2018. Gene editing restores dystrophin expression in a canine model of Duchenne muscular dystrophy. *Science*, 362(6410), pp. 86-91.

ANDERSON, J. E., GARRETT, K., MOOR, A., MCINTOSH, L. AND PENNER, K. 1998. Dystrophy and myogenesis in mdx diaphragm muscle. *Muscle Nerve*, 21(9), pp. 1153-65.

ANDREEVA, E. R., PUGACH, I. M. AND OREKHOV, A. N. 1997. Subendothelial smooth muscle cells of human aorta express macrophage antigen in situ and in vitro. *Atherosclerosis*, 135(1), pp. 19-27.

ANGELINI, C. AND PETERLE, E. 2012. Old and new therapeutic developments in steroid treatment in Duchenne muscular dystrophy. *Acta Myol*, 31(1), pp. 9-15.

AYALON, G., DAVIS, J. Q., SCOTLAND, P. B. AND BENNETT, V. 2008. An ankyrin-based mechanism for functional organization of dystrophin and dystroglycan. *Cell*, 135(7), pp. 1189-200.

BATCHELOR, C. L. AND WINDER, S. J. 2006. Sparks, signals and shock absorbers: how dystrophin loss causes muscular dystrophy. *Trends Cell Biol*, 16(4), pp. 198-205.

BELGIOVINE, C., D'INCALCI, M., ALLAVENA, P. AND FRAPOLLI, R. 2016. Tumor-associated macrophages and anti-tumor therapies: complex links. *Cell Mol Life Sci*, 73(13), pp. 2411-24.

BELJAARS, L., SCHIPPERS, M., REKER-SMIT, C., MARTINEZ, F. O., HELMING, L., POELSTRA, K. AND MELGERT, B. N. 2014. Hepatic Localization of Macrophage Phenotypes during Fibrogenesis and Resolution of Fibrosis in Mice and Humans. *Front Immunol*, 5, pp. 430.

BENDECK, M. P., CONTE, M., ZHANG, M., NILI, N., STRAUSS, B. H. AND FARWELL, S. M. 2002. Doxycycline modulates smooth muscle cell growth, migration, and matrix remodeling after arterial injury. *Am J Pathol*, 160(3), pp. 1089-95.

BERTORINI, T. E., BHATTACHARYA, S. K., PALMIERI, G. M., CHESNEY, C. M., PIFER, D. AND BAKER, B. 1982. Muscle calcium and magnesium content in Duchenne muscular dystrophy. *Neurology*, 32(10), pp. 1088-92.

BORTHWICK, L. A., BARRON, L., HART, K. M., VANNELLA, K. M., THOMPSON, R. W., OLAND, S., CHEEVER, A., SCIURBA, J., RAMALINGAM, T. R., FISHER, A. J. AND WYNN, T. A. 2016. Macrophages are critical to the maintenance of IL-13-dependent lung inflammation and fibrosis. *Mucosal Immunol*, 9(1), pp. 38-55.

BOWMAN, C. G., IMHOFF, J. G. AND BONVENTRE, P. F. 1970. Specificity of diphtheria toxin action on heart and muscle tissues of Guinea pigs. *Infect Immun*, 2(5), pp. 686-8.

BURNETT, S. H., KERSHEN, E. J., ZHANG, J., ZENG, L., STRALEY, S. C., KAPLAN, A. M. AND COHEN, D. A. 2004. Conditional macrophage ablation in transgenic mice expressing a Fas-based suicide gene. *J Leukoc Biol*, 75(4), pp. 612-23.

BURZYN, D., KUSWANTO, W., KOLODIN, D., SHADRACH, J. L., CERLETTI, M., JANG, Y., SEFIK, E., TAN, T. G., WAGERS, A. J., BENOIST, C. AND MATHIS, D. 2013. A special population of regulatory T cells potentiates muscle repair. *Cell*, 155(6), pp. 1282-95.

CASTILLO, L. AND MACCALLUM, D. M. 2012. Cytokine measurement using cytometric bead arrays. *Methods Mol Biol*, 845, pp. 425-34.

CHANG, R. F. AND MUBARAK, S. J. 2012. Pathomechanics of Gowers' sign: a video analysis of a spectrum of Gowers' maneuvers. *Clin Orthop Relat Res*, 470(7), pp. 1987-91.

CHAZAUD, B. 2015. Inflammation during skeletal muscle regeneration and tissue remodeling: application to exercise-induced muscle damage management. *Immunol Cell Biol*.

CHUNG, J., SMITH, A. L., HUGHES, S. C., NIIZAWA, G., ABDEL-HAMID, H. Z., NAYLOR, E. W., HUGHES, T. AND CLEMENS, P. R. 2015. Twenty-year follow-up of newborn screening for patients with muscular dystrophy. *Muscle Nerve*.

CIRAK, S., FENG, L., ANTHONY, K., ARECHAVALA-GOMEZA, V., TORELLI, S., SEWRY, C., MORGAN, J. E. AND MUNTONI, F. 2012. Restoration of the dystrophin-associated glycoprotein complex after exon skipping therapy in Duchenne muscular dystrophy. *Mol Ther*, 20(2), pp. 462-7.

COULTON, G. R., CURTIN, N. A., MORGAN, J. E. AND PARTRIDGE, T. A. 1988. The mdx mouse skeletal muscle myopathy: II. Contractile properties. *Neuropathol Appl Neurobiol*, 14(4), pp. 299-314.

CUDA, C. M., POPE, R. M. AND PERLMAN, H. 2016. The inflammatory role of phagocyte apoptotic pathways in rheumatic diseases. *Nat Rev Rheumatol*, 12(9), pp. 543-58.

DAVIES, K. E. AND NOWAK, K. J. 2006. Molecular mechanisms of muscular dystrophies: old and new players. *Nat Rev Mol Cell Biol*, 7(10), pp. 762-73.

DE JONG, W. H. AND BORM, P. J. 2008. Drug delivery and nanoparticles: applications and hazards. *Int J Nanomedicine*, 3(2), pp. 133-49.

DONG, S., CHEN, Q. L., SONG, Y. N., SUN, Y., WEI, B., LI, X. Y., HU, Y. Y., LIU, P. AND SU, S. B. .2016. Mechanisms of CCl<sub>4</sub>-induced liver fibrosis with combined transcriptomic and proteomic analysis. *J Toxicol Sci*, 41(4), pp. 561-72.

DUFFIELD, J. S., FORBES, S. J., CONSTANDINO, C. M., CLAY, S., PARTOLINA, M., VUTHOORI, S., WU, S., LANG, R. AND IREDALE, J. P. 2005. Selective depletion of macrophages reveals distinct, opposing roles during liver injury and repair. *J Clin Invest*, 115(1), pp. 56-65.

DUMONT, N. A., WANG, Y. X., VON MALTZAHN, J., PASUT, A., BENTZINGER, C. F., BRUN, C. E. AND RUDNICKI, M. A. 2015. Dystrophin expression in muscle stem cells regulates their polarity and asymmetric division. *Nat Med*, 21(12), pp. 1455-63.

EL REFAEY, M., XU, L., GAO, Y., CANAN, B. D., ADESANYA, T. M. A., WARNER, S. C., AKAGI, K., SYMER, D. E., MOHLER, P. J., MA, J., JANSSEN, P. M. L. AND HAN, R. 2017. In Vivo Genome Editing Restores Dystrophin Expression and Cardiac Function in Dystrophic Mice. *Circ Res*, 121(8), pp. 923-929.

FALZARANO, M. S., SCOTTON, C., PASSARELLI, C. AND FERLINI, A. 2015. Duchenne Muscular Dystrophy: From Diagnosis to Therapy. *Molecules*, 20(10), pp. 18168-84.

FAMENINI, S., RIGALI, E. A., OLIVERA-PEREZ, H. M., DANG, J., CHANG, M. T., HALDER, R., RAO, R. V., PELLEGRINI, M., PORTER, V., BREDESEN,

D. AND FIALA, M. 2017. Increased intermediate M1-M2 macrophage polarization and improved cognition in mild cognitive impairment patients on  $\omega$ -3 supplementation. *FASEB J*, 31(1), pp. 148-160.

GAIAD, T. P., OLIVEIRA, M. X., LOBO, A. R., LIBÓRIO, L. R., PINTO, P. A. F., FERNANDES, D. C., SANTOS, A. P., AMBRÓSIO, C. E. AND MACHADO, A. S. D. 2017. Low-intensity training provokes adaptive extracellular matrix turnover of a muscular dystrophy model. *J Exerc Rehabil*, 13(6), pp. 693-703.

GASPER, M. C. AND GILCHRIST, J. M. 2005. Creatine kinase: a review of its use in the diagnosis of muscle disease. *Med Health R I*, 88(11), pp. 398, 400-4.

GHERYANI, N., COFFELT, S. B., GARTLAND, A., RUMNEY, R. M., KISS-TOTH, E., LEWIS, C. E., TOZER, G. M., GREAVES, D. R., DEAR, T. N. AND MILLER, G. 2013. Generation of a novel mouse model for the inducible depletion of macrophages in vivo. *Genesis*, 51(1), pp. 41-9.

GILBERT, R., NALBANTOGLU, J., PETROF, B. J., EBIHARA, S., GUIBINGA, G. H., TINSLEY, J. M., KAMEN, A., MASSIE, B., DAVIES, K. E. AND KARPATI, G. 1999. Adenovirus-mediated utrophin gene transfer mitigates the dystrophic phenotype of mdx mouse muscles. *Hum Gene Ther*, 10(8), pp. 1299-310.

GIORDANO, C., MOJUMDAR, K., LIANG, F., LEMAIRE, C., LI, T., RICHARDSON, J., DIVANGAHI, M., QURESHI, S. AND PETROF, B. J. 2015. Toll-like receptor 4 ablation in mdx mice reveals innate immunity as a

therapeutic target in Duchenne muscular dystrophy. *Hum Mol Genet*, 24(8), pp. 2147-62.

GOEMANS, N., MERCURI, E., BELOUSOVA, E., KOMAKI, H., DUBROVSKY, A., MCDONALD, C. M., KRAUS, J. E., LOURBAKOS, A., LIN, Z., CAMPION, G., WANG, S. X., CAMPBELL, C. AND GROUP, D. I. S. 2018. A randomized placebo-controlled phase 3 trial of an antisense oligonucleotide, drisapersen, in Duchenne muscular dystrophy. *Neuromuscul Disord*, 28(1), pp. 4-15.

GOEMANS, N. M., TULINIUS, M., VAN DEN AKKER, J. T., BURM, B. E., EKHART, P. F., HEUVELMANS, N., HOLLING, T., JANSON, A. A., PLATENBURG, G. J., SIPKENS, J. A., SITSEN, J. M., AARTSMA-RUS, A., VAN OMMEN, G. J., BUYSE, G., DARIN, N., VERSCHUUREN, J. J., CAMPION, G. V., DE KIMPE, S. J. AND VAN DEUTEKOM, J. C. 2011. Systemic administration of PRO051 in Duchenne's muscular dystrophy. *N Engl J Med*, 364(16), pp. 1513-22.

GOSSELIN, L. E. AND WILLIAMS, J. E. 2006. Pentoxifylline fails to attenuate fibrosis in dystrophic (mdx) diaphragm muscle. *Muscle Nerve*, 33(6), pp. 820-3.

GOTTFRIED, E., KUNZ-SCHUGHART, L. A., WEBER, A., REHLI, M., PEUKER, A., MÜLLER, A., KASTENBERGER, M., BROCKHOFF, G., ANDREESEN, R. AND KREUTZ, M. 2008. Expression of CD68 in non-myeloid cell types. *Scand J Immunol*, 67(5), pp. 453-63.

GOULDING, J., ABOUD, G., TAHILIANI, V., DESAI, P., HUTCHINSON, T. E. AND SALEK-ARDAKANI, S. 2014. CD8 T cells use IFN- $\gamma$  to protect against the lethal effects of a respiratory poxvirus infection. *J Immunol*, 192(11), pp. 5415-25.

GREGOREVIC, P., PLANT, D. R. AND LYNCH, G. S. 2004. Administration of insulin-like growth factor-I improves fatigue resistance of skeletal muscles from dystrophic mdx mice. *Muscle Nerve*, 30(3), pp. 295-304.

GROUNDS, M. D., RADLEY, H. G., LYNCH, G. S., NAGARAJU, K. AND DE LUCA, A. 2008. Towards developing standard operating procedures for pre-clinical testing in the mdx mouse model of Duchenne muscular dystrophy. *Neurobiol Dis*, 31(1), pp. 1-19.

GUMERSON, J. D. AND MICHELE, D. E. 2011. The dystrophin-glycoprotein complex in the prevention of muscle damage. *J Biomed Biotechnol*, 2011, pp. 210797.

GUTPELL, K. M., HRINIVICH, W. T. AND HOFFMAN, L. M. 2015. Skeletal muscle fibrosis in the mdx/utrn $\pm$  mouse validates its suitability as a murine model of Duchenne muscular dystrophy. *PLoS One*, 10(1), pp. e0117306.

HUANG, P., ZHAO, X. S., FIELDS, M., RANSOHOFF, R. M. AND ZHOU, L. 2009. Imatinib attenuates skeletal muscle dystrophy in mdx mice. *FASEB J*, 23(8), pp. 2539-48.

JOHNSON, B. D., SCHEUER, T. AND CATTERALL, W. A. 2005. Convergent regulation of skeletal muscle Ca<sup>2+</sup> channels by dystrophin, the actin cytoskeleton, and cAMP-dependent protein kinase. *Proc Natl Acad Sci U S A*, 102(11), pp. 4191-6.

KANG, P. B. 2013. Beyond the gowers sign: measuring outcomes in Duchenne muscular dystrophy. *Muscle Nerve*, 48(3), pp. 315-7.

KARALAKI, M., FILI, S., PHILIPPOU, A. AND KOUTSILIERIS, M. 2009. Muscle regeneration: cellular and molecular events. *In Vivo*, 23(5), pp. 779-96.

KAWANISHI, N., MIZOKAMI, T., NIIHARA, H., YADA, K. AND SUZUKI, K. 2016. Macrophage depletion by clodronate liposome attenuates muscle injury and inflammation following exhaustive exercise. *Biochem Biophys Res*, 5, pp. 146-151.

KINOSHITA, M., UCHIDA, T., SATO, A., NAKASHIMA, M., NAKASHIMA, H., SHONO, S., HABU, Y., MIYAZAKI, H., HIROI, S. AND SEKI, S. 2010. Characterization of two F4/80-positive Kupffer cell subsets by their function and phenotype in mice. *J Hepatol*, 53(5), pp. 903-10.

KLEOPA, K. A., DROUSIOTOU, A., MAVRIKIOU, E., ORMISTON, A. AND KYRIAKIDES, T. 2006. Naturally occurring utrophin correlates with disease severity in Duchenne muscular dystrophy. *Hum Mol Genet*, 15(10), pp. 1623-8.

KUNKEL, L. M., LALANDE, M., MONACO, A. P., FLINT, A., MIDDLESWORTH, W. AND LATT, S. A. 1985. Construction of a human X-chromosome-enriched phage library which facilitates analysis of specific loci. *Gene*, 33(3), pp. 251-8.

LA ROCCA, G., ANZALONE, R. AND FARINA, F. 2009. The expression of CD68 in human umbilical cord mesenchymal stem cells: new evidences of presence in non-myeloid cell types. *Scand J Immunol*, 70(2), pp. 161-2.

LE RUMEUR, E. 2015. Dystrophin and the two related genetic diseases, Duchenne and Becker muscular dystrophies. *Bosn J Basic Med Sci*, 15(3), pp. 14-20.

LI, J., HSU, H. C. AND MOUNTZ, J. D. 2012. Managing macrophages in rheumatoid arthritis by reform or removal. *Curr Rheumatol Rep*, 14(5), pp. 445-54.

LIU, X., LIU, Y., ZHAO, L., ZENG, Z., XIAO, W. AND CHEN, P. 2017. Macrophage depletion impairs skeletal muscle regeneration: The roles of regulatory factors for muscle regeneration. *Cell Biol Int*, 41(3), pp. 228-238.

LOVE, D. R., HILL, D. F., DICKSON, G., SPURR, N. K., BYTH, B. C., MARSDEN, R. F., WALSH, F. S., EDWARDS, Y. H. AND DAVIES, K. E. 1989. An autosomal transcript in skeletal muscle with homology to dystrophin. *Nature*, 339(6219), pp. 55-8.

MAH, J. K., KORNGUT, L., DYKEMAN, J., DAY, L., PRINGSHEIM, T. AND JETTE, N. 2014. A systematic review and meta-analysis on the epidemiology of Duchenne and Becker muscular dystrophy. *Neuromuscul Disord*, 24(6), pp. 482-91.

MALERBA, A., BOLDRIN, L. AND DICKSON, G. 2011. Long-term systemic administration of unconjugated morpholino oligomers for therapeutic expression of dystrophin by exon skipping in skeletal muscle: implications for cardiac muscle integrity. *Nucleic Acid Ther*, 21(4), pp. 293-8.

MALIK, V., RODINO-KLAPAC, L. R., VIOLLET, L. AND MENDELL, J. R. 2010a. Aminoglycoside-induced mutation suppression (stop codon readthrough) as a therapeutic strategy for Duchenne muscular dystrophy. *Ther Adv Neurol Disord*, 3(6), pp. 379-89.

MALIK, V., RODINO-KLAPAC, L. R., VIOLLET, L., WALL, C., KING, W., AL-DAHAK, R., LEWIS, S., SHILLING, C. J., KOTA, J., SERRANO-MUNUERA, C., HAYES, J., MAHAN, J. D., CAMPBELL, K. J., BANWELL, B., DASOUKI, M., WATTS, V., SIVAKUMAR, K., BIEN-WILLNER, R., FLANIGAN, K. M., SAHENK, Z., BAROHN, R. J., WALKER, C. M. AND MENDELL, J. R. 2010b. Gentamicin-induced readthrough of stop codons in Duchenne muscular dystrophy. *Ann Neurol*, 67(6), pp. 771-80.

MAO, H., SU, P., QIU, W., HUANG, L., YU, H. AND WANG, Y. 2016. The use of Masson's trichrome staining, second harmonic imaging and two-photon excited fluorescence of collagen in distinguishing intestinal tuberculosis from Crohn's disease. *Colorectal Dis*, 18(12), pp. 1172-1178.

MARIOL, M. C. AND SÉGALAT, L. 2001. Muscular degeneration in the absence of dystrophin is a calcium-dependent process. *Curr Biol*, 11(21), pp. 1691-4.

MARTINEZ, F. O. AND GORDON, S. 2014. The M1 and M2 paradigm of macrophage activation: time for reassessment. *F1000Prime Rep*, 6, pp. 13.

MERCURI, E. AND MUNTONI, F. 2013. Muscular dystrophies. *Lancet*, 381(9869), pp. 845-60.

MESSINA, S., VITA, G. L., AGUENNOUZ, M., SFRAMELI, M., ROMEO, S., RODOLICO, C. AND VITA, G. 2011. Activation of NF-kappaB pathway in Duchenne muscular dystrophy: relation to age. *Acta Myol*, 30(1), pp. 16-23.

MILLER, G., MOORE, C. J., TERRY, R., LA RIVIERE, T., MITCHELL, A., PIGGOTT, R., DEAR, T. N., WELLS, D. J. AND WINDER, S. J. 2012. Preventing phosphorylation of dystroglycan ameliorates the dystrophic phenotype in mdx mouse. *Hum Mol Genet*, 21(20), pp. 4508-20.

MILLS, C. D., LENZ, L. L. AND LEY, K. 2015. Macrophages at the fork in the road to health or disease. *Front Immunol*, 6, pp. 59.

MOJUMDAR, K., LIANG, F., GIORDANO, C., LEMAIRE, C., DANIALOU, G., OKAZAKI, T., BOURDON, J., RAFEI, M., GALIPEAU, J., DIVANGAHI, M. AND PETROF, B. J. 2014. Inflammatory monocytes promote progression of Duchenne muscular dystrophy and can be therapeutically targeted via CCR2. *EMBO Mol Med*, 6(11), pp. 1476-92.

MURRAY, P. J., ALLEN, J. E., BISWAS, S. K., FISHER, E. A., GILROY, D. W., GOERDT, S., GORDON, S., HAMILTON, J. A., IVASHKIV, L. B., LAWRENCE, T., LOCATI, M., MANTOVANI, A., MARTINEZ, F. O., MEGE, J. L., MOSSER, D. M., NATOLI, G., SAEIJ, J. P., SCHULTZE, J. L., SHIREY, K. A., SICA, A., SUTTLES, J., UDALOVA, I., VAN GINDERACHTER, J. A., VOGEL, S. N. AND WYNN, T. A. 2014. Macrophage activation and polarization: nomenclature and experimental guidelines. *Immunity*, 41(1), pp. 14-20.

MUSARO, A. 2014. The Basis of Muscle Regeneration. *Advances in Biology*, 16.

NAMGOONG, J. H. AND BERTONI, C. 2016. Clinical potential of ataluren in the treatment of Duchenne muscular dystrophy. *Degener Neurol Neuromuscul Dis*, 6, pp. 37-48.

NEDACHI, T., HATAKEYAMA, H., KONO, T., SATO, M. AND KANZAKI, M. 2009. Characterization of contraction-inducible CXC chemokines and their roles in C2C12 myocytes. *Am J Physiol Endocrinol Metab*, 297(4), pp. E866-78.

NERI, M., TORELLI, S., BROWN, S., UGO, I., SABATELLI, P., MERLINI, L., SPITALI, P., RIMESSI, P., GUALANDI, F., SEWRY, C., FERLINI, A. AND MUNTONI, F. 2007. Dystrophin levels as low as 30% are sufficient to avoid muscular dystrophy in the human. *Neuromuscul Disord*, 17(11-12), pp. 913-8.

PARTRIDGE, T. A. 2013. The mdx mouse model as a surrogate for Duchenne muscular dystrophy. *FEBS J*, 280(17), pp. 4177-86.

PASSAMANO, L., TAGLIA, A., PALLADINO, A., VIGGIANO, E., D'AMBROSIO, P., SCUTIFERO, M., ROSARIA CECIO, M., TORRE, V., DE LUCA, F., PICILLO, E., PACIELLO, O., PILUSO, G., NIGRO, G. AND POLITANO, L. 2012. Improvement of survival in Duchenne Muscular Dystrophy: retrospective analysis of 835 patients. *Acta Myol*, 31(2), pp. 121-5.

PESSINA, P. AND MUÑOZ-CÁNOVES, P. 2016. Fibrosis-Inducing Strategies in Regenerating Dystrophic and Normal Skeletal Muscle. *Methods Mol Biol*, 1460, pp. 73-82.

PIGOZZO, S. R., DA RE, L., ROMUALDI, C., MAZZARA, P. G., GALLETTA, E., FLETCHER, S., WILTON, S. D. AND VITIELLO, L. 2013. Revertant fibers in the mdx murine model of Duchenne muscular dystrophy: an age- and muscle-related reappraisal. *PLoS One*, 8(8), pp. e72147.

PLANT, D. R. AND LYNCH, G. S. 2003. Depolarization-induced contraction and SR function in mechanically skinned muscle fibers from dystrophic mdx mice. *Am J Physiol Cell Physiol*, 285(3), pp. C522-8.

RAIMONDO, T. M. AND MOONEY, D. J. 2018. Functional muscle recovery with nanoparticle-directed M2 macrophage polarization in mice. *Proc Natl Acad Sci U S A*, 115(42), pp. 10648-10653.

RIGAMONTI, E., ZORDAN, P., SCIORATI, C., ROVERE-QUERINI, P. AND BRUNELLI, S. 2014. Macrophage plasticity in skeletal muscle repair. *Biomed Res Int*, 2014, pp. 560629.

ROMFH, A. AND MCNALLY, E. M. 2010. Cardiac assessment in duchenne and becker muscular dystrophies. *Curr Heart Fail Rep*, 7(4), pp. 212-8.

ROSENBERG, A. S., PUIG, M., NAGARAJU, K., HOFFMAN, E. P., VILLALTA, S. A., RAO, V. A., WAKEFIELD, L. M. AND WOODCOCK, J. 2015. Immune-mediated pathology in Duchenne muscular dystrophy. *Sci Transl Med*, 7(299), pp. 299rv4.

ROUILLON, J., POUPIOT, J., ZOCEVIC, A., AMOR, F., LÉGER, T., GARCIA, C., CAMADRO, J. M., WONG, B., PINILLA, R., COSETTE, J., COENENSTASS, A. M., MCCLOREY, G., ROBERTS, T. C., WOOD, M. J., SERVAIS, L., UDD, B., VOIT, T., RICHARD, I. AND SVINARTCHOUK, F. 2015. Serum proteomic profiling reveals fragments of MYOM3 as potential biomarkers for monitoring the outcome of therapeutic interventions in muscular dystrophies. *Hum Mol Genet*, 24(17), pp. 4916-32.

RUEGG, U. T., NICOLAS-MÉTRAL, V., CHALLET, C., BERNARD-HÉLARY, K., DORCHIES, O. M., WAGNER, S. AND BUETLER, T. M. 2002. Pharmacological control of cellular calcium handling in dystrophic skeletal muscle. *Neuromuscul Disord*, 12 Suppl 1, pp. S155-61.

RUMNEY, R. M. H., COFFELT, S. B., NEALE, T. A., DHAYADE, S., TOZER, G. M. AND MILLER, G. 2017. PyMT-Maclow: A novel, inducible, murine model

for determining the role of CD68 positive cells in breast tumor development. *PLoS One*, 12(12), pp. e0188591.

RÓSZER, T. 2015. Understanding the Mysterious M2 Macrophage through Activation Markers and Effector Mechanisms. *Mediators Inflamm*, 2015, pp. 816460.

SHAPOURI-MOGHADDAM, A., MOHAMMADIAN, S., VAZINI, H., TAGHADOSI, M., ESMAEILI, S. A., MARDANI, F., SEIFI, B., MOHAMMADI, A., AFSHARI, J. T. AND SAHEBKAR, A. 2018. Macrophage plasticity, polarization, and function in health and disease. *J Cell Physiol*, 233(9), pp. 6425-6440.

SHARP, P. S., BYE-A-JEE, H. AND WELLS, D. J. 2011. Physiological characterization of muscle strength with variable levels of dystrophin restoration in mdx mice following local antisense therapy. *Mol Ther*, 19(1), pp. 165-71.

SHIBUYA, A. AND IKEWAKI, N. 2002. High serum glyceraldehyde-3-phosphate dehydrogenase levels in patients with liver cirrhosis. *Hepatol Res*, 22(3), pp. 174-179.

SPURNEY, C. F., GORDISH-DRESSMAN, H., GUERRON, A. D., SALI, A., PANDEY, G. S., RAWAT, R., VAN DER MEULEN, J. H., CHA, H. J., PISTILLI, E. E., PARTRIDGE, T. A., HOFFMAN, E. P. AND NAGARAJU, K. 2009. Preclinical drug trials in the mdx mouse: assessment of reliable and sensitive outcome measures. *Muscle Nerve*, 39(5), pp. 591-602.

SUMMAN, M., WARREN, G. L., MERCER, R. R., CHAPMAN, R., HULDERMAN, T., VAN ROOIJEN, N. AND SIMEONOVA, P. P. 2006. Macrophages and skeletal muscle regeneration: a clodronate-containing liposome depletion study. *Am J Physiol Regul Integr Comp Physiol*, 290(6), pp. R1488-95.

TEDESCO, F. S., DELLAVALLE, A., DIAZ-MANERA, J., MESSINA, G. AND COSSU, G. 2010. Repairing skeletal muscle: regenerative potential of skeletal muscle stem cells. *J Clin Invest*, 120(1), pp. 11-9.

TIDBALL, J. G. AND VILLALTA, S. A. 2010. Regulatory interactions between muscle and the immune system during muscle regeneration. *Am J Physiol Regul Integr Comp Physiol*, 298(5), pp. R1173-87.

TIDBALL, J. G. AND WEHLING-HENRICKS, M. 2007. Macrophages promote muscle membrane repair and muscle fibre growth and regeneration during modified muscle loading in mice in vivo. *J Physiol*, 578(Pt 1), pp. 327-36.

UDALOVA, I. A., MANTOVANI, A. AND FELDMANN, M. 2016. Macrophage heterogeneity in the context of rheumatoid arthritis. *Nat Rev Rheumatol*, 12(8), pp. 472-85.

VAN ROOIJEN, N. AND SANDERS, A. 1994. Liposome mediated depletion of macrophages: mechanism of action, preparation of liposomes and applications. *J Immunol Methods*, 174(1-2), pp. 83-93.

VILLALTA, S. A., DENG, B., RINALDI, C., WEHLING-HENRICKS, M. AND TIDBALL, J. G. 2011a. IFN- $\gamma$  promotes muscle damage in the mdx mouse model of Duchenne muscular dystrophy by suppressing M2 macrophage activation and inhibiting muscle cell proliferation. *J Immunol*, 187(10), pp. 5419-28.

VILLALTA, S. A., NGUYEN, H. X., DENG, B., GOTOH, T. AND TIDBALL, J. G. 2009. Shifts in macrophage phenotypes and macrophage competition for arginine metabolism affect the severity of muscle pathology in muscular dystrophy. *Human molecular genetics*, 18(3), pp. 482-496.

VILLALTA, S. A., RINALDI, C., DENG, B., LIU, G., FEDOR, B. AND TIDBALL, J. G. 2011b. Interleukin-10 reduces the pathology of mdx muscular dystrophy by deactivating M1 macrophages and modulating macrophage phenotype. *Human molecular genetics*, 20(4), pp. 790-805.

WANG, H., MELTON, D. W., PORTER, L., SARWAR, Z. U., MCMANUS, L. M. AND SHIREMAN, P. K. 2014a. Altered macrophage phenotype transition impairs skeletal muscle regeneration. *Am J Pathol*, 184(4), pp. 1167-1184.

WANG, Y., MARINO-ENRIQUEZ, A., BENNETT, R. R., ZHU, M., SHEN, Y., EILERS, G., LEE, J. C., HENZE, J., FLETCHER, B. S., GU, Z., FOX, E. A., ANTONESCU, C. R., FLETCHER, C. D., GUO, X., RAUT, C. P., DEMETRI, G. D., VAN DE RIJN, M., ORDOG, T., KUNKEL, L. M. AND FLETCHER, J. A. 2014b. Dystrophin is a tumor suppressor in human cancers with myogenic programs. *Nat Genet*, 46(6), pp. 601-6.

WANG, Y., WEHLING-HENRICKS, M., SAMENGO, G. AND TIDBALL, J. G. 2015. Increases of M2a macrophages and fibrosis in aging muscle are influenced by bone marrow aging and negatively regulated by muscle-derived nitric oxide. *Aging Cell*, 14(4), pp. 678-88.

WATKINS, S. C. AND CULLEN, M. J. 1982. Muscle fibre size and shape in Duchenne muscular dystrophy. *Neuropathol Appl Neurobiol*, 8(1), pp. 11-7.

WEHLING, M., SPENCER, M. J. AND TIDBALL, J. G. 2001. A nitric oxide synthase transgene ameliorates muscular dystrophy in mdx mice. *The Journal of Cell Biology*, 155(1), pp. 123-132.

WEHLING-HENRICKS, M., LEE, J. J. AND TIDBALL, J. G. 2004. Prednisolone decreases cellular adhesion molecules required for inflammatory cell infiltration in dystrophin-deficient skeletal muscle. *Neuromuscul Disord*, 14(8-9), pp. 483-90.

WEIN, N., ALFANO, L. AND FLANIGAN, K. M. 2015. Genetics and emerging treatments for Duchenne and Becker muscular dystrophy. *Pediatr Clin North Am*, 62(3), pp. 723-42.

WEISSER, S. B., VAN ROOIJEN, N. AND SLY, L. M. 2012. Depletion and reconstitution of macrophages in mice. *J Vis Exp*, (66), pp. 4105.

WONG, W. W., VINCE, J. E., LALAOUI, N., LAWLOR, K. E., CHAU, D., BANKOVACKI, A., ANDERTON, H., METCALF, D., O'REILLY, L., JOST, P. J., MURPHY, J. M., ALEXANDER, W. S., STRASSER, A., VAUX, D. L. AND

SILKE, J. 2014. cIAPs and XIAP regulate myelopoiesis through cytokine production in an RIPK1- and RIPK3-dependent manner. *Blood*, 123(16), pp. 2562-72.

WU, B., CLOER, C., LU, P., MILAZI, S., SHABAN, M., SHAH, S. N., MARSTON-POE, L., MOULTON, H. M. AND LU, Q. L. 2014. Exon skipping restores dystrophin expression, but fails to prevent disease progression in later stage dystrophic dko mice. *Gene Ther*, 21(9), pp. 785-93.

WYNN, T. A., CHAWLA, A. AND POLLARD, J. W. 2013. Macrophage biology in development, homeostasis and disease. *Nature*, 496(7446), pp. 445-55.

YIN, H., MOULTON, H. M., BETTS, C., MERRITT, T., SEOW, Y., ASHRAF, S., WANG, Q., BOUTILIER, J. AND WOOD, M. J. 2010. Functional rescue of dystrophin-deficient mdx mice by a chimeric peptide-PMO. *Mol Ther*, 18(10), pp. 1822-9.

YU, X., BAO, B., ECHIGOYA, Y. AND YOKOTA, T. 2015. Dystrophin-deficient large animal models: translational research and exon skipping. *Am J Transl Res*, 7(8), pp. 1314-31.

YUCEL, N., CHANG, A. C., DAY, J. W., ROSENTHAL, N. AND BLAU, H. M. 2018. Humanizing the mdx mouse model of DMD: the long and the short of it. *NPJ Regen Med*, 3, pp. 4.

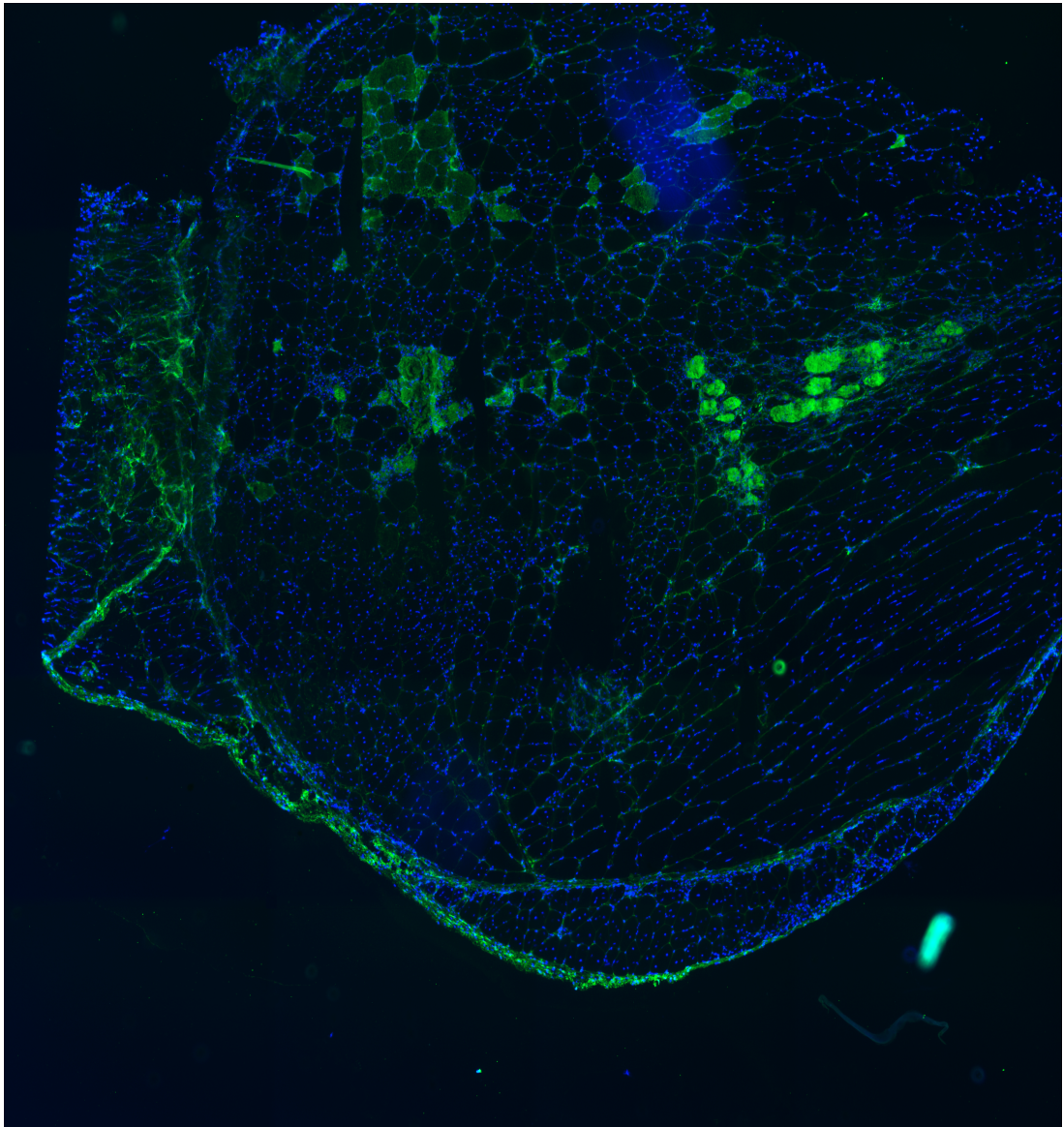
ZHOU, L. AND LU, H. 2010. Targeting fibrosis in Duchenne muscular dystrophy. *J Neuropathol Exp Neurol*, 69(8), pp. 771-6.

## Chapter 8: Appendices

---

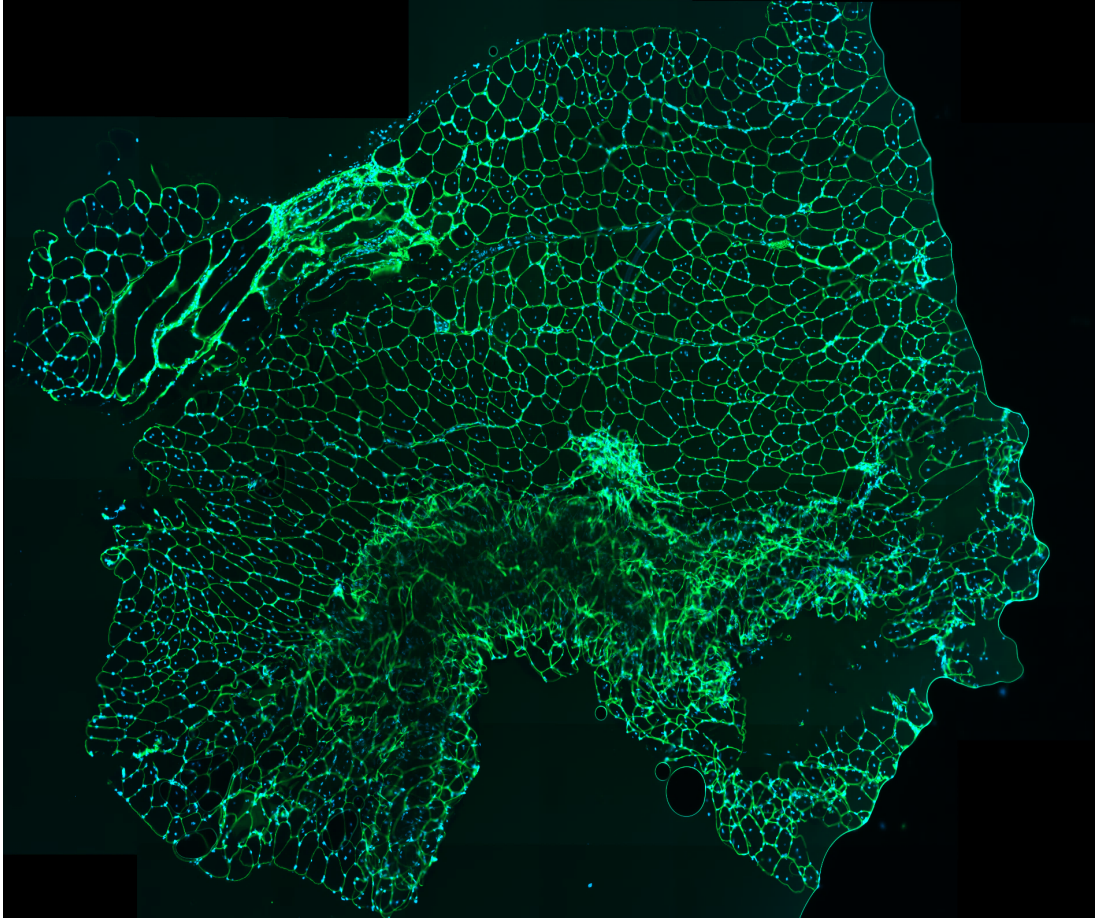
### 8.1 Appendix I

#### Complete IgG Stained Six Week Doxycycline Treated MacLowMD TA



## 8.2 Appendix II

### Complete Laminin Stained Six Week Doxycycline Treated MacLowMD TA



## 8.3 Appendix III

### Animal Work Reagents

#### Genotyping Reagents and Buffers

##### 10 mg/ml Proteinase K Stock Solution

- 100mg Proteinase K (Proteinase K from Tritirachium album supplied by SIGMA- P2308)
- 10 ml storage buffer Aliquoted and stored at -200C

##### 10X TBE buffer

- 108g Tris base
- 55g Boric acid
- 800ml dH<sub>2</sub>O
- Stir in magnetic stirrer
- 40ml 0.5M EDTA (pH8)
- Make up to 1000ml with dH<sub>2</sub>O

Stored at room temperature away from light. For X1 working solution dilute with deionized dH<sub>2</sub>O.

##### 10% Formalin

- 4g sodium phosphate (NaH<sub>2</sub>PO<sub>4</sub>)
- 7.1g Di-sodium hydrogen orthophosphate (Na<sub>2</sub>HPO<sub>4</sub>)
- 100ml formaldehyde
- 900ml dH<sub>2</sub>O

Stored at room temperature away from direct sunlight.

## 8.4 Appendix III

### Immunohistochemistry and Immunofluorescent Antibodies and Regents

Primary antibodies used in immunohistochemistry and immunofluorescent staining of tissue sections

<b>Antibody</b>	<b>Clone</b>	<b>Catalogue Number and Supplier</b>	<b>Reactivity</b>	<b>Dilution Used</b>	<b>Storage</b>
<b>Anti-F4/80 antibody</b>	Cl: A3-1	Ab6640 abcam Cambridge, UK	Mouse	1:100	2 -8°C
<b>CD68 alexafluor647 conjugated antibody</b>	FA-11	MCA1957 Biorad California, USA	Mouse	1:10	2 -8°C
<b>Purified anti-mouse CD206 (MMR) antibody</b>	C068C2	141701 BioLegend California, USA	Mouse	1:200	-20°C
<b>Anti-CD163 antibody</b>	EPR195 18	ab182422 abcam Cambridge, UK	Mouse	1:200	2 -8°C
<b>Biotinylated Horse Anti-Mouse IgG antibody</b>	Polyclonal	BA-2000, Vector Laboratories, Peterborough, UK	Mouse	1:500	2 -8°C
<b>Laminin antibody <math>\alpha</math>1</b>	4H8-2	ALX-804-190- C100, Enzo, Exeter, UK	Mouse	1:500	2 -8°C
<b>Collagen Type I antibody</b>	Monoclonal	AB765P, Merck Millipore, Massachusetts, USA	Mouse	1:500	-20°C

Secondary antibodies used in immunohistochemistry and immunofluorescent staining of tissue sections

All antibodies were stored at 2- 8°C.

<b>Antibody</b>	<b>Catalogue Number and Supplier</b>
<b>Biotinylated Rabbit Anti-Rat IgG Antibody</b>	BA-4000, Vector Laboratories, Peterborough, UK
<b>Biotinylated goat anti-rabbit IgG</b>	BA-1000 Vector Laboratories, Peterborough, UK
<b>Fluorescein Streptavidin</b>	SA-5001 Vector Laboratories, Peterborough, UK
<b>Fluorescein Rabbit Anti-Rat IgG Antibody</b>	FL-4000 Vector Laboratories, Peterborough, UK
<b>Fluorescein Goat Anti-Rabbit IgG Antibody</b>	FL-1000 Vector Laboratories, Peterborough, UK

## 8.5 Appendix V

### Western Blot Antibodies and Regents

#### Primary antibodies used in blood serum western blots

<b>Antibody</b>	<b>Clone</b>	<b>Catalogue Number and Supplier</b>	<b>Reactivity</b>	<b>Dilution Used</b>	<b>Storage</b>
<b>MYOM3 Antibody</b>	Rabbit polyclonal	17692-1-AP Proteintech Group, Manchester, UK	Mouse	1:500	-20°C
<b>Anti-GAPDH antibody</b>	Rabbit polyclonal	MCA1957 BioRad California, USA	Mouse, Rat, Rabbit, Chicken, Human, Fish	1:10,000	-20°C

#### Secondary antibodies used in blood serum western blots

Antibody was stored at 2- 8°C.

<b>Antibody</b>	<b>Catalogue Number and Supplier</b>
<b>Goat Anti-Rabbit Immunoglobulins</b>	P044801-2, Agilent Technologies, California, USA